JOURNAL OF MATERIALS SCIENCE 33 (1998) 561–624

Review
Room-temperature reactions in thin metal couples

V. SIMIĆ, Ž. MARINKOVIĆ
Institute of Physics, Maksima Gorkog 118, Zemun, 11080 Belgrade, Federal Republic of Yugoslavia

Results of a 40 year-long investigation of room-temperature formation of compounds in 144 thin-film couples obtained by combining 23 metals (Ag, Al, Au, Bi, Cd, Co, Cr, Cu, Ga, Ge, In, Mg, Mn, Ni, Pb, Pd, Pt, Sb, Sm, Sn, Te, Ti, Zn) are presented. The data from published papers of the present and other authors have been complemented by unpublished data of the present authors. The systematized results and their analysis point to the following. In 39 couples, a total of 65 compounds are formed. The reactions of compound formation last from ~1 min to ~10 y, depending on the specimen type and procedure of film deposition. In the bulk–film specimens, the number of compounds formed is smaller and the reaction is slower than in the film–film specimens prepared by thermal evaporation. In the specimens with the sputtered top layer, a greater number of compounds is formed and the compound formation reaction proceeds more rapidly than in the couples prepared by thermal evaporation of both metals. The compounds formed can be transformed into others containing higher percentage of one of the constituents, until the specimen contains an excess of that constituent, provided that such compounds exist in the respective phase diagram. At the beginning of the reaction, compounds are formed in a broad concentration range, while at the reaction end the range is narrowed down, becoming close to that in the corresponding phase diagram. The optimum conditions for compound formation exist in the couples consisting of a high-melting metal and a low-melting one, provided that the potential compound is not high-melting. If the potential compound is high-melting, or if both metals in the couple have melting points in the same temperature range, no compound formation takes place at room temperature. In the couples consisting of a given high-melting metal and one of the low- melting metals, a linear relationship exists between the interdiffusion coefficient and the melting point of the low-melting metal. If, for a couple consisting of a high-melting metal and a low-melting one, there is a solid solubility range of the low-melting metal, during the course of long ageing, the compound formed is decomposed and the low-melting metal is amorphized. During the long ageing, the ambient atmosphere acts on the metal films (alone or in a couple) leading to formation of oxides, hydroxides or carbonates. The results obtained complement the low-temperature range results in the respective phase diagrams.

1. Introduction

In modern research and development procedures, as well as in the process of production and exploitation of devices and their components, it is very often the case that two metals come into intimate contact. It is usually required that the characteristics of such a contact couple remain unchanged during its exploitation. It is sometimes necessary to induce (by heating or by some other means) characteristics different from the initial ones, but these should also remain unchanged during the subsequent exploitation. However, it is not unusual that undesirable changes take place in the metal couple, either in the process of its formation or in the ageing process, i.e. during exploitation. In the former case, the necessary component cannot be produced. In the latter more unfavourable case, the component is built in a device, but characteristics of the device become progressively changed during its exploitation, so that finally it must be discarded.

Because of the mentioned problems, a systematic investigation of the phenomena occurring in metal couples, especially those often used, has to be made.

When two metals come into intimate contact, interdiffusion processes take place to a greater or lesser degree, i.e. there is a mass transfer of one metal into the other and *vice versa*. Probably the first systematic

study of the interdiffusion of metals (diffusion of gold in lead) was that made approximately a century ago [1]. Roberts-Austen combined techniques of sectioning and chemical analysis to measure the diffusion and found that gold atoms had diffused a distance of the order of centimetres in lead with an annealing time of about 30 d at temperatures ranging from 100–250 °C.

A consequence of such a diffusion in this and other metal couples may be the formation of intermetallic compounds. Properties of the compounds formed may differ considerably from those of the starting metals. This may result in a deterioration of the regime on contact and, therefore, in undesirable changes of the device characteristics.

So far, the contacts between two bulk metals have been considered. The involved phenomena may be strongly accentuated if the contact is made of thin metal layers.

It is known from the existing literature that a metal in the form of a thin layer was first obtained in 1857 [2]. Thin metal layers have since been gradually establishing their place in science and technology.

In the 1940s and 1950s an explosive development of thin metal-film preparation and application technologies has taken place, these being a prerequisite of the development of certain important branches of technology, especially military. Thin films are increasingly employed in optics, micro- and opto-electronics, sensor and computation technologies. They are used as mirrors with front-reflecting surfaces, conduction paths, contact and barrier layers, antireflection and anticorrosion layers, etc. The real physical dimensions of the layers used range from less than 1 mm in the rocket-guiding sensors, up to as much as 5 m in optical mirrors for large telescopes. This dynamic development continues.

Because of the character of a thin metal film as a physical medium, diffusion and compound formation in thin metal couples is more vigorous than in the corresponding bulk couples, especially if the processes at several hundred degrees centigrade are considered.

Development of microelectronics and, particularly, sensor technology has led to the demand to deposit the layers at as low a temperature as possible. If the sensor is exposed to an elevated temperature, its characteristics may become undesirably changed. Such contacts are often deposited nowadays even at room temperature. This has led to the necessity of a systematic investigation of the phenomena in thin metal film couples at room temperature. Knowledge of the reaction process in the couples is one of the preconditions of a correct design and fabrication of the critical components and devices in many branches of modern technology, military in particular.

In the mid sixties, sporadic investigation began of the phenomenon of compound formation in thin metal films at room temperature. It was a part (in fact a periferal part) of a study which was made, due to scientific and technical needs, at elevated temperatures. The investigation was continued for the whole of the seventies.

At the beginning of the eighties, the room-temperature formation of compounds on the contact of two thin metal films could be considered rather a rare phenomenon. Only four or five compounds had been identified. However, the investigation became systematic. Intensification of the research in a number of laboratories, primarily in Oslo and Belgrade, has led to identification of 65 compounds formed at room temperature in the evaporated thin metal couples.

The process of a spontaneous compound formation at room temperature could not be detected and followed during a reasonable time on contact of two bulk metals. This is made possible, however, by the characteristics of a thin film, i.e. by presence of many defects which favour diffusion. Thus, on the contact of two thin films, there exist optimum conditions for compound formation.

It was interesting, therefore, to establish whether compound formation could take place on the bulk-metal/evaporated thin film interface, i.e. whether only one thin film takes part in the reaction, and, if so, in which couple this occurs and what will be the transformations of the compounds formed during ageing. In brief, is there any difference between the processes taking place when two thin films are involved, and those when bulk metal reacts with a thin film. These questions are interesting from both theoretical and practical aspects, in particular if the contact phenomena in microelectronics, optoelectronics, sensor techniques and integral circuits are considered.

It is of particular interest to study contact phenomena in semiconductor technology. Namely, it is often the case to have a thin metal film contact evaporated on a semiconducting bulk single-crystal compound. For such a study, the films were evaporated on both the bulk metal and the metal film.

For the bulk–film and film–film specimen types, the upper film can also be obtained by radio-frequency (r.f.) sputtering. Because this procedure is often used in practice, its study is of significant interest.

Finally, the question concerning the conclusions to be derived on analysing the results obtained with the given couples, but of different types, should be considered.

The present review has been compiled as follows. Most of the available material, dispersed over more significant relevant journals, has been accumulated and organized, and is presented in a consistent manner. The material encompasses compound formation at room temperature in the metal couples most frequently applied. In order to make as comprehrensive a survey as possible, the collected material has been coupled by adding results of the authors own recent studies. The 144 investigated couples formed from 23 metals are presented in Table I.

The material thus assembled offers the possibility of having in a single place an up-to-date survey of investigations in the field, which also facilitates its use for practical purposes (Section 2).

The kinetics of compound formation have been arranged in a similar manner (Section 3).

The organization of the material offers the possibility of its analysis by separate parameters. Thus different

TABLE I 144 investigated couples combined from 23 metals

Ag–Al	Ag–Cd	Ag–Ga	Ag–In	Ag–Mg	Ag–Sb	Ag–Sm	Ag–Sn
Ag–Te	Ag–Zn	Al–Au	Al–Co	Al–Cr	Al–Cu	Al–Mg	Al–Mn
Al–Ni	Al–Sb	Al–Sm	Al–Te	Al–Ti	Al–Zn	Au–Bi	Au–Cd
Au–Cu	Au–Ga	Au–Ge	Au–In	Au–Mg	Au–Mn	Au–Pb	Au–Sb
Au–Sm	Au–Sn	Au–Te	Au–Ti	Au–Zn	Bi–In	Bi–Mg	Bi–Mn
Bi–Ni	Bi–Pd	Bi–Te	Bi–Ti	Cd–Cu	Cd–Mg	Cd–Ni	Cd–Pd
Cd–Sb	Cd–Sm	Cd–Te	Cd–Ti	Co–Cr	Co–Ga	Co–Ge	Co–In
Co–Mg	Co–Sb	Co–Sm	Co–Sn	Co–Te	Co–Zn	Cr–Ga	Cr–Ge
Cr–Mn	Cr–Sb	Cr–Sn	Cr–Te	Cr–Zn	Cu–Ga	Cu–Ge	Cu–In
Cu–Mg	Cu–Mn	Cu–Sb	Cu–Sm	Cu–Sn	Cu–Te	Cu–Ti	Cu–Zn
Ga–Mg	Ga–Mn	Ga–Ni	Ga–Pd	Ga–Sb	Ga–Sm	Ga–Te	Ga–Ti
Ge–Mg	Ge–Mn	Ge–Ni	Ge–Sm	Ge–Te	Ge–Ti	In–Mg	In–Mn
In–Ni	In–Pd	In–Sb	In–Sm	In–Sn	In–Te	In–Ti	Mg–Ni
Mg–Pb	Mg–Sb	Mg–Sm	Mg–Sn	Mg–Te	Mg–Zn	Mn–Ni	Mn–Sb
Mn–Sm	Mn–Sn	Mn–Te	Mn–Ti	Mn–Zn	Ni–Sb	Ni–Sm	Ni–Sn
Ni–Te	Ni–Zn	Pb–Pd	Pb–Pt	Pb–Sm	Pb–Te	Pb–Ti	Pd–Sb
Pd–Sn	Pd–Te	Pd–Zn	Pt–Sn	Sb–Sm	Sb–Sn	Sb–Te	Sb–Zn
Sm–Sn	Sm–Te	Sm–Zn	Sn–Te	Sn–Ti	Te–Ti	Te–Zn	Ti–Zn

aspects of the compound formation process have been analysed within a time interval from a few minutes to nearly a decade (Section 4).

The processes taking place during a period of about 15 y after completion of the reaction have also been followed and analysed, particularly the influence of the atmosphere (Section 5).

It has been found that some of the compounds formed are susceptible to changes during long ageing, obeying rules which passed unnoticed until present (Section 6). This is important, especially because thin-film couples, in the form of conducting paths or contacts, should not be susceptible to changes in their characteristics during long exploitation.

The review is completed by analysis of the results obtained so far and by reflections regarding trends of further investigation. It contains very abundant experimental material, including the authors' so-far unpublished results.

The authors feel that the knowledge gained during their, and other authors', long-lasting research is, in this way, presented in the optimum form, that will be useful to both the specialists working in the field and those using thin films.

2. Formation of compounds

2.1. Formation of compounds on the contact of two evaporated thin metal films

This section contains data published so far relative to the formation of compounds in 39 investigated couples. The results are presented, as far as possible, in a uniform manner. Within the limits of the available data, the following information has been presented for each couple:

(i) reference to the phase diagram used;

(ii) reference to the first published paper containing the data about the compound formation, together with authors' names and the methods used for analysis;

(iii) table of formation of compounds from the elements and their transformations during ageing;

(iv) the data of the ASTM standards [3] on the basis of which the formed compounds have been identified;

(v) the X-ray powder results, prepared on the basis of the relevant authors' standards used for identification of the compounds in the absence of the corresponding ASTM standards.

When in the later published papers more data are contained than in the previous ones, comments on the data from the latter are given. If the papers by different authors contain different results, they have been compared, commented upon and, if possible, interpreted.

2.1.1. Ag–Cd

The first results about the room-temperatue compound formation in the Ag–Cd couple (phase diagram [4]) have been presented by Simić and Marinković [5]. This couple has been studied in some detail using specimens 850–904 nm thick with three different cadmium concentrations: 38.5% (solid solubility range), 51.0% (AgCd) and 75.8% ($AgCd_3$). (All concentrations are given in weight per cent.)

The specimens were analysed by X-ray diffractometry (XRD). It has been found that, irrespective of the cadmium content, $AgCd_3$ (ASTM 28–199) is always formed first. This compound is formed during the first hour after evaporation (Table II). By following the specimen changes during 5–6 mon, the following transformations have been found to take place in the specimens containing 38.5% and 51.0% Cd

$$8AgCd_3 + 7Ag = 3Ag_5Cd_8 \quad (1)$$

and

$$Ag_5Cd_8 + 3Ag = 8AgCd \quad (2)$$

A consequence of the transformation in the specimen with 38.5% Cd is that cadmium and $AgCd_3$ disappear, while Ag_5Cd_8 (ASTM 14–4) and AgCd (C) (cubic) (ASTM 28-197) remain, together with excess silver. A similar situation exists for the specimen containing 51.0% Cd, except that in this case $AgCd_3$ also remains. In the specimen with 75.8% Cd, only $AgCd_3$

TABLE II Structural transformations in the Ag–Cd couple during ageing

Time after evaporation	Cd concentration (wt%)		
	38.5	51.0	75.8
0.5 h	Cd	Cd	Cd
	Ag	Ag	Ag
	$AgCd_3$	$AgCd_3$	$AgCd_3$
2 h	Cd		Cd
	Ag	Ag	Ag
	$AgCd_3$	$AgCd_3$	$AgCd_3$
	Ag_5Cd_8	Ag_5Cd_8	
6 d	Ag	Ag	Cd
	$AgCd_3$	$AgCd_3$	$AgCd_3$
	Ag_5Cd_8	Ag_5Cd_8	
14 d	Ag	Ag	
	$AgCd_3$	$AgCd_3$	$AgCd_3$
	Ag_5Cd_8	Ag_5Cd_8	
41 d	Ag	Ag	
	$AgCd_3$	$AgCd_3$	$AgCd_3$
	Ag_5Cd_8	Ag_5Cd_8	
	AgCd(C)		
99, 150, 155, d	Ag	Ag	
		$AgCd_3$	$AgCd_3$
	Ag_5Cd_8	Ag_5Cd_8	
	AgCd(C)	AgCd(C)	

remains. As can be seen, the compounds are formed following the sequence of cadmium content: $AgCd_3$, Ag_5Cd_8, AgCd.

2.1.2. Ag–Ga

The first results concerning room-temperature compound formation in the Ag–Ga couple (phase diagram [4]) were presented by Simić and Marinković [6]. This couple has been thoroughly studied using specimens 172–192 nm thick and containing five different gallium concentrations: 17.5% and 24.0% Ga (x′ phase existing in the 17.7–24.0% Ga concentration range, i.e. about the Ag_3Ga stoichiometric value), 39.0% (AgGa), 49.0% (Ag_2Ga_3) and 75.0%. The specimens were analysed by XRD. The identification of the obtained powder diagrams was done by means of the authors own Ag_3Ga standard prepared by fusing stoichiometric amounts of the elements in the evacuated quartz tube. The XRD powder diagrams of the Ag_3Ga standard and of the film specimen containing 24.0% Ga are identical. The powder diffraction results of the standard are presented in Table III.

TABLE IV Structural transformations in the Ag–Ga couple during ageing

Time after evaporation	Ga concentration (wt%)		
	17.5	24.0	39.0 49.0 75.0
1 d	Ag	Ag	
	Ag_3Ga	Ag_3Ga	Ag_3Ga
20–30 d	Ag	Ag	
	Ag_3Ga	Ag_3Ga	Ag_3Ga
3–4 mon	Ag		
	Ag_3Ga	Ag_3Ga	Ag_3Ga
8.5 mon	Ag_3Ga	Ag_3Ga	Ag_3Ga

The obtained results are presented in Table IV, which shows the following parts. Because gallium is amorphous for these layer thicknesses, it does not appear in the XRD diagram. The process of compound formation is virtually finished during the first day (in the case of 24.0% Ga, somewhat later) and there are no further transformations during the following 3–4 mon.

2.1.3. Ag–In

The first data concerning room-temperature compound formation in the Ag–In couple (phase diagram [4]) were presented by Simić and Marinković [6]. This couple was studied in some detail using specimens 180–215 nm thick and containing six different indium concentrations: 11.2% (solid solubility range), 26.2% (Ag_3In), 34.7% (Ag_2In), 50.0%, 68.0% ($AgIn_2$) and 80.0% ($AgIn_2$ + In).

The specimens were analysed using XRD. Identification of the compound reflections was done by means of the authors own standards for Ag_2In and $AgIn_2$, prepared by fusing stoichiometric amounts of the elements in an evacuated quartz tube.

The XRD diagrams of the Ag_2In standard and the film specimen containing the same indium concentration are identical, but the diagrams of the $AgIn_2$ standard and the film specimen having the same indium concentrations are different.

TABLE III X-ray powder results of the Ag_3Ga standard

Bulk standard (24 wt% Ga) (200 °C/24h)				Thin-film standard (17.5 and 24.0 wt% Ga)(20 °C)			
d (nm)	I/I_0	d (nm)	I/I_0	d (nm)	I/I_0	d (nm)	I/I_0
0.3883	4	0.1866	2	0.3883	6	0.1866	6
0.2644	2	0.1611	4	0.2644	3	0.1613	30
0.2543	4	0.1437	2	0.2549	10	0.1442	7
0.2478	1	0.1360	4			0.1363	14
0.2309	41	0.1308	4	0.2315	100	0.1310	23
0.2241	100	0.1295	2	0.2245	100	0.1296	19
0.2186	6	0.1210	4	0.2191	19	0.1213	29
0.1906	3	0.1121	4	0.1906	16	0.1121	11

Note: In all the tables with X-ray powder results, d-values are given in nanometres (nm), and not in Angstroms as in the ASTM, standards.

Annealing of the specimens with 68.0% In at 60 and 120 °C has shown that the transformation temperature is between these two values. Below the transformation temperature, the $LTAgIn_2$ (the low-temperature phase) exists, while above it the $MTAgIn_2$ (the medium-temperature phase) is present.

Structural transformations take place during ageing, as shown in Table V.

The compound containing more indium ($LTAgIn_2$) is always formed first. If the specimen contains excess silver, the following transformation takes place

$$3\,Ag + AgIn_2 = 2\,Ag_2In \quad (3)$$

The transformation process is completed in less than 5 d in the specimens containing 50.0% In or more. In the specimens with less than 50.0% In, the process is completed only after 9 mon. When the transformation is completed, the specimens with less than 50.0% In contain Ag_2In and excess silver, and those with more than 50.0% In contain only $LTAgIn_2$. The specimen with 50.0% In is an intermediate state, i.e. a combination of the two states mentioned.

2.1.4. Ag–Sn

In 1959, Fujiki [7] found, using electron diffraction, that in the Ag–Sn couple the γ-AgSn phase was formed. However, his results seem not too persuasive. Considerably later, Tu and Rosenberg [8] claim to have obtained Ag_3Sn. In their presented powder diagram, it is seen that several hours after evaporation, several very weak reflections of Ag_3Sn were already present. The reflection intensities increase very slowly with time at room temperature.

The results of a thorough study of this couple (phase diagram [4, 9]) are presented in a paper by Simić and Marinković [6]. Specimens 170–210 nm thick with four different tin concentrations have been used: 15.0% (Ag_5Sn), 27.0% (Ag_3Sn), 50.0% and 75.0%.

TABLE V Structural transformations in the Ag–In couple during ageing

Time after evaporation (d)	In concentration (wt%)			
	11.2	26.2	50.0	68.0
1	Ag	Ag	Ag	Ag
			In	In
	$LTAgIn_2$	$LTAgIn_2$	$LTAgIn_2$	$LTAgIn_2$
2	Ag	Ag	Ag	Ag
	$LTAgIn_2$	$LTAgIn_2$	In	In
		Ag_2In	$LTAgIn_2$	$LTAgIn_2$
3	Ag	Ag	Ag	
		$LTAgIn_2$	In	
		Ag_2In	$LTAgIn_2$	
4, 120	Ag	Ag	Ag	
	$LTAgIn_2$	$LTAgIn_2$	$LTAgIn_2$	$LTAgIn_2$
		Ag_2In	Ag_2In	
275	Ag	Ag	Ag	
			$LTAgIn_2$	$LTAgIn_2$
	Ag_2In	Ag_2In	Ag_2In	

Note: The specimen with 34.7% In was measured only after 275 d (Ag_2In was formed). The specimen with 80.0% In was measured only after 2 d ($LTAgIn_2$ was formed).

The specimens were analysed using XRD. It has been found that only the Ag_3Sn compound (ASTM 4–0798) is formed during the day of evaporation. The process of 6 mon transformation is presented in Table VI. Irrespective of the tin concentration, Ag_3Sn is already formed during the first day. The stable state (disappearance of silver or tin) is reached in the specimen with 75.0% Sn after 2 d and with 50.0% Sn after 15 d. In the case of specimens containing less tin, the stable state is reached after 6 mon.

On the basis of these data, the results obtained by Tu and Rosenberg [8] could be interpreted. Their specimens contained 500 nm Ag and 300 nm Sn, i.e. 27.0% Sn. From Table VI, it follows that the longest time necessary to complete the process (6 mon) is for the case of the specimen with 27.0% Sn. The fact that this was for the specimen 170 nm thick, i.e. five times less than theirs, means that the process of compound formation was even slower in the latter case. This explains why Tu and Rosenberg found that Ag_3Sn almost does not grow at room temperature [8].

2.1.5. Ag–Te

The first results concerning room-temperature compound formation in the Ag–Te couple (phase diagram [4]) were presented by Simić and Marinković [6]. This couple was studied in some detail using specimens 187–197 nm thick with four different tellurium concentrations: 35.0% ($\sim Ag_2Te$), 44.0% ($\sim Ag_3Te_2$), 54.0% ($\sim AgTe$) and 78.0%. Specimens were analysed using XRD. The process of compound formation and transformation is represented in Table VII. Although all the specimens were measured a number of times, the transformation process is presented until the moment only when the stable state has been reached.

The stable compounds which do not subsequently transform are already obtained in specimens containing 35.0% and 54.0% Te during the first day. In the specimen containing 78% Te, the process is completed

TABLE VI Structural transformations in the Ag–Sn couple during ageing

Time after evaporation (d)	Sn concentration (wt%)			
	15.0	27.0	50.0	75.0
1	Ag	Ag	Ag	Ag
	Sn	Sn	Sn	Sn
	Ag_3Sn	Ag_3Sn	Ag_3Sn	Ag_3Sn
2	Ag	Ag	Ag	
	Sn	Sn	Sn	Sn
	Ag_3Sn	Ag_3Sn	Ag_3Sn	Ag_3Sn
4	Ag	Ag	Ag	
	Sn	Sn	Sn	
	Ag_3Sn	Ag_3Sn	Ag_3Sn	
15	Ag	Ag		
	Sn	Sn	Sn	Sn
	Ag_3Sn	Ag_3Sn	Ag_3Sn	Ag_3Sn
34, 126	Ag	Ag		
	Sn	Sn	Sn	
	Ag_3Sn	Ag_3Sn	Ag_3Sn	
174	Ag	Ag		
	Ag_3Sn	Ag_3Sn		

TABLE VII Structural transformations in the Ag–Te couple during ageing

Time after evaporation (d)	Te concentration (wt%)			
	35.0	44.0	54.0	78.0
1	Ag	Ag_2Te		Te
	Ag_2Te	Ag_5Te_3	Ag_5Te_3	Ag_2Te
2		Ag_2Te		Te
		Ag_5Te_3		Ag_2Te
8	Ag			Te
	Ag_2Te	Ag_2Te		Ag_2Te
		Ag_5Te_3	Ag_5Te_3	Ag_5Te_3
17				Te
		Ag_2Te		Ag_2Te
		Ag_5Te_3		Ag_5Te_3
25	Ag	Ag_2Te		Te
	Ag_2Te	Ag_5Te_3	Ag_5Te_3	Ag_2Te
				Ag_5Te_3
37, 101		Ag_2Te		
		Ag_5Te_3		
168		Ag_5Te_3		

after 3 wks, and in that with 44.0% Te after 6 mon. The final result of the transformation in the specimens containing less than 40.0% Te is Ag_2Te (ASTM 12–695) with a possible excess of silver. In the specimens with more than 40.0% Te, Ag_5Te_3 (ASTM 16–372) finally remains with a possible excess of tellurium.

2.1.6. Ag–Zn

The first results concerning room-temperature compound formation in the Ag–Zn couple (phase diagram [4]) were presented by Simić and Marinković [5]. The couple was thoroughly studied using specimens 665–1265 nm thick with three different zinc concentrations: 37.9% (AgZn), 52.3% (Ag_5Zn_8) and 64.0% ($AgZn_3$).

The specimens were analysed using XRD (Table VIII). It was found that, irrespective of the zinc concentration, $AgZn_3$ (ASTM 25–1325) was always formed first, within 1 h after evaporation. The $AgZn_3$ formed transforms during the following 5–6 mon in the following way

$$AgZn_3 + 2\,Ag = 3\,AgZn \quad (4)$$

and

$$Ag + 2\,AgZn + 2\,AgZn_3 = Ag_5Zn_8 \quad (5)$$

As a result of the transformation, $AgZn_3$ disappeared in the sample with 37.9% Zn. This was transformed into AgZn and Ag_5Zn_8 (ASTM 29–956), with excess silver. In the specimen with 64.0% Zn, the $AgZn_3$ dominates, with both AgZn modifications present. The compounds are formed following the sequence: $AgZn_3$, AgZn (C) (cubic) (ASTM 29–1155), AgZn (H) (hexagonal) (ASTM 29–1156), Ag_5Zn_8.

2.1.7. Al–Au

During the sixties and seventies there was considerable activity on the identification of the compounds

TABLE VIII Structural transformations in the Ag–Zn couple during ageing

Time after evaporation	Zn concentration (wt%)		
	37.9	52.3	64.0
0.5 h	Zn	Zn	Zn
	Ag	Ag	Ag
	$AgZn_3$	$AgZn_3$	$AgZn_3$
3 h	Ag	Zn	Zn
	$AgZn_3$	Ag	Ag
	AgZn(C)	$AgZn_3$	$AgZn_3$
4 h	Ag	Ag	Zn
	$AgZn_3$	$AgZn_3$	Ag
	AgZn (C)	AgZn (C)	$AgZn_3$
2–4 d			Zn
	Ag	Ag	Ag
	$AgZn_3$	$AgZn_3$	$AgZn_3$
	AgZn (C)	AgZn (C)	AgZn (C)
21–22 d	Ag	Ag	Ag
	$AgZn_3$	$AgZn_3$	$AgZn_3$
	AgZn (C)	AgZn (C)	AgZn (C)
		AgZn (H)	
60 d	Ag	Ag	Ag
	$AgZn_3$	$AgZn_3$	$AgZn_3$
	AgZn (C)	AgZn (C)	AgZn (C)
		AgZn (H)	AgZn (H)
		Ag_5Zn_8	
105 d	Ag	Ag	
	$AgZn_3$	$AgZn_3$	$AgZn_3$
	AgZn (C)	AgZn (C)	AgZn (C)
	AgZn (H)	AgZn (H)	AgZn (H)
		Ag_5Zn_8	
120 d	Ag	Ag (trace)	
	$AgZn_3$	$AgZn_3$	$AgZn_3$
	AgZn (C)	AgZn (C)	AgZn (C)
	AgZn (H)	AgZn (H)	AgZn (H)
	Ag_5Zn_8	Ag_5Zn_8	
164–173 d	Ag	$AgZn_3$	$AgZn_3$
	AgZn (C)	AgZn (C)	AgZn (C)
	AgZn (H)	AgZn (H)	AgZn (H)
	Ag_5Zn_8	Ag_5Zn_8	

formed in the thin Al–Au couples, but at elevated temperatures (above 84 °C) [10].

There were some indications that the reaction also takes place at room temperature. Hunter *et al.* [11] performed measurements using a diffraction grating with golden surfaces, on which the Al + MgF_2 layers were evaporated. They observed that the efficiency of the grating was considerably weakened with time – after 15 mon it was 25 times less. Their hypothesis was that perhaps compounds were formed due to interdiffusion, which leads to a change of the film properties and also of the diffraction grating.

First results concerning room-temperature behaviour of the Al–Au couple (phase diagram [4, 12]) were presented by Marinković and Simić [13]. A detailed study of the couple was made using specimens 75–170 nm thick with five different gold concentrations: 41.7%, 78.0% ($AuAl_2$), 89.3%, 93.6% (Au_2Al) and 96.6% (Au_4Al). The specimens were analysed by XRD. Identification of the obtained powder diagrams was made by means of the ASTM 17–0877 ($AuAl_2$) and the authors' own standard prepared by fusing stoichiometric amounts of the elements in an evacuated quartz tube (Au_2Al). The XRD powder results of this standard are represented in Table IX.

TABLE IX X-ray powder diagram of the Au_2Al standard

d (nm)	I/I_0	d (nm)	I/I_0	d (nm)	I/I_0	d (nm)	I/I_0
0.4417	14	0.2706	6	0.2108	8	0.1335	13
0.3376	5	0.2515	9	0.2067	7	0.1308	23
0.3153	11	0.2332	36	0.1933	7	0.1249	22
0.3038	12	0.2267	40	0.1610	24	0.1163	11
0.2968	8	0.2222	100	0.1587	11	0.1114	8
0.2814	5	0.2181	49	0.1479	18	0.1098	7

TABLE X Structural transformations in the Al–Au couple during ageing

Time after evaporation	Au concentration (wt%)				
	41.7	78.0	89.3	93.6	96.6
3–5 d	Au	Au	Au	Au	Au
	Al	Al	Al	Al	Al
		Au_2Al		Au_2Al	Au_2Al
15–20 d	Au		Au	Au	Au
	Al	Al	Al	Al	Al
		Au_2Al	Au_2Al	Au_2Al	Au_2Al
50–60 d	Au	Al	Al		Au
	Al	Au_2Al	Au_2Al	Au_2Al	Au_2Al
3 y	Au	Au_2Al	Au_2Al		Au
	$AuAl_2$	$AuAl_2$	$AuAl_2$	Au_2Al	Au_2Al

The results obtained are presented in Table X. It can be seen that starting with a gold concentration of 78.0%, Au_2Al is formed within the first few days. The process is virtually completed within 2 mon by the disappearance of one or both metals. However, longer ageing leads to a transformation in the samples containing an excess of aluminium

$$Au_2Al + 3\,Al = 2\,AuAl_2 \quad (6)$$

In this manner, $AuAl_2$ is formed, either alone or together with Au_2Al. After 3 y the powder diagram of $AuAl_2$ is quite clear, and its reflection intensities relatively high.

2.1.8. Au–Cd

The first published data concerning room-temperature compound formation in the Au–Cd couple (phase diagram [4, 12]) were presented by Marinković and Simić [14]. The couple was thoroughly studied using specimens 130–217 nm thick with seven different cadmium concentrations: 15.0% ($\sim Au_3Cd$), 22.0% 30.0%, 36.0% ($\sim AuCd$), 51.0%, 64.0% ($\sim AuCd_3$) and 71.0%.

Analysis of the specimens was performed using XRD. The results are presented in Table XI.

It follows from Table XI that, irrespective of the cadmium concentration, $AuCd_3$ (own standard) is immediately formed, together with excess of gold or cadmium. If the specimen contains gold in addition to $AuCd_3$, the following reaction takes place

$$AuCd_3 + 2\,Au = 3\,AuCd \quad (7)$$

and AuCd (ASTM 5–0675) is formed. In the specimens containing 15.0–36.0% Cd, this compound remains stable during the first 1.5–3 mon. In the specimens containing 51.0–71.0% Cd, the $AuCd_3$ formed (alone or with cadmium) is stable to about 1.5–3.0 mon. After that a structural transformation takes place. In the XRD diagram of the phase produced, the position of the reflections depends on the cadmium concentration in the specimen. The phase (or phases) produced could not be identified.

Recently, the ASTM 31–0226 C (calculated) card for $AuCd_3$ has been published. The d values contained in it are identical to those in the author's own standard, prepared by fusing the stoichiometric mixture in an evacuated quartz tube. The only difference is that the ASTM card contains reflections up to 116.5° 2θ, and for their own standard up to 60°2θ.

2.1.9. Au–Ga

The first data concerning room temperature compound formation in the Au–Ga couple (phase diagram [4, 12]) were presented by Simic and Marinković [15]. A detailed study of the couple was performed by means of specimens 150–760 nm thick with seven different gallium concentrations, some of them being relatively close to the stoichiometric values of the expected compounds: 5.0%, 12.0% ($\sim Au_7Ga_2$), 17.0% ($\sim Au_2Ga$), 33.0%, 40.0% ($\sim AuGa_2$), 60.0% and 70.0%. Analysis of the specimens was effected by XRD.

The gold and gallium films react readily at room temperature, giving rise to four different compounds.

TABLE XI Structural transformations in the Au–Cd couple during ageing

Time after evaporation (d)	Cd concentration (wt%)						
	15.0	22.0	30.0	36.0	51.0	64.0	71.0
1–4	Au	Au	Au	Cd	Cd	Cd	Cd
	$AuCd_3$	$AuCd_3$	Cd	Au	Au	$AuCd_3$	$AuCd_3$
			$AuCd_3$	$AuCd_3$			
8	Au	Au	Au	Au		Cd	Cd
	AuCd	AuCd	AuCd	AuCd	$AuCd_3$	$AuCd_3$	$AuCd_3$
40–46	Au			Au			Cd
	AuCd			AuCd	$AuCd_3$	$AuCd_3$	$AuCd_3$
78–95	Au			Au			
	AuCd			AuCd	[a]	[a]	[a]

[a] Transformation.

TABLE XII Structural transformations in the Au–Ga couple during ageing

Time after evaporation (d)	Ga concentration (wt %)					
	5.0	12.0	17.0	33.0	40.0	60.0 70.0
1	Au $AuGa_2$ AuGa Au_2Ga Au_7Ga_2				Au $AuGa_2$ AuGa	$AuGa_2$
2		Au AuGa Au_2Ga		Au $AuGa_2$ AuGa Au_2Ga		
3			Au $AuGa_2$ Au_2Ga Au_7Ga_2			
7				Au AuGa Au_2Ga	$AuGa_2$ AuGa	$AuGa_2$
43–45	Au Au_2Ga Au_7Ga_2	Au Au_2Ga Au_7Ga_2	Au AuGa Au_2Ga Au_7Ga_2			
100				Au AuGa Au_2Ga	$AuGa_2$ AuGa	$AuGa_2$
360	Au Au_2Ga Au_7Ga_2	Au Au_2Ga Au_7Ga_2	AuGa Au_2Ga Au_7Ga_2	Au AuGa Au_2Ga	 $AuGa_2$ AuGa	Au_2Ga

The formation and transformations of the compounds during 1 y are presented in Table XII.

When the specimen contains 60.0% Ga or more, $AuGa_2$ (ASTM 3–0967) is formed and there are no further transformations. If the gallium concentration is lower, the specimen contains excess gold in addition to $AuGa_2$ and a reaction

$$AuGa_2 + Au = 2AuGa \quad (8)$$

takes place in which AuGa (ASTM 7–126) is formed, as well as another reaction

$$2AuGa_2 + 6Au = 4Au_2Ga \quad (9)$$

If the specimen contains less than 10% Ga, all four compounds are formed simultaneously, but transformations take place during ageing

$$AuGa + Au = Au_2Ga \quad (10)$$

and

$$2Au_2Ga + 3Au = Au_7Ga_2 \quad (11)$$

in which AuGa and Au_2Ga (ASTM 29–0619) concentrations are decreasing and the Au_7Ga_2 concentration is increasing.

Au_2Ga and Au_7Ga_2 have been identified on the basis of the literature data [16].

2.1.10. Au–In

The first data concerning room-temperature compound formation in the Au–In couple (phase diagram [4, 12]) were presented by Grebenik and Tonkopryad [17]. By evaporating gold (10 nm) and indium (70 nm) and analysing the specimens by electron diffraction, they found indium and $AuIn_2$ diffraction lines.

Somewhat later, Finstad *et al.* [18] found, in the specimens containing more than 70 at%. In using the Rutherford back-scattering method, that $AuIn_2$ was formed.

The Au–In couple was studied in some detail by Simić and Marinkovic [19] using specimens 85–400 nm thick with 14 different indium concentrations, from 3.4%–76.0%. The specimens were analysed using XRD. The results are presented in Table XIII. It can be seen that in the specimens with indium concentrations higher than 40.0%, $AuIn_2$ (ASTM 3–0939) is immediately formed, either alone or together with excess indium, depending on the indium concentration (53.0% In is the stoichiometric value for $AuIn_2$). This compound remains stable during the subsequent 9 mon.

In the specimens with indium concentrations in the 15.0%–36.0% range, $AuIn_2$ is also immediately formed, with excess gold. Gold reacts with the initially formed compound

$$AuIn_2 + Au = 2AuIn \quad (12)$$

whereby AuIn (own standard) is formed. This compound remains stable during the subsequent 9 mon in the specimens containing 23.0%–36.0% In. If there is more gold (specimens with 5.2%–20.0% In), the following reactions take place

$$3AuIn + 4Au = Au_7In_3 \quad (13)$$

TABLE XIII Structural transformations in the Au–In couple during ageing

Time after evaporation (d)	In concentration (wt %)					
	3.4, 3.6	5.2, 7.0	15.0, 20.0	23.0, 29.0, 36.0	45.0, 53.0	57.0, 70.0, 76.0
1	Au	Au AuIn Au_7In_3	Au $AuIn_2$	Au $AuIn_2$ AuIn	$AuIn_2$	In $AuIn_2$
4			Au AuIn			
7, 15				AuIn		
120	Au	Au Au_4In	Au Au_7In_3 Au_4In		$AuIn_2$	In $AuIn_2$
180	Au	Au Au_4In	Au Au_7In_3 Au_4In			
270				AuIn	$AuIn_2$	In $AuIn_2$

and

$$AuIn + 3Au = Au_4In \quad (14)$$

The Au_7In_3 compound (20.0% In) was identified on the basis of the literature data [20], and Au_4In (12.2% In) using the authors own standard prepared by fusing the stoichiometric mixture in an evacuated quartz tube.

Investigation of the Au–In couple was continued intensively [21–24]. It was found, among other results, that $AuIn_2$ can be formed at temperatures lower than ambient [22].

2.1.11. Au–Pb

The first data concerning room-temperature compound formation in the Au–Pb couple (phase diagram [4, 12]) were presented by Fujiki [7]. By analysing evaporated specimens containing different Au/Pb concentration ratios (from 80 : 20 to 15 : 85) using electron diffraction, Fujiki found that three compounds were formed: $AuPb_3$, $AuPb_2$ and Au_2Pb. The reflections in the XRD diagrams of these specimens were most often of low or medium intensity. Which compound will be formed depends on the constituent concentrations in the specimen. Similar results were published by Leder, one decade later [25].

Weaver and Brown [26] used a different approach. They followed the procedure used by Schopper [27], who studied change in reflectivity of the Au–Pb specimen golden surface during heating in a vacuum. Weaver and Brown studied the change of gold reflectivity in the Au–Pb specimen during its room-temperature ageing. The decrease in reflectivity stopped after approximately 1 h, when the XRD of the specimen was taken. The obtained compound was identified as $AuPb_2$.

Using the Au–Pb specimens 800 nm thick with 26.1 wt % Pb, Tu and Rosenberg [8] found that $AuPb_2$ was formed. However, the process was followed only for 2–3 wks.

Pariset and Galtier [28] found that $AuPb_2$ was formed in the thin film specimen at a temperature as low as $-150\,^{\circ}C$.

Marinković and Simić [13] made a detailed XRD study of the transformation process of the compounds formed during 2 mon. Specimens 37–300 nm thick containing different lead concentrations were used: 24.0%, 34.0% (Au_2Pb), 44.0%, 67.0% ($\sim AuPb_2$), 76.0% ($\sim AuPb_3$) and 85.0%. The transformation process is represented in Table XIV.

Depending on the lead concentration in the specimen, $AuPb_3$ (ASTM 11–573) and/or $AuPb_2$ (ASTM 8–419) were formed already during the first day. In the specimens containing 85.0% Pb, only $AuPb_3$ was formed and there was no further transformation during subsequent ageing. In the specimens containing 67.0% Pb, $AuPb_3$ transforms into $AuPb_2$, and in the specimens with less than 50.0% Pb, $AuPb_2$ is transformed to Au_2Pb [26]. The transformation can be expressed by

$$2AuPb_3 + Au = 3AuPb_2 \quad (15)$$

TABLE XIV Structural transformations in the Au–Pb couple during ageing

Time after evaporation (d)	Pb concentration (wt %)			
	24.0	34.0, 44.0	67.0	76.0, 85.0
1–3	Au $AuPb_2$	Au $AuPb_2$	Au $AuPb_2$ $AuPb_3$	Pb $AuPb_3$
8 10		Au $AuPb_2$	Au $AuPb_2$ $AuPb_3$	Pb $AuPb_3$
15 20	Au $AuPb_2$	Au $AuPb_2$		Pb $AuPb_3$
30–40	Au $AuPb_2$	Au $AuPb_2$ Au_2Pb	$AuPb_2$	Pb $AuPb_3$
50–60	Au $AuPb_2$ Au_2Pb	Au $AuPb_2$ Au_2Pb	$AuPb_2$	Pb $AuPb_3$

and

$$AuPb_2 + 3Au = 2Au_2Pb \quad (16).$$

From the data in Table XIV it can be inferred why certain authors did not identify all three compounds. Weaver and Brown [26] used specimens containing two different constituent concentrations, one with (unknown) excess lead and the other with 37.0% Pb. In both cases, the formation of Au_2Pb is possible. However, if the specimen contains 37.0% Pb, the compound is formed only after 1–1.5 mon, which is considerably longer than the time during which the authors followed their specimens, although they had supposed the possibility of Au_2Pb formation. A similar interpretation is possible for the results obtained by Tu and Rosenberg [8]. Studies of the Au–Pb system continued in the following decade [29].

2.1.12. Au–Sb

The first results concerning room-temperature compound formation in the Au–Sb couple (phase diagram [4, 12]) were presented by Simić and Marinković [30]. A detailed study of this couple was made using the samples 100–257 nm thick with eight different antimony concentrations.

Analysis of the samples was made using the XRD. Only $AuSb_2$ (ASTM 8–460) was found to be formed. The compound is formed in certain specimens only some 10 d after evaporation (Table XV)

In all the specimens, the compound appeared only after 1.5–2 mon and the process was completed within about 3 mon in the specimens containing less than 40% Sb. From the XRD powder diagrams it can be seen that the specimens with 43.0% and 56.0% Sb, i.e. near the stoichiometric $AuSb_2$ value, contain the highest compound concentrations.

TABLE XV Structural transformations in the Au–Sb couple during ageing

Time after evaporation (d)	Sb concentration (wt %)				
	8.7	17.7	25.7	30.0	43.0; 56.0, 75.0, 86.0
1–3	Au Sb	Au Sb	Au Sb	Au Sb	Au Sb
8–10		Au Sb	Au Sb $AuSb_2$		Au Sb $AuSb_2$
46–50	Au	Au $AuSb_2$	Au $AuSb_2$	Au Sb $AuSb_2$	Au Sb $AuSb_2$
81–85	Au	Au $AuSb_2$	Au $AuSb_2$	Au $AuSb_2$	Au Sb $AuSb_2$

2.1.13. Au–Sn

The first results concerning room-temperature compound formation in the Au–Sn couple (phase diagram [4, 12]) were presented by Tu and Rosenberg [8]. The tables presenting the compounds formed contain $AuSn_4$. The authors concluded that this compound was formed just because it contains the most tin. The analysis was made by XRD.

Buene *et al.*, using Rutherford, back-scattering [31], inferred that in the Au–Sn couple the compounds were formed during or immediately after evaporation. The authors supposed that in their specimens, depending on the Au/Sn ratio, AuSn, $AuSn_2$ and $AuSn_4$ were formed. They stated that only the formation of $AuSn_4$ was confirmed by X-ray and electron diffraction, i.e. by reliable identification methods.

The Au–Sn couple was the subject of a detailed study by Simić and Marinković [32] using specimens 215–480 nm thick with ten different concentrations (3.0–73.0 wt % Sn). Analysis of the specimens was made by XRD. The obtained results are presented in Table XVI.

Table XVI shows that already during the first day, four compounds are formed: $AuSn_4$ (own standard), $AuSn_2$ (literature data [33, 34]), AuSn (ASTM 8–463) and Au_5Sn (own standard). The constituent concentrations in the specimen determine the compound to be formed. During 1 y ageing, a number of transformations take place.

In the specimens with constituent concentration ratios close to the stoichiometric $AuSn_4$ value (70.76%

TABLE XVI Structural transformations in the Au–Sn couple during ageing

Time after evaporation (d)	Sn concentration (wt %)					
	3.0, 9.0, 13.0	24.0, 32.0	37.0	53.0	58.0	65.0, 73.0
1	Au Au_5Sn	Au AuSn	AuSn	$AuSn_2$	$AuSn_2$ $AuSn_4$	Sn $AuSn_2$ $AuSn_4$
30					$AuSn_2$	
150	Au Au_5Sn		AuSn			
180						Sn $AuSn_2$ $AuSn_4$
210	Au Au_5Sn					
300 and 360		Au Au_5Sn AuSn	AuSn	$AuSn_2$	$AuSn_2$ $AuSn_4$	Sn $AuSn_4$

Sn), $AuSn_2$ is transformed to $AuSn_4$, which remains stable

$$AuSn_2 + 2Sn = AuSn_4 \quad (17)$$

In the specimens having constituent concentrations close to the $AuSn_2$ stoichiometric value (54.62% Sn), the compound is stable and has no transformation. The same holds for the remaining two compounds, which remain stable in the specimens with the constituent concentrations close to the respective stoichiometric values: AuSn (37.57% Sn) and Au_5Sn (10.1% Sn). In the concentration range 20.0%–30.0% Sn the following transformation takes place

$$AuSn + 4Au = Au_5Sn \quad (18)$$

Later, the ASTM standards became available for the remaining three compounds: ASTM 28–0441 ($AuSn_4$), ASTM 31–0568 (Au_5Sn) and ASTM 28–0440 ($AuSn_2$). The first two ASTM cards correspond to the internal standards prepared by Simić and Marinković [32], and the third one corresponds to the standard published by Mirkin [34]. All three cards are of the "calculated" type and have more reflections than the mentioned internal standards.

The paper by Buene [35] contains data relative to the Au–Sn specimens studied in the range 20–400 °C. Thereby a paper by the same author [31] is considered to be a preliminary one. Analysis was performed by the X-ray and electron diffraction, as well as by the Rutherford back-scattering method. It has been found that, in unheated specimens, the $AuSn_4$, $AuSn_2$ and AuSn compounds appear. An unidentified additional phase has been found at elevated temperatures, considered to be the ξ phase (in fact, this is Au_5Sn).

Room-temperature compound formation and their transformations in the Au–Sn couple have since been extensively analysed. An essential contribution has been supplied by the Oslo group [36–41], and by Sharma *et al.* [42]. The ξ phase, Au_5Sn, was finally identified by the Oslo group [40].

2.1.14. Au–Te

The first results concerning compound formation in the Au–Te couple (phase diagram [4, 12]) were presented by Bernède *et al.* [43, 44]. The formation of the compound, the XRD powder diagram of which corresponds completely to $AuTe_2$, was found by the authors to take place 1 y after evaporation. Marinković and Simić did not find this compound [13].

2.1.15. Au–Zn

The first results concerning room-temperature compound formation in the Au–Zn couple (phase diagram [4, 12]) were presented by Marinković and Simić [14]. A detailed study of the couple was made using specimens 216–350 nm thick with eight different zinc concentrations: 10.0% ($\sim Au_3Zn$), 15.0%, 27.0% ($\sim$AuZn), 47.0% and 56.0% ($\sim AuZn_3$), 65.0%, 72.0% and 83.0%. Analysis of the specimens was performed by XRD. The results are presented in Table XVII.

During the first 2 d, $AuZn_3$ (ASTM 12–84) formed in all the specimens. In the specimens containing more than 50.0% Zn, this compound, with an excess of zinc, remained unchanged for 5 mon. In the samples with less than 50.0% Zn, a transformation takes place: $AuZn_3$ with an excess of gold is transformed to AuZn (own standard), the rate of the presented transformation depending on the zinc concentration. This compound with an excess of gold remains stable for 5 mon.

2.1.16. Bi–Pd

The first results concerning room-temperature compound formation in the Bi–Pd couple (phase diagram [4, 45]) were presented by Simić and Marinković [46]. A detailed study was made using specimens 150–550 nm thick with three different Palladium concentrations: 20.3% ($PdBi_2$), 33.8% (PdBi) and 62.9%. The specimens were analysed by XRD. The results are presented in Table XVIII.

TABLE XVII Structural transformations in the Au–Zn couple during ageing

Time after evaporation (d)	Zn concentration (wt %)				
	10.0	15.0	27.0	47.0	56.0, 65.0 72.0, 83.0
1–2	Au $AuZn_3$	Au $AuZn_3$	Au $AuZn_3$ AuZn	Au Zn $AuZn_3$	Zn $AuZn_3$
4	Au AuZn				
8–9		Au AuZn	Au $AuZn_3$ AuZn		
13–15	Au AuZn		Au AuZn		
40–50	Au AuZn	Au AuZn		$AuZn_3$ AuZn	Zn $AuZn_3$
78–82		Au AuZn		$AuZn_3$ AuZn	Zn $AuZn_3$
140–160	Au AuZn	Au AuZn	Au AuZn		

TABLE XVIII Structural transformations in the Bi–Pd couple during ageing

Time after evaporation	Pd concentration (wt%)		
	20.3	33.8	62.9
1 h	Bi Pd	Bi Pd	Bi Pd
2 d	Bi Pd $PdBi_2$		Bi Pd
5 d	Bi Pd $PdBi_2$	Bi Pd	Bi Pd
14 d	Bi Pd $PdBi_2$	Bi Pd $PdBi_2$	Bi Pd
61 d 52 mon	Pd $PdBi_2$	Pd $PdBi_2$	Bi Pd

It can seen that only $PdBi_2$ (ASTM 27–0436) has formed. The rate of formation depends on the constituent concentrations.

2.1.17. Cd–Cu

In the Cd–Cu couple (phase diagram [4]), the first results relative to room-temperature compound formation were in a paper by Simić and Marinković [47] and complemented by the same authors [48]. A detailed study of the couple was performed using specimens 120–220 nm thick containing five different copper concentrations: 10.0%, 15.0%, 25.0%, 50.0% (Cu_4Cd_3) and 75.0% (Cu_5Cd_8). Analysis of the specimens was performed using the XRD. The results are presented in Table XIX. It can be seen that in the specimens containing less copper, the Cu_4Cd_3 compound (ASTM 20–178) was formed already in the first days. After 15 d, this compound was formed in all the specimens and remained stable for 3 mon. In the specimens with the least copper, the $CuCd_3$ compound (ASTM 16–17) was observed, which remained stable within the time interval studied.

TABLE XIX Structural transformations in the Cd–Cu couple during ageing

Time after evaporation (d)	Cu concentraton (wt%)				
	10.0	15.0	25.0	50.0	75.0
2–3	Cd Cu_4Cd_3	Cd Cu_4Cd_3[a]	Cd Cu_4Cd_3[a]	Cd Cu	Cd Cu
5–8	Cd Cu_4Cd_3	Cd Cu_4Cd_3	Cd Cu_4Cd_3	Cd Cu	Cd Cu Cu_4Cd_3
15	Cd Cu_4Cd_3	Cd Cu_4Cd_3	Cd Cu_4Cd_3	Cd Cu Cu_4Cd_3[a]	Cd Cu Cu_4Cd_3
30	Cd Cu_4Cd_3 $CuCd_3$[a]	Cd Cu_4Cd_3	Cd Cu_4Cd_3	Cd[a] Cu Cu_4Cd_3[a]	Cd Cu Cu_4Cd_3
60	Cd Cu_4Cd_3 $CuCd_3$	Cd Cu_4Cd_3	Cd Cu_4Cd_3	Cu Cu_4Cd_3	Cu Cu_4Cd_3
90	Cd Cu_4Cd_3 $CuCd_3$		Cd Cu_4Cd_3		

[a] Trace.

2.1.18. Cd–Te

The first results concerning room-temperature compound formation in the Cd–Te couple (phase diagram [4]) were presented by Marinković and Simić [49]. A detailed study of the couple was made using specimens 170–200 nm thick with five different tellurium concentrations; 34.0%, 47.0%, 53.2% (CdTe), 58.0% and 69.8%. XRD was used to analyse the specimens. The results are presented in Table XX. The CdTe compound (ASTM 15–770) was formed in trace amounts only in the specimen containing 53.2% Te (stoichiometric value) after 1 wk. The concentration of the compound slowly increased with time. In the specimens in which CdTe had not been formed, some oxide compounds formed due to the action of the atmosphere on cadmium, appeared during ageing.

TABLE XX Structural transformation in the Cd–Te couple during ageing

Time after evaporation (d)	Te concentraton (wt%)				
	34.0	47.0	53.2	58.0	69.8
1	Cd Te	Cd Te	Cd Te	Cd Te	Cd Te
15	Cd Te	Cd Te	Cd Te CdTe	Cd Te	Cd Te
90	Cd Te	Cd Te	Cd Te CdTe	Cd Te	Cd Te [a]
240	Cd Te	Cd Te	Cd Te CdTe	Cd Te [a]	Cd Te [a]

[a] Product of atmospheric action on cadmium.

2.1.19. Cu–Ga

The first results on the room-temperature compound formation in the Cu–Ga couple (phase diagram [4]) were presented by Simić and Marinković [47]. A detailed study of the couple was made with specimens 180–190 nm thick with six different gallium concentrations from 15.0–68.0%. Irrespective of the gallium concentration, the CuGa compound (ASTM 3–1048) was already formed during the first day and there were no further changes with time (Table XXI).

TABLE XXI Structural transformation in the Cu–Ga couple during ageing

Time after evaporation (d)	Ga concentration (wt%)	
	15.0, 25.0, 42.0, 52.0	62.0, 68.0
1	Cu CuGa	Cu[a] CuGa
2, 30 120, 900	Cu CuGa	CuGa

[a] Trace.

2.1.20. Cu–In

The first results relative to room-temperature compound formation in the Cu–In couple (phase diagram [4]) were presented by Simić and Marinković [47]. A detailed study of the couple was made on specimens 176–200 nm thick, with six different indium concentrations from 15.0–85.0%. XRD was used to analyse the specimens. Irrespective of the indium concentration, a certain compound was already formed during the first day, together with an excess of copper (specimens with 15.0%–46.0% In) or indium (specimens with 70.0–85.0% In).

Identification of the compound formed could not be done on the basis of the available ASTM cards, because the XRD powder diagram obtained from the specimens was different from the data in the cards. The fact that Indium and copper disappeared in the specimen containing 70.0% In, so that only the formed compound remained, suggested that the compound had a formula corresponding to about 70.0% In. An additional fact is that the intensity of all reflections in the diagram of the 70.0% In specimen is higher than in the other specimens. Both these facts led the authors to the conclusion that the compound formed is CuIn (65.0 wt% In). The XRD powder results of the compound are presented in Table XXII. These results were later accepted as the ASTM 35–1150 standard for CuIn. Chen *et al.* [50] and Albin *et al.* [51] also identified CuIn in thin-film couples at room temperature. Structural transformations in the Cu–In couple are presented in Table XXIII.

TABLE XXII X-ray powder diagram of compound formed in the Cu–In thin film specimens

d (nm)	I/I_0	d (nm)	I/I_0	d (nm)	I/I_0	d (nm)	I/I_0
0.7250	6	0.1656	3	0.1485	5	0.1367	3
0.3312	12	0.1563	6	0.1481	3	0.1202	4
0.2596	100	0.1561	4	0.1411	3	0.1198	4
0.2347	18	0.1542	12	0.1409	2	0.1196	3
0.2099	56	0.1537	8	0.1370	7	0.1104	1
0.1661	3						

TABLE XXIII Structural transformation in the Cu–In couple during ageing

Time after evaporation (d)	In concentration (wt%)		
	15.0, 25.0, 32.0, 46.0	70.0	85.0
1	Cu	In	In
	CuIn	CuIn	CuIn
10, 106	Cu		In
	CuIn	CuIn	CuIn
900	Cu		
	CuIn	CuIn	CuIn

2.1.21. Cu–Sb

The first results concerning room-temperature compound formation in the Cu–Sb couple (phase diagram [4]) were presented by Simić and Marinković [47]. A detailed study of the couple was made with specimens 175–220 nm thick containing five different antimony concentrations: 22.9%, 34.9%, 44.2% ($\sim Cu_3Sb$), 52.0% ($\sim Cu_2Sb$) and 75.0%. XRD was used to analyse the specimens. The results are presented in Table XXIV.

It can be seen that only Cu_2Sb (ASTM 3-1024) has formed during the 8 mon period studied. The process of compound formation is very slow, its rate increasing with antimony concentration. Thus the first trace of Cu_2Sb is observed after more than 1 mon in the specimen with 75.0% Sb, but in the specimen containing the least Sb (22.9%) it is observed after 3 mon. After 10 mon, the intensity of the formed compound is higher, but the process of compound formation is not completed.

TABLE XXIV Structural transformations in the Cu Sb couple during ageing

Time after evaporation (d)	Sb concentration (wt%)			
	22.9	34.9, 44.2	52.0	75.0
1	Cu	Cu	Cu	Cu[a]
	Sb	Sb	Sb	Sb
34	Cu	Cu	Cu	Cu[a]
	Sb	Sb	Sb	Sb
				Cu_2Sb[a]
51	Cu	Cu	Cu	Cu[a]
	Sb	Sb	Sb	Sb
		Cu_2Sb[a]	Cu_2Sb	Cu_2Sb[a]
91	Cu	Cu	Cu	Cu[a]
	Sb	Sb	Sb	Sb
	Cu_2Sb[a]	Cu_2Sb	Cu_2Sb	Cu_2Sb
150, 250	Cu	Cu	Cu	Cu[a]
	Sb	Sb	Sb	Sb
	Cu_2Sb	Cu_2Sb	Cu_2Sb	Cu_2Sb

[a] Trace.

2.1.22. Cu–Sn

The first results relative to room-temperature compound formation in the Cu–Sn couple (phase diagram [4]) were presented by Tu [52]. The couple was studied using specimens 0.5–3 μm thick containing three different tin concentrations: ~ 37%, ~ 66% and ~ 81%. XRD was used to analyse the specimens.

In all the specimens studied, only Cu_6Sn_5 was observed. Three powder diagrams taken during 1 y ageing were presented for the specimen with ~37% Sn. It can be seen that the specimens aged for 1 and 15 d contain three phases, Cu + Sn + Cu_6Sn_5, while the third 1 y aged specimen contains only copper and Cu_6Sn_5. The statement that Cu_6Sn_5 has been obtained in the specimen containing about 37% Sn has been repeated in another paper by the same author [8].

The Cu–Sn couple was the subject of a detailed study presented by Simić and Marinković [47]. Specimens 183–189 nm thick with five different tin concentrations were used: 20.0%, 39.0% (Cu_3Sn), 50.0%, 61.0% (Cu_6Sn_5) and 85.0%. XRD was used to analyse the specimens.

The results of compound formation and transformations during ageing are presented in Table XXV. It can be seen that Cu_6Sn_5 (ASTM 2–0693) is immediately formed in all the specimens and that the reaction is completed within 3 wks, except for the specimen with 50.0% Sn. Comparison of the results for 39.0% Sn from this paper with those for 37.0% Sn from the previous paper [52] shows that they are similar to each other, the exception being that the reaction took more time in the previous work because the specimen was three times thicker.

2.1.23. Cu–Te

The first published results regarding room-temperature compound formation in the Cu–Te couple (phase

TABLE XXV Structural transformations in the Cu Sn couple during ageing

Time after evaporation (d)	Sn concentration (wt%)				
	20.0	39.0	50.0	61.0	85.0
1	Cu	Cu	Cu	Cu	
	Sn	Sn	Sn	Sn	Sn
		Cu_6Sn_5		Cu_6Sn_5	Cu_6Sn_5
2,	Cu	Cu	Cu	Cu	
3	Sn	Sn	Sn	Sn	Sn
	Cu_6Sn_5	Cu_6Sn_5	Cu_6Sn_5	Cu_6Sn_5	Cu_6Sn_5
5	Cu	Cu	Cu	Gu	
		Sn	Sn	Sn	Sn
	Cu_6Sn_5	Cu_6Sn_5	Cu_6Sn_5	Cu_6Sn_5	Cu_6Sn_5
20,	Cu	Cu	Cu		
49			Sn	Sn	Sn
	Cu_6Sn_5	Cu_6Sn_5	Cu_6Sn_5	Cu_6Sn_5	Cu_6Sn_5
101,	Cu	Cu	Cu	Sn	Sn
930	Cu_6Sn_5	Cu_6Sn_5	Cu_6Sn_5	Cu_6Sn_5	Cu_6Sn_5

TABLE XXVI Structural transformations in the Cu–Te couple during ageing

Time after evaporation (d)	Te concentration (wt%)				
	20.0	50.1	60.1	66.7	85.0
1			Te	Te	Te
	Cu_3Te	Cu_7Te_5	Cu_7Te_5	Cu_7Te_5	X[a]
2			Te	Te	Te
	Cu_3Te	Cu_7Te_5	Cu_7Te_5	Cu_7Te_5	X[a]
		CuTe		CuTe	
3				Te	Te
	Cu_3Te	Cu_7Te_5	Cu_7Te_5	Cu_7Te_5	X[a]
		CuTe	CuTe	CuTe	
4				Te	Te
	Cu_3Te	Cu_7Te_5	Cu_7Te_5	Cu_7Te_5	X[a]
		CuTe	CuTe	CuTe	CuTe
13,				Te	Te
43	Cu_3Te	Cu_7Te_5	Cu_7Te_5	Cu_7Te_5	X[a]
			CuTe	CuTe	CuTe
83				Te	Te
	Cu_3Te	Cu_7Te_5	Cu_7Te_5	Cu_7Te_5	
			CuTe	CuTe	CuTe
900		Cu_7Te_5	Cu_7Te_5	Cu_7Te_5	
			CuTe	CuTe	CuTe

[a]X: Unidentified phase.

diagram [4]) were reported by Simić and Marinković [47]. A detailed study of the couple was made with specimens 182–195 nm thick with five different tellurium concentrations: 20.0% ($CuTe_x$), 50.1% (Cu_2Te), 60.1% (Cu_4Te_3), 66.67% (CuTe) and 85.0%.

The formation of compounds depends on the constituent concentrations in the specimens. Table XXVI presents structural transformations during ageing. Thus, Cu_3Te (ASTM 18–456) (previously designated $CuTe_x$ [53]) is immediately formed in the specimen containing 20.0% Te and no further transformations occur during 3 mon ageing.

The Cu_7Te_5 compound (ASTM 19–409) (previously designated $Cu_{1.44}Te$ [53]) is formed in the specimens containing 50.1%, 60.1% and 66.67% Te. The CuTe compound (ASTM 13–258) is formed by transformation during ageing. Domination of this compound increases with increasing tellurium concentration in the specimen.

In the specimen containing 85.0% Te, some unidentified phase, X (which perhaps contains more tellurium than would correspond to the CuTe formula), is formed in the beginning, and then CuTe.

2.1.24. Cu–Zn

The first results concerning room-temperature compound formation in the Cu–Zn couple (phase diagram [4]) were reported by Simić and Marinković [47]. A detailed study of this couple was performed using specimens 185–187 nm thick, containing four different zinc concentrations: 26.0%, 49.0%, 62.0% (Cu_5Zn_8) and 83.0% ($CuZn_4$). Analysis of the specimens was made by XRD. Identification of the obtained powder diagrams was made using the authors own standard prepared by fusing a mixture of the stoichiometric amounts of the elements corresponding to the $CuZn_4$ formula (i.e. 83.0% Zn) in an evacuated quartz tube.

Only one compound, $CuZn_4$, was present in all the specimens (Table XXVII). Its concentration increased at the beginning, then showed saturation and finally began to decrease and even disappeared. It disappeared first in the specimen with the lowest zinc concentration (26.0%), then in the specimen with 49.0% Zn. In the specimen with 62.0% Zn, only trace of $CuZn_4$ remained after 8 mon. In the specimen containing the highest zinc concentration (83.0%), $CuZn_4$ remained stable during the investigated period. The data from the XRD diagram obtained with the standard are presented in Table XXVIII.

At the time of publication of the mentioned paper [47], the authors thought that the phenomenon in question was a reorientation of the microcrystals in the film. Only quite recently they found that it is a new phenomenon which appears in a number of couples during their ageing [54].

TABLE XXVII Structural transformations in the Cu–Zn couple during ageing

Time after evaporation (d)	Zn concentration (wt%)			
	26.0	49.0	62.0	83.0
1	Zn	Zn	Zn	Zn
	Cu	Cu	Cu	
		$CuZn_4$		$CuZn_4$
4–5	Zn	Zn	Zn	Zn
	Cu	Cu	Cu	
	$CuZn_4$	$CuZn_4$	$CuZn_4$	$CuZn_4$
10–15	Cu	Cu	Cu	Zn
	$CuZn_4$	$CuZn_4$	$CuZn_4$	$CuZn_4$
40	Cu	Cu	Cu	
	$CuZn_4$	$CuZn_4$	$CuZn_4$	$CuZn_4$
105	Cu	Cu	Cu	
		$CuZn_4$	$CuZn_4$	$CuZn_4$
130	Cu	Cu	Cu	
			$CuZn_4$	$CuZn_4$
240	Cu	Cu	Cu	
			$CuZn_4$[a]	$CuZn_4$

[a] Trace.

TABLE XXVIII X-ray powder diagram of the Cu–83% Zn standard

d (nm)	I/I_0	d (nm)	I/I_0
0.2380	30	0.1226	20
0.2150	70	0.1192	4
0.2076	100	0.1158	15
0.1592	16	0.1148	10
0.1374	14	0.1074	14

The results from Table XXVII were later accepted as the ASTM 35–1151 and 35–1152 standard (bulk and thin film, respectively) as $CuZn_5$. This formula was adopted because the specimens in question contain 83.0% Zn. Both formulae can be accepted temporarily, until further investigations show which one is more adequate.

2.1.25. Ga–Mg

In the Ga-Mg couple (phase diagram [4,53]) the first results relative to room-temperature compound formation were presented by Marinković and Simić [55]. The couple was studied in some detail using specimens 175–188 nm thick with four different magnesium concentrations: 15.0% ($MgGa_2$), 26.5% (MgGa), 41.0% (Mg_2Ga) and 55.0% (Mg_5Ga_2). XRD was used to analyse the specimens. It was found that, depending on magnesium concentration, one or two compounds were formed: Mg_2Ga (ASTM 23–260) and Mg_2Ga_5 (ASTM 25–277) (Table XXIX).

In the specimens containing 15%–41% Mg, the compound Mg_2Ga was formed already during the first day, while in the specimen with 55% Mg, this happened after 2 wks. In the former specimens, the compound reacted with an excess of gallium to produce another compound

$$Mg_2Ga + 4Ga = Mg_2Ga_5 \qquad (19)$$

while in the latter specimens this reaction did not take place. Both these compounds are unstable: the first disappeared within 2 wks and the second within 3 mon.

2.1.26. Ga–Ni

In the Ga–Ni couple (phase diagram [4]), the first results concerning room-temperature compound formation were presented by Marinković and Simić [56]. A detailed study of the couple was made with specimens 147–176 nm thick with seven different nickel concentrations: 10.0%, 17.0% ($NiGa_4$), 36.0% (Ni_2Ga_3), 44.7% (NiGa), 55.7% (Ni_3Ga_2), 63.0% (Ni_2Ga) and 70.0% ($\sim Ni_3Ga$). The specimens were analysed by the XRD. Identification of the XRD diagrams obtained could not be performed by means of the available ASTM standards which differed from the diagrams obtained. The results were as follows. In the specimens with 10.0% and 17.0% Ni one compound was formed together with excess gallium, and in those containing 36.0%–55.7% Ni the same compound was formed with excess nickel. Only nickel and gallium were identified in the specimens with 63.0% and 70.0% Ni. Because identification of the compound could not be done, the specimens were annealed in vacuum at 40–100 °C. Ni_2Ga and Ni_2Ga_3 were formed in the annealed specimens with 36.0%–70.0% Ni. In the specimens containing 10.0% and 17.0% Ni (i.e. with highest gallium content) no change was produced by annealing at 100 °C, i.e. the formed compound remained. This led the authors to conclude that the compound formed was $NiGa_4$. By annealing with excess nickel, the Ni_2Ga_3 compound is produced

$$3\,NiGa_4 + 5\,Ni = 4\,Ni_2Ga_3 \qquad (20)$$

which is obtained experimentally.

According to Hansen and Anderko [53], $NiGa_4$ has a cubic structure, $a = 0.842$ nm. The measurements made by the authors show that the compound formed has a lattice constant $a = 0.85$ nm, with hkl values presented in Table XXX.

The XRD results from Table XXX were later accepted as the ASTM 36-1146 standard for $NiGa_4$ and then deleted, probably because a new ASTM 37-1095 card for $NiGa_4$ appeared. However, the two structures differ considerably and should not be concurrent. Further studies will show to which structure the $NiGa_4$ formula corresponds. A possibility exists that one of

TABLE XXIX Structural transformations in the Ga–Mg couple during ageing

Time after evaporation (d)	Mg concentration (wt%)			
	15.0	26.5	41.0	55.0
1–2	Mg_2Ga_5	Mg	Mg	Mg
	Mg_2Ga	Mg_2Ga	Mg_2Ga	
7		Mg	Mg	
		Mg_2Ga_5	Mg_2Ga	
14–16		All disappeared	Mg	Mg
			Mg_2Ga	Mg_2Ga
			Mg_2Ga_5	
33				Mg
				Mg_2Ga
81				Mg
				Mg_2Ga[a]
106				All disappeared

[a] Trace.

TABLE XXX X-ray diagram of thin film $NiGa_4$ specimen

d (nm)	h k l	I/I_0
0.2675	3 1 0	70
0.2436	2 2 2	45
0.2260	3 2 1	55
0.1989	3 3 0, 4 1 1	100

TABLE XXXI Structural transformations in the Ga–Ni couple during ageing

Time after evaporation (d)	Ni concentration (wt%)				
	10.0, 17.0	36.0	44.7	55.7	63.0, 70.0
1–3	Ga	Ni	Ni	Ni	Ni
	$NiGa_4$		$NiGa_4$	$NiGa_4$[a]	Ga
21	Ga		Ni	Ni	Ni
	$NiGa_4$		Ga		Ga
			$NiGa_4$	$NiGa_4$	
30, 90, 150	Ga	Ni	Ni	Ni	Ni
	$NiGa_4$	$NiGa_4$	$NiGa_4$	$NiGa_4$	Ga

Note: Although gallium is amorphous in thin films (< 10 μm), it has been formed here in a polycrystalline state.
[a] Trace.

them corresponds to the low-temperature phase (ASTM 36-1146) and the other to the high- or medium-temperature one (ASTM 37-1095).

Table XXXI shows the formation and tranformation of the compound over 5 mon.

2.1.27. Ga–Pd

The first results relative to room-temperature compound formation in the Ga–Pd couple (phase diagram [4, 45]) were presented by Simić and Marinković [46]. The couple was studied using specimens 200–450 nm thick with three different palladium concentrations: 40.0% and 45.0% ($\sim Pd_3Ga_7$) and 74.0% ($\sim Pd_2Ga$). The specimens were analysed by XRD. The results are presented in Table XXXII. It can be seen that only one compound, $PdGa_5$ (ASTM 15-0577), was formed. There was no transformation during the period in which the process was followed.

TABLE XXXII Structural transformations in the Ga–Pd couple during ageing

Time after evaporation	Pd concentration (wt%)		
	40.0	45.0	74.0
1 d	Pd	Pd	Pd
	$PdGa_5$	$PdGa_5$	$PdGa_5$
35 d	Pd		Pd
	$PdGa_5$	$PdGa_5$	$PdGa_5$
50 mon[a]	Pd		Pd
	$PdGa_5$	$PdGa_5$	$PdGa_5$

[a] Reaction continued–the concentration of $PdGa_5$ increased with time.

TABLE XXXIII Structural transformations in the Ga–Sb couple during ageing

Time after evaporation	Sb concentration (wt%)		
	53.0	63.0	73.0
7 d	Sb	Sb	Sb
		GaSb	
2, 6 mon, 2 y	Sb	Sb	Sb
		GaSb	
9.25, 10.75 y	Sb	Sb	Sb
		GaSb	

TABLE XXXIV Change in X-ray intensity ratio $I_{GaSb(1\,1\,1)}/I_{Sb(0\,0\,3)}$ during ageing

Ageing time (mon)	$I_{GaSb(1\,1\,1)}/I_{Sb(0\,0\,3)}$	Ageing time (y)	$I_{GaSb(1\,1\,1)}/I_{Sb(0\,0\,3)}$
0.3	0.16	1	2.50
2	1.6	2	2.57
3	1.85	9.25	2.93
4	2.00	10.75	2.92
6	2.40		

2.1.28. Ga–Sb

The first results concerning the room-temperature compound formation in the Ga–Sb system (phase diagram [4, 57]) were presented by Marinković and Simić [55]. A detailed study of the system was performed on specimens 160–187 nm thick, with three different antimony concentrations: 53.0%, 63.0% (GaSb) and 73.0%. The specimens were analysed using XRD, and the results are presented in Table XXXIII.

It can be seen that GaSb (ASTM 7–215) has formed only in the specimen containing 63.0% Sb, which shows that its range of existence is narrow. In fact, a barely seen trace of the main GaSb reflection is also present in the other two specimens, but its intensity does not increase with time.

The GaSb formation is extremely slow. This can be seen from Table XXXIV, into which the results of the new measurements have been also inserted. Table XXXIV shows that the reaction is completed and the process of compound formation is finished after less than 9 y (probably after 7–8 y). Thus, it is the slowest room-temperature reaction of all the thin film couples analysed.

2.1.29. In–Ni

The first results concerning the room-temperature compound formation in the In–Ni couple (phase diagram [4, 58]) were presented by Marinković and Simić [56]. A detailed study of the couple was made using specimens 180–184 nm thick with four different nickel concentrations: 18.0% (Ni_3In_7), 25.3% (Ni_2In_3), 32.8% (NiIn) and 60.6% (Ni_3In). The specimens were analysed using XRD and the results are presented in Table XXXV. The table shows that $LTNi_2In_3$ is formed in the

TABLE XXXV Structural transformations in the In–Ni couple during ageing. LT = low-temperature phase

Time after evaporation (d)	Ni concentration (wt%)			
	18.0	25.3	32.8	60.6
1	Ni In	Ni In	Ni In	
2				Ni In $LTNi_2In_3$[a]
3				Ni In $LTNi_2In_3$
21			Ni	Ni
	In $LTNi_2In_3$	In $LTNi_2In_3$	In $LTNi_2In_3$	In[a] $LTNi_2In_3$
53			Ni	
	In $LTNi_2In_3$	In $LTNi_2In_3$	In $LTNi_2In_3$	
90	In $LTNi_2In_3$ $Ni_{10}In_{27}$[a]	In[a] $LTNi_2In_3$	Ni In $LTNi_2In_3$	Ni $LTNi_2In_3$
135	In $LTNi_2In_3$ $Ni_{10}In_{27}$	In[a] $LTNi_2In_3$		
360			Ni[a]	
	In[a] $LTNi_2In_3$ $Ni_{10}In_{27}$	In[a] $LTNi_2In_3$	In[a] $LTNi_2In_3$	

[a] Trace.

TABLE XXXVI X-ray powder diagram of $LTNi_2In_3$ thin film standard

d (nm)	I/I_0	d (nm)	I/I_0	d (nm)	I/I_0	d (nm)	I/I_0
0.2797	40	0.2368	14	0.1556	16	0.1427	8
0.2675	100	0.2310	34	0.1535	12	0.1379	8
0.2529	86	0.2207	30	0.1513	16	0.1355	12
0.2495	40	0.2085	32	0.1488	8	0.1321	8
0.2462	50	0.2045	60	0.1465	8		

specimen containing the highest nickel concentration already within a few days after evaporation. Within 3 wks, it is also formed in the other specimens. In the specimens containing 25%–60% Ni the process is virtually completed within 1 y, without any further transformations. The compound reflections are most intensive in the powder diagram of the specimen with 25.3% Ni (74.7% In). It was supposed, therefore, that the compound in question is $LTNi_2In_3$. The XRD powder results of our own thin-film standard for this compound are presented in Table XXXVI. These results were later accepted as the ASTM 36-1147 standard.

In the specimen containing 18.0% Ni, a structural transformation takes place after 3 mon. The reflections due to the originally formed compound become weaker and a new compound, $Ni_{10}In_{27}$ (ASTM 7-299), appears in the XRD diagram according to the reaction

$$5LTNi_2In_3 + 12In = Ni_{10}In_{27} \qquad (21)$$

2.1.30. In–Pd

The first results relative to the room-temperature compound formation in the In–Pd couple (phase diagram [4, 45]) were presented by Simić and Marinković [46]. The couple was studied using specimens 125–300 nm thick with three different palladium concentrations: 35.0% ($\sim Pd_2In_3$), 48.2% (PdIn) and 73.6% (Pd_3In). XRD was used to analyse the specimens.

Only $PdIn_3$ (ASTM 21-407) was formed in the investigated specimens (Table XXXVII). Its concentration gradually increases with time.

TABLE XXXVII Structural transformations in the In–Pd couple during ageing

Time after evaporation	Pd concentration (wt%)		
	35.0	48.2	73.6
2 d		Pd In $PdIn_3$[a]	Pd In
7 d		Pd In $PdIn_3$	Pd In[a] $PdIn_3$
56 d		Pd $PdIn_3$	Pd In[a] $PdIn_3$
51 mon	Pd In $PdIn_3$	Pd $PdIn_3$	Pd $PdIn_3$

[a] Trace.

2.1.31. Ni–Sn

In the Ni–Sn couple (phase diagram [4, 59]), the first results concerning the room temperature compound formation were presented by Tu and Rosenberg [8]. The table presenting the intermetallic compounds formed at room temperature contains Ni_3Sn_4. XRD was used to analyse the specimens.

A detailed study of the Ni–Sn couple was performed by Marinković and Simić [56] using specimens 171–183 nm thick with four different tin concentrations: 40.2% (Ni_3Sn), 57.5% (Ni_3Sn_2), 66.9% (NiSn) and 72.9% (Ni_3Sn_4).

The results are presented in Table XXXVIII. It can be seen that only NiSn (ASTM 26-1289) has been formed, irrespective of the tin concentration.

It is interesting why there is a difference in the results of the two studies performed by the same techniques. Tu and Rosenberg [8] have used a specimen four times thicker and therefore the process presumably occurred more slowly. The authors followed the reaction for only 2–3 weeks. According to the ASTM card for NiSn (published later), NiSn and Ni_3Sn_4 have some common reflections. The reason for the confusion might be that the key reflections were not yet present in their specimen. Their specimen (which contained 32.7 wt% Sn), because of its thickness, during the course of a long observation would produce a greater number of better-defined reflections in the XRD diagram, which would solve the dilemma.

TABLE XXXVIII Structural transformations in the Ni–Sn couple during ageing

Time after evaporation	Sn concentration (wt%)	
	40.2	57.5, 66.9, 72.9
10–13 d	Ni	Ni
	Sn	Sn
	NiSn	NiSn
2.5, 4 mon	Ni	Ni
		Sn
	NiSn	NiSn

2.1.32. Ni–Te

The first results relative to the room-temperature compound formation in the Ni–Te couple (phase diagram [4, 45]) were given by Marinković and Simić [49]. A detailed study of the couple was made using specimens 180–185 nm thick with two different tellurium concentrations: 68.5% (NiTe) and 81.3% ($NiTe_2$). The specimens were analysed by XRD. The results are presented in Table XXXIX. The $NiTe_2$ compound (ASTM 8-4) appears after about 10 d in the specimen containing 81.3% Te. At the same time, only a trace of this compound is observed in the specimen with 68.5% Te, while its formation is completed after 35 d. The situation remains unchanged during 7 mon.

TABLE XXXIX Structural transformations in the Ni–Te couple during ageing

Time after evaporation	Te concentration (wt%)	
	68.5	81.3
9–10 d	Ni	Ni
	Te	Te
	$NiTe_2$[a]	$NiTe_2$
35 d,	Ni	Ni
3, 7 mon	Te	Te
	$NiTe_2$	$NiTe_2$

[a] Trace.

2.1.33. Pb–Pd

The first results concerning the room-temperature compound formation in the Pb–Pd couple (phase diagram [4, 53]) were reported by Tu and Rosenberg [8]. It is shown in the table presenting the authors' results that $PdPb_2$ is formed, with a note that the compound is formed because it contains the highest lead concentration. The specimens were studied using XRD over 2–3 wks. A detailed analysis of the couple was made by Simić and Marinković [46] using specimens 195–520 nm thick with four different palladium concentrations: 20.5% ($PdPb_2$), 39.9% ($\sim PdPb$), 44.0% (Pd_3Pb_2) and 53.4% ($\sim Pd_3Pb$). The results are presented in Table XL. It can be seen that only $PdPb_2$ (ASTM 8-365) is formed and without any further transformations during ageing. Depending on the constituent concentrations, in addition to the compound, lead and/or palladium are present too.

TABLE XL Structural transformations in the Pb–Pd couple during ageing

Time after evaporation	Pd concentration (wt%)			
	20.5	39.9	44.0	53.4
1 h	Pd	Pd	Pd	Pd
	Pb	Pb	Pb	Pb
	$PdPb_2$		$PdPb_2$	$PdPb_2$
2.5–5 h		Pd		Pd
		Pb		$PdPb_2$
		$PdPb_2$		
4 d			Pd	
			$PdPb_2$	
26 d	Pd	Pd	Pd	Pd
	Pb	Pb		
	$PdPb_2$	$PdPb_2$	$PdPb_2$	$PdPb_2$
43 d,		Pd	Pd	Pd
80 d	Pb	Pb		
	$PdPb_2$	$PdPb_2$	$PdPb_2$	$PdPb_2$
52 mon	Pb	Pb	Pd	Pd
	$PbCO_3$	$PbCO_3$	$PbCO_3$	$PbCO_3$
	Pb (X)[a]	Pb (X)	Pb (X)	Pb (X)

[a] Unidentified compound.

2.1.34. Pb–Pt

The first results relative to the room-temperature compound formation in the Pb–Pt couple (phase diagram [4, 53]) were also presented in the paper by Tu and Rosenberg [8]. It is mentioned in the table presenting their results that $PtPb_4$ is formed. Specimens

TABLE XLI Structural transformations in the Pb–Te couple during ageing. X = unidentified phase

Time after evaporation (d)	Te concentration (wt%) / specimen thickness (nm)						
	0 / 120	15 / 100	34 / 129	38 / 200	46 / 120	59.9 / 180	100 / 120
1	Pb	Pb Te	Pb Te PbTe	Pb Te PbTe	Pb Te PbTe	Pb Te	Te
8		Pb Te PbTe	Pb Te PbTe	Pb Te PbTe	Pb Te PbTe X	Pb Te PbTe X	
15		Pb Te PbTe	Pb Te PbTe X	Pb Te PbTe	Pb Te PbTe X	Pb Te PbTe X	
30		Pb Te PbTe X	Pb PbTe X				
60		Pb PbTe X		Pb Te PbTe		Te PbTe X	
120					Pb Te PbTe		
730			PbTe	Pb Te PbTe X	Te PbTe	Te PbTe X	Te
	$PbCO_3$		$PbCO_3$		$PbCO_3$	$PbCO_3$	

containing 500 nm Pt and 300 nm Pb were used and the compound formation was followed over 2–3 wks.

2.1.35. Pb–Te

The first results concerning the room-temperature compound formation in the Pb–Te couple (phase diagram [4, 53]) were given by Marinković and Simić [49]. A detailed study of the couple was made using specimens 100–200 nm thick with five different tellurium concentrations: 15%, 34%, 38% (PbTe), 46% and 59.9%. The specimens were analysed using XRD.

Table XLI contains the results. It can be seen that the evaporated tellurium layer is not changed, even after 2 y. The evaporated lead layer is progressively transformed to $PbCO_3$, so that after 2 y the specimen contains only this compound. In all the Pb–Te specimens, the PbTe compound (ASTM 8–28) is formed after 1 wk. An unidentified phase, denoted X in the table, is formed immediately afterwards. This phase appears first in the specimens containing higher tellurium concentration. The intensity of the phase X reflection increases as the lead reflection intensities decrease. Phase X is not formed by the action of the atmospheric gases on lead or tellurium. It is probably a complex compound formed by a simultaneous action of the atmospheric gases on lead and tellurium. The sequence of the transformations caused by the atmospheric gases is as follows. Lead is transformed first to $PbCO_3$. Then phase X is progressively transformed to $PbCO_3$. It can be supposed that, given sufficient time, the specimens will contain only $PbCO_3$ + Te. A similar transformation takes place in the thin-film Au–Pb specimens, in which $AuPb_2$ is formed first. After 3.5 y the specimens contain only $PbCO_3$ + Au [49].

2.1.36. Pd–Sb

A detailed study of the couple was made using specimens 317 nm thick, with two different antimony concentrations: 40.0% Sb (γ phase) and 54.0% Sb (PdSb) [46]. The specimens were analysed using XRD. During the first month, no compound was observed. The completely finished reaction with the PdSb compound formed (ASTM 26–0888) was observed after a long ageing time.

2.1.37. Pd–Sn

The first results pertaining to the room-temperature compound formation in the Pd–Sn couple (phase diagram [4, 45]) were due to Tu and Rosenberg [8]. The table containing the authors' results contains $PdSn_4$, with a statement that the compound is formed because it contains the highest tin concentration. The specimens containing 500 nm Pd and 300 nm Sn were followed by XRD for 2–3 wks.

A detailed study of the couple was made in the paper by Simić and Marinković [46], using specimens 170–800 nm thick with four different concentrations:

TABLE XLII Structural transformations in the Pd–Sn couple during ageing

Time after evaporation (d)	Sn concentration (wt %)			
	27.0	42.0	76.0	81.7
1	Pd Sn	Pd Sn	Pd Sn $PbSn_4$[a]	Pd Sn $PdSn_4$[a]
3	Pd Sn $PdSn_4$[a]			
6	Pd Sn $PdSn_4$	Pd Sn $PdSn_4$	Pd Sn $PdSn_4$	Pd Sn $PdSn_4$
13	Pd Sn $PdSn_4$	Pd Sn $PdSn_4$	Pd Sn $PdSn_4$ $PdSn_3$[a]	Pd Sn $PdSn_4$
48, 71	Pd Sn $PdSn_4$	Pd Sn $PdSn_4$	Pd Sn $PdSn_4$ $PdSn_3$	Pd Sn $PdSn_4$
83	Pd Sn $PdSn_4$	Pd Sn $PdSn_4$	Pd Sn $PdSn_4$ $PdSn_3$	Pd Sn $PdSn_4$ $PdSn_3$[a]
99			Pd Sn $PdSn_4$ $PdSn_3$	Pd Sn $PdSn_4$ $PdSn_3$
52 mon		Pd Sn $PdSn_4$ $PdSn_3$	Pd Sn $PdSn_4$ $PdSn_3$	Pd Sn $PdSn_4$ $PdSn_3$

[a] Trace.

27.0% (Pd_3Sn), 42.0% (Pd_3Sn_2), 76.0% ($PdSn_3$) and 81.7% ($PdSn_4$). The specimens were analysed by XRD.

The results are presented in Table XLII which shows the following. In the specimens containing more than 50.0% Sn, traces of $PdSn_4$ (ASTM 36–137) are observed already during the first day.

Compound formation takes place several days later in the specimens containing less than 50.0% Sn. After 1 wk, all the specimens contain $PdSn_4$. In the specimens with less than 50.0% Sn the situation remains virtually unchanged for three months, only the $PdSn_4$ concentration is somewhat higher. In the specimen with 76.0% Sn, a trace of $PdSn_3$ (ASTM 15–575) is observed after 2 wks, and after 1.5 mon all the compound reflections are present. Its concentration increases over the following 2 mon. In this specimen, the constituents are in the stoichiometric ratio of $PdSn_3$. It can be seen from the XRD diagrams that the tin reflection intensities continually decrease and after 3 mon the intensity of the $PdSn_4$ decreases too. The $PdSn_3$ compound was formed from $PdSn_4$ according to the reaction.

$$3PdSn_4 + Pd = 4\,PdSn_3 \qquad (22)$$

In the specimen containing 81.7% Sn, the same process takes place, but considerably more slowly. The reason is that in this compound the constituents are in the stoichiometric ratio corresponding to $PdSn_4$. Over 4 y the reaction has continued without essential changes.

Tu and Rosenberg [8] did not observe the transformation of $PdSn_4$ to $PdSn_3$ because they followed the process for too short a time and they had a considerably thicker specimen (i.e. a slower process).

TABLE XLIII Structural transformations in the Pd–Te couple during ageing

Time after evaporation (d)	Te concentration (wt %)		
	38.1	55.0	70.5
1 d	Pd Te		Pd Te
2 d		Pd Te $PdTe_2$	
5 d			Pd Te $PdTe_2$
12, 30, 51, 67 d	Pd Te $PdTe_2$	Pd Te $PdTe_2$	Pd Te $PdTe_2$
51 mon	Pd $PdTe_2$	Pd Te $PdTe_2$	Pd Te $PdTe_2$

TABLE XLIV Compounds formed at room temperature in thin-film metal couples evaporated in vacuum

No	Metal couple	Compounds formed			
1	Ag–Cd	AgCd	Ag_5Cd_8	$AgCd_3$	
2	Ag–Ga	Ag_3Ga			
3	Ag–In	Ag_2In	$LTAgIn_2$		
4	Ag–Sn	Ag_3Sn			
5	Ag–Te	Ag_2Te	Ag_5Te_3		
6	Ag–Zn	AgZn	Ag_5Zn_8	$AgZn_3$	
7	Al–Au	Au_2Al	$AuAl_2$		
8	Au–Cd	AuCd	$AuCd_3$		
9	Au–Ga	Au_7Ga_2	Au_2Ga	AuGa	$AuGa_2$
10	Au–In	Au_4In	Au_7In_3	AuIn	$AuIn_2$
11	Au–Pb	Au_2Pb	$AuPb_2$	$AuPb_3$	
12	Au–Sb	$AuSb_2$			
13	Au–Sn	Au_5Sn	AuSn	$AuSn_2$	$AuSn_4$
14	Au–Te	$AuTe_2$			
15	Au–Zn	Au_3Zn	AuZn	$AuZn_3$	
16	Bi–Pd	$PdBi_2$			
17	Cd–Cu	Cu_4Cd_3	$CuCd_3$		
18	Cd–Te	CdTe			
19	Cu–Ga	CuGa			
20	Cu–In	CuIn			
21	Cu–Sb	Cu_2Sb			
22	Cu–Sn	Cu_6Sn_5			
23	Cu–Te	Cu_3Te	Cu_7Te_5	CuTe	
24	Cu–Zn	$CuZn_4$			
25	Ga–Mg	Mg_2Ga	Mg_2Ga_5		
26	Ga–Ni	$NiGa_4$			
27	Ga–Pd	$PdGa_5$			
28	Ga–Sb	GaSb			
29	In–Ni	$LTNi_2In_3$	$Ni_{10}In_{27}$		
30	In–Pd	$PdIn_3$			
31	Ni–Sn	NiSn or Ni_3Sn_4			
32	Ni–Te	$NiTe_2$			
33	Pb–Pd	$PdPb_2$			
34	Pb–Pt	$PtPb_4$			
35	Pb–Te	PbTe			
36	Pd–Sb	PdSb[a]			
37	Pd–Sn	$PdSn_3$	$PdSn_4$		
38	Pd–Te	$PdTe_2$			
39	Pt–Sn	$PtSn_4$			

[a] In the Pd–Sb couple, PdSb compound was noticed after 4 y.

2.1.38. Pd–Te

The first results relative to the room-temperature compound formation in the Pd–Te couple (phase diagram [4, 45]) were presented by Simić and Marinković [46]. A detailed study of the couple was made using specimens 185–580 nm thick with three different tellurium concentrations: 38.1%, (earlier Pd_2Te), 55.0% (PdTe) and 70.5% ($PdTe_2$). The specimens were analysed using XRD. The results are presented in Table XLIII.

It can be seen that only one compound, $PdTe_2$ (ASTM 29–0970) is formed, irrespective of the constituent concentrations. The maximal concentration of $PdTe_2$ is in the specimens with maximal concentration of tellurium.

2.1.39. Pt–Sn

The first results regarding the room-temperature compound formation in the Pt–Sn couple (phase diagram [4, 53]) were given by Tu and Rosenberg [8]. In the table presenting the authors' results it is only noted that $PtSn_4$ is formed. The specimens contained 500 nm Pt and 300 nm Sn and the compound formation was followed for 2–3 wks.

2.2. Formation of compounds on the contact of the bulk metal with evaporated thin metal film

The first results concerning compound formation on the contact of a bulk metal and a thin-film evaporated on to it at room temperature were published in 1983 [60]. Bulk noble metals (silver, aluminium, gold and copper) with high crystal symmetry (cubic), distinct metallic character and relatively high melting points, were used. Another group of bulk metals consisted of low melting point metals (indium, lead, tin and gallium) having crystal symmetry mostly lower than cubic. Silver, aluminium, gold, cadmium, copper, gallium, indium, lead, tin, antimony, tellurium and zinc were used for evaporation. Only the couples known to form compounds at room temperature

TABLE XLV Compounds formed at bulk metal–evaporated thin metal film interface

Metal		State after			Metal		State after		
Bulk	Film	1–3 mon [61]	5–8 y [61]	13 y [62]	Bulk	Film	1–3 mon [61]	5–8 y [61]	13 y [62]
Ag	Ga	Ag_3Ga	Ag_3Ga	Ag_3Ga	Ga	Ag	Ag_3Ga		
Ag	In	Ag_2In	CD[a]	CD[a]	In	Ag	$LTAgIn_2$	$LTAgIn_2$	
Ag	Sn	Ag_3Sn	Ag_3Sn	CD[a]	Sn	Ag	Ag_3Sn	Ag_3Sn	Ag_3Sn
Ag	Te	Ag_2Te	Ag_2Te	Ag_2Te	Te	Ag	Ag_5Te_3	Ag_5Te_3 [62]	
Ag	Zn	$AgZn_3$	Ag_5Zn_8	Ag_5Zn_8	Zn	Ag[b]	$AgZn_3$	$AgZn_3$ [62]	
		Ag_5Zn_8		AgZn			Ag_5Zn_8 AgZn	Ag_5Zn_8 AgZn	
Au	Al	0	0	[c]	Al	Au	0	0	0
Au	Cd	$AuCd_3$	$AuCd_3$	[c]	Cd	Au	$AuCd_3$ AuCd	$AuCd_3$ AuCd	
Au	Ga	$AuGa_2$ AuGa Au_2Ga	AuGa Au_2Ga Au_7Ga_2	[c]	Ga	Au	$AuGa_2$		
Au	In	$AuIn_2$ AuIn		[c]	In	Au	$AuIn_2$	$AuIn_2$ [62]	$AuIn_2$
Au	Pb	$AuPb_3$ $AuPb_2$	[d] [62]	[d]	Pb	Au	$AuPb_3$	[d] [62]	[d]
Au	Sb	$AuSb_2$	$AuSb_2$	[c]	Sb	Au	0	0 [62]	
Au	Sn	AuSn	AuSn	[c]	Sn	Au	$AuSn_4$ $AuSn_2$ AuSn	$AuSn_4$ $AuSn_2$ AuSn	$AuSn_4$ $AuSn_2$ AuSn
Au	Zn	$AuZn_3$ AuZn	$AuZn_3$ AuZn	$AuZn_3$ AuZn	Zn	Au	0	0	0
Cu	Cd	Cu_4Cd_3	Cu_4Cd_3	Cu_4Cd_3	Cd	Cu	0	Cu_4Cd_3	Cu_4Cd_3
Cu	Ga	CuGa	CD[a]	CD[a]	Ga	Cu	CuGa		
Cu	In	CuIn	CuIn	CuIn	In	Cu	CuIn	CuIn	CuIn
Cu	Sb	0	0	0	Sb	Cu	0	0	
Cu	Sn	Cu_6Sn_5	Cu_6Sn_5	Cu_6Sn_5	Sn	Cu	Cu_6Sn_5	Cu_6Sn_5	Cu_6Sn_5
Cu	Te	0	0	0	Te	Cu	Cu_7Te_5 CuTe	CuTe [62]	
Cu	Zn	$CuZn_4$			Zn	Cu	0	0	0
Pb	Te	PbTe	[d]	[d]	Te	Pb	0 [62]	0 [62]	0

[a] CD, compound disappears.
[b] It is incorrectly noted in [56] that compounds did not form.
[c] Specimens destroyed – gold plates were used for some other purposes.
[d] Oxidation of lead and lead compounds.

(Table XLIV) were prepared and analysed. The total number of the prepared, measured and analysed couples amounts to 31.

The following conclusions have been derived from the results presented. The compounds were formed in 27 out of 31 couples, showing that the compound formation in the bulk–film specimens takes place for almost all the couples in which the compounds are formed in the film–film specimens.

This conclusion was stimulating, so that research was continued. New bulk materials (cadmium, antimony, tellurium and zinc), having lower crystal symmetry and usually lower melting points, were used [61]. In this way, ten new couples (designated in Table 1 in [61], "*"), were obtained, making a total number of 41 (32 with and 9 without compounds formed) measured couples. In addition, changes occurring in these couples during ageing were studied. Thus, results are obtained for 42 fresh specimens, 37 specimens 5–8 y old, and for 25 specimens 13 y old (Table XLV).

The results obtained in this way (104 measurements) present a sufficient statistics for analysis and conclusions.

2.2.1. Number of compounds formed

In general, the number of the compounds formed in the bulk–film specimens is smaller than the corresponding number for the film–film ones. Thus, four compounds are formed in the Au–Sn film–film specimen, but there is only one compound in the Au bulk–Sn film. Similarly, four compounds are formed in the Au–Ga film–film specimen, there are three compounds in the Au bulk–Ga film, and only one in the Ga bulk–Au film specimen. There are two compounds in the Ag–In film–film specimen: Ag_2In and $LTAgIn_2$. However, only Ag_2In is formed in the Ag bulk–In film specimen, while in the In bulk–Ag film, the only compound formed is $LTAgIn_2$.

The offered explanation is as follows. The constituent concentrations in thin-film specimens can be changed voluntarily, and in this way all the compounds which form at room temperature can be produced. If one of the constituents is in bulk form, the compounds formed are mostly those with a predominant concentration of bulk metal. In the In bulk–Ag film such a compound is $AgIn_2$, and in the Ag bulk–In film it is Ag_2In. The same reasoning is valid for the Ag–Te couple, which produces two compounds if in thin-film form: Ag_2Te and Ag_5Te_3. If, in a thin-film specimen, only one compound is formed, the same compound is formed in the corresponding bulk–film specimen (Ag–Ga, Ag–Sn, Cu–Ga, Cu–In, etc.).

In the bulk–film type couples (Table XLV), 20 compounds are formed when the low-melting metal is in the bulk form and 24 compounds when the high-melting metal is in the bulk form, which is approximately the same. In the same couples of the film–film type, 42 compounds are formed (Table XLIV).

2.2.2. Rate of reaction

The reaction rates may greatly differ in the bulk–film specimens. In general, they are smaller than in the corresponding *film–film specimens*. It has been observed that they may depend on the manner in which the bulk metal is treated prior to evaporation of the film.

Table XLVI presents, for three couples with different reaction rates, comparative data on the time when the compound formation was first observed and on the time when the reaction was completed. In the most rapid processes, all the reactions are completed during the first day. In the medium-rate processes, the reactions are completed after some months, and the slowest processes are completed after several years, or are not completed within the investigated period.

It can be seen that the reaction is faster and a greater number of compounds is produced if the *low-melting metal is present as a film*. It can also be seen that the bulk metal surface treatment influences the reaction. Thus, cadmium, lead and zinc react with a gold film only if their surface is etched in suitable reactants, while gallium and indium also react if their surface is washed in alcohol.

2.2.3. Transformation of compounds

In the bulk–film specimens, the same compounds are formed as in the corresponding film–film ones, but the reaction rate is lower. For example, the reaction

$$AuIn_2 + Au = 2AuIn \qquad (23)$$

TABLE XLVI Comparative data on reaction rates in bulk–film and film–film specimens[a]

Metal couple	Specimen type	Compound is observed	Process is completed
Ag–Ga	Ag film–Ga film (24% or 49% Ga)	1st day	1st day
	Ag bulk–Ga film	1st day	1st day
	Ga bulk–Ag film	1st day	2nd day
Cu–Sn	Cu film–Sn film (20% or 85% Sn)	2nd day	5th day
	Cu bulk (treated mechanically)–Sn film	9th day	Not completed after 3 mon
	Cu bulk (untreated)–Sn film	14th day	Not completed after 5 mon
	Sn bulk (etched)–Cu film	30th day	After several years
Au–Al	Au film–Al film	5th day	Between 1 and 3 y
	Au bulk–Al film	No compound formation after 6.5 y	
	Al bulk–Au film	No compound formation after 6.5 y	

[a] Table completed from [60].

takes 4 mon in the bulk–film specimen, and about 1 mon in the film–film one.

The transformation process (for which the Au–Ga couple is taken as an example) is the following. The $AuGa_2$ is formed first, then it transforms to another (second) compound containing more gold. Then the second compound is transformed into the third, etc.

$$AuGa_2 + Au = 2AuGa \quad (24)$$

then

$$AuGa + Au = Au_2Ga, \quad (25)$$

and

$$Au_2Ga + AuGa + 4Au = Au_7Ga_2 \quad (26)$$

Another interesting example is the Ag–Zn couple. In this case the process is as follows. The $AgZn_3$ is formed first and it is then transformed

$$8AgZn_3 + 7Ag = 3Ag_5Zn_8 \quad (27)$$

and then

$$Ag_5Zn_8 + 3Ag = 8AgZn \quad (28)$$

The transformations start already during the vacuum evaporation. In the course of time in both the couples analysed (and in Te bulk–Cu film couple), the compounds with more metal, which is in the bulk, are formed.

The times at which the compounds were first observed in the bulk gold–metal film and bulk metal–gold film specimens, as examples, are presented elsewhere [29].

2.3. Formation of compounds on contact of metal film or bulk with sputtered thin metal film

This section presents the results of investigations of compounds that are formed when on a fresh metal film or bulk metal another film is deposited using radio frequency (r.f.) sputtering. The results presented here are taken from both published and unpublished [62] papers by Simić and Marinković.

The results are presented in a concise manner in three tables, each table being followed by necessary comments and explanations in text. The tables contain results obtained with both film–$film_{r.f.}$ and bulk–$film_{r.f.}$ specimens. Also, in addition to the results obtained immediately after the r.f. film formation, those obtained after 5 and 11 y ageing (Tables XLVII and XLVIII) and 8 or 10 y (Table XLIX) were presented.

In certain cases, the specimens of the film–$film_{r.f.}$ type were not prepared. Namely, if well-defined compounds had been formed in the film–film specimens obtained by evaporation, attention was directed primarily to bulk–$film_{r.f.}$ specimens. However, if the evaporated film–film specimens had not been prepared, or when in such specimens no compound was formed, attention was directed more to the film–$film_{r.f.}$ specimens. Only in some cases were bulk–$film_{r.f.}$ specimens also studied in order to see if compound formation would occur.

It should be mentioned that the essential phenomena occurring in the metal couples, as well as the existing regularities, are most clearly found by long observation of the vacuum-evaporated film–film specimens. The phenomena observed in thin-film specimens in which the second film has been obtained by sputtering, contribute only to complete and/or to extend the already gathered knowledge.

2.3.1. *Me–$Ag_{r.f.}$ Me–$AlAg_{r.f.}$ and Me–$AuAg_{r.f.}$ couples*

The results are presented in Table XLVII.

In the *Al–$Ag_{r.f.}$* couple, no compound was formed both in the film–$film_{r.f.}$ and bulk–$film_{r.f.}$ specimens.*

TABLE XLVII Formation of compounds in couples containing top sputtered Ag, Al or Au film

Couple	Film–$film_{r.f.}$ [62,63]					Bulk–$film_{r.f.}$				
	Bottom	Top	Compound identified after			Bottom	Top	Compound identified after		
			1–5 d	5 y	11 y			1–5 d [61]	5 y [61]	11 y [62]
Ag–Al	Al	Ag	0	0	0	Al	Ag	0	0	0
Ag–In						In	Ag	$LTAgIn_2$	$LTAgIn_2$	$LTAgIn_2$
Ag–Sb	Sb	Ag	Ag_3Sb	Ag_3Sb	Ag_3Sb[a]	Sb	Ag	Ag_3Sb	Ag_3Sb	Ag_3Sb[a]
Ag–Sn	Sn	Ag	Ag_3Sn	Ag_3Sn	Ag_3Sb[a]	Sn	Ag	Ag_3Sn		
Ag–Te						Te	Ag	Ag_5Te_3	Ag_5Te_3	Ag_5Te_3
Al–Au						Au	Al	0	0	0
Al–Sb	Sb	Al	AlSb[b]	AlSb[b]	AlSb[b]	Sb	Al	AlSb[b]		
Au–Al						Al	Au	Au_2Al	Au_2Al	Au_2Al
								$AuAl_2$	$AuAl_2$	$AuAl_2$
Au–Cd						Cd	Au	$AuCd_3$	$AuCd_3$	$AuCd_3$
								AuCd	AuCd	AuCd
Au–In						In	Au	$AuIn_2$	$AuIn_2$	$AuIn_2$
Au–Sb						Sb	Au	$AuSb_2$		
Au–Zn						Zn	Au	$AuZn_3$	$AuZn_3$	$AuZn_3$

[a] After 8.5 y.
[b] Trace.

* When first mentioned, couples which in evaporated thin film specimens do not form compounds are printed in italics, and those in which compounds are formed, are printed in bold

TABLE XLVIII Formation of compounds in couples containing top-sputtered copper film

Couple	Film–film$_{r.f.}$					Bulk film$_{r.f.}$				
	Bottom	Top	Compound identified after			Bottom	Top	Compound identified after		
			1–5 d [48, 63]	5 y [48, 63]	11 y [62]			1–5 d [61]	5 y [61]	11 y [62]
Cu-Al	Al	Cu	0	0	0	Al	Cu	0	0	0
Cu-Au	Au	Cu	0	0	0	Au	Cu	0	0	0
Cu-Cd	Cd	Cu	Cu_4Cd_3	Cu_4Cd_3	Cu_4Cd_3	Cd	Cu	Cu_4Cd_3	Cu_4Cd_3	Cu_4Cd_3
Cu-Ga	Ga	Cu	CuGa Cu_9Ga_4	CuGa Cu_9Ga_4	CuGa Cu_9Ga_4					
Cu-Ge	Ge	Cu	Cu_3Ge Cu_5Ge	Cu_3Ge Cu_5Ge	Cu_3Ge Cu_5Ge	Ge	Cu	Cu_3Ge Cu_5Ge	Cu_3Ge Cu_5Ge	Cu_3Ge Cu_5Ge
Cu-In						In	Cu	CuIn Cu_4In	CuIn	CuIn
Cu-Sb	Sb	Cu	Cu_2Sb	Cu_2Sb	Cu_2Sb	Sb	Cu	Cu_2Sb Cu_3Sb[a]		
Cu-Sn	Sn	Cu	Cu_6Sn_5 Cu_3Sn	Cu_6Sn_5 Cu_3Sn	Cu_6Sn_5 Cu_3Sn	Sn	Cu	Cu_6Sn_5 Cu_3Sn[a]	Cu_6Sn_5 Cu_3Sn[a]	Cu_6Sn_5 Cu_3Sn[a]
Cu-Te						Te	Cu	Cu_7Te_5		
Cu-Zn	Zn	Cu	Cu_5Zn_8 $CuZn_4$	Cu_5Zn_8 $CuZn_4$	Cu_5Zn_8 $CuZn_4$	Zn	Cu	$CuZn_4$	$CuZn_4$	$CuZn_4$

[a] Trace.

TABLE XLIX Formation of compounds in couples containing top-sputtered chromium and titanium film

Couple	Film–film$_{r.f.}$				Bulk–film$_{r.f.}$			
	Bottom	Top	Compound identified after		Bottom	Top	Compounded identified after	
			1–5 d [66, 69]	8 y (Me–Cr) 10 y (Me–Ti) [62]			1–5 d [66, 69]	8 y (Me–Cr) 10 y (Me–Ti) [62]
Cr–Al	Al	Cr	0	0				
Cr–Ga	Ga	Cr	$CrGa_4$	$CrGa_4$				
Cr–In	In	Cr	0	0	In	Cr	0	0
Cr–Sb	Sb	Cr	0	0				
Cr–Sn	Sn	Cr	Cr_2Sn_3	Cr_2Sn_3	Sn	Cr	0	0
Cr–Te	Te	Cr	0	0	Te	Cr	0	0
Cr–Zn	Zn	Cr	0	0	Zn	Zr	0	0
Ti–Al	Al	Ti	0	0				
Ti–Au	Au	Ti	0	0				
Ti–Bi	Bi	Ti	LT(Bi–Ti)	Compound disappeared				
Ti–Cd	Cd	Ti	CdTi $CdTi_2$	[a]	Cd	Ti	CdTi $CdTi_2$	[a]
Ti–Cu	Cu	Ti	0	0				
Ti–Ga	Ga	Ti	α-Ti_3Ga	α-Ti_3Ga				
Ti–Ge	Ge	Ti	0	0				
Ti–In	In	Ti	Ti_3In_4	Ti_3In_4	In	Ti	Ti_3In_4	Ti_3In_4
Ti–Mn	Mn	Ti	0	0				
Ti–Pb	Pb	Ti	LT(Pb–Ti)	LT(Pb–Ti) [b]				
Ti–Sn	Sn	Ti	α-Ti_6Sn_5	α-Ti_6Sn_5	Sn	Ti	α-Ti_6Sn_5	α-Ti_6Sn_5
Ti–Te	Te	Ti	$TiTe_2$	$TiTe_2$				
Ti–Zn	Zn	Ti	0	0	Zn	Ti	0	0

[a] In these specimens, the situation remained unchanged after 3.5 y. After 10 y compound formed and Cd-film disappeared under the influence of the atmosphere.
[b] compound stable but $PbCO_3$ and Pb(X) are also present.

The $LTAgIn_2$ compound was formed in the **In bulk–Ag$_{r.f.}$** specimen, which could be expected because indium was in excess.

The *Sb–Ag* couple (phase diagram [4, 53]) was investigated in the form of a film–film$_{r.f.}$ specimen, in which the Ag_3Sb (ASTM 10-452) compound formation was found to take place [62]. The experiments with the bulk–film$_{r.f.}$ specimens led also to Ag_3Sb compound formation [61].

The compounds expected from the study with corresponding evaporated specimens [6] were formed in the **Sn–Ag$_{r.f.}$** and **Te–Ag$_{r.f.}$** specimens. For the compound

formed in the **Te bulk–$Ag_{r.f.}$** [63], the same comment is valid as for the **In bulk–$Ag_{r.f.}$** specimen.

The AlSb (ASTM 6-0233) compound was formed in the *Sb–Al* couple (phase diagram [4]), in both film–$film_{r.f.}$ and bulk–$film_{r.f.}$ specimens. It is interesting that in both specimen types, weak compound reflections are obtained, i.e. trace amounts.

In the **Me–Au** system, compounds were formed in all the vacuum-evaporated thin-film specimens, as presented in Section 2.1. Attention was therefore directed to a study of the couples in the metal bulk–$Au_{r.f.}$ form. In general, the expected results were obtained.

The table also shows that the 5 and 11 y ageing did not lead to any essential change.

In the couples in which the upper layer is obtained by r.f. sputtering, the reaction is usually completed when the sputtering is ended, but some exceptions exist. The reaction continues during ageing in the specimens: In bulk–Ag, Te bulk–Ag, Zn bulk–Au and In bulk–Cu.

It can be concluded that the compounds formed in the Me–$Ag_{r.f.}$, Me–$Al_{r.f.}$ and Me–$Au_{r.f.}$ couples are stable during ageing.

2.3.2. Me–$Cu_{r.f.}$ couples

The results are presented in Table XLVIII.

In both the *film–*$film_{r.f.}$ and *bulk–*$film_{r.f.}$ Al–Cu and Au–Cu couples, no compound is formed when the upper (copper) film is deposited by r.f. sputtering.

In the **Cd–Cu** couple, Cu_4Cd_3 is formed, irrespective of the specimen type.

In the **Ga–Cu** couple, Cu_9Ga_4 (ASTM 2-1250) is formed in addition to CuGa. When the sputtering time is shorter, the specimen contains less copper and CuGa is formed. If the sputtering time is longer, the copper concentration is higher and therefore Cu_9Ga_4 is formed in addition to CuGa. It is interesting that the first-formed compound does not create a barrier to the second compound (Cu_9Ca_4) formation.

In the *Ge–Cu* couple (phase diagram [4]), specimens of the film–$film_{r.f.}$ and bulk–$film_{r.f.}$ types have been prepared and measured [48]. It has been found that the Cu_3Ge compound (ASTM 6-0693) is formed when the copper concentration is lower. When more copper was deposited, in addition to Cu_3Ge, the specimen contained a compound which did not correspond to CuGe (ASTM 36-1134). Because the compound contains more copper, the authors have concluded that it is Cu_5Ge, which is also mentioned by Hansen [53].

In the **In–Cu** couple, it was easy to prepare the evaporated specimens and therefore no In film–$Cu_{r.f.}$ specimen was prepared. In the In bulk–$Cu_{r.f.}$ type specimens, the compound formation depended on the amount of sputtered copper. CuIn was formed with less copper, and Cu_4In with more copper [48].

In the **Sb–Cu** couple, Cu_2Sb was formed irrespective of the form of antimony (film or bulk). However, in the bulk–film specimen only a Cu_3Sb trace was formed. Cu_3Sb was formed at 200–300 °C in thin-film specimens [64].

In the **Sn–Cu** couple, two compounds were formed in both film–$film_{r.f.}$ and bulk–$film_{r.f.}$ type specimens: Cu_6Sn_5 and Cu_3Sn [48]. Because of a small amount of the sputtered copper, the Cu_3Sn formed in the bulk–$film_{r.f.}$ specimens gives low X-ray reflection intensity. In evaporated thin-film specimens, Cu_3Sn was formed at 90 °C [65] or at 60 °C [62].

In the **Zn–Cu** couple, $CuZn_4$ is formed in the film–$film_{r.f.}$ type specimen [48]. If the copper concentration is sufficient (longer sputtering), Cu_5Zn_8 appears in addition to $CuZn_4$. It is formed by the transformation

$$2CuZn_4 + 3Cu = Cu_5Zn_8 \qquad (29)$$

In the Zn bulk–$Cu_{r.f.}$ specimen, only $CuZn_4$ is formed. In this specimen, zinc is always present in excess, and the mentioned transformation cannot occur.

The table also shows that no substantial change occurred in the specimens during 11 y ageing. The only exception is the In bulk–$Cu_{r.f.}$ specimen in which, during ageing, Cu_4In was transformed to CuIn. This is a consequence of the fact that indium is in excess in the specimen.

It follows that the compounds formed in the Me–$Cu_{r.f.}$ couples are stable during ageing.

2.3.3. Me–$Cr_{r.f.}$ and Me–$Ti_{r.f.}$ couples

A detailed study of the *Ga–Cr* couple (phase diagram [4]) was made using ten specimens with different concentrations [66]. The obtained results show that only one compound is formed, the XRD powder results of which, presented in Table L, differ from all the available ASTM standards for Ga–Cr.

The obtained results are presented in Table XLIX. The first part of the table shows the results obtained from a study of the specimens in the Me–$Cr_{r.f.}$ system. In five out of seven investigated couples, no compound is formed.

Analysis of the phase diagram [4], *Walser-Bené's rule* [67] and the authors' own results [66], allowed them to conclude that the compound formed is $CrGa_4$. For the reasons mentioned at the beginning of this section, the specimens with gallium bulk were not investigated.

A detailed study of the *Sn–Cr* couple (phase diagram [68]) was made using five specimens with different tin concentrations [66]. Only Cr_2Sn_3 compound (ASTM 19–333) was found. In the specimens obtained by r.f. sputtering of chromium on tin bulk, no compound was found [62].

In the lower part of Table XLIX, the results obtained by studying the couples in the Me–$Ti_{r.f.}$ are presented. The results are from a paper by Simić and Marinković [69] and an additional study by the same authors [62]. In 6 out of 13 couples studied, no compound was formed. In the couples of $Ti_{r.f.}$ with Al, Au, Cu, Ge and Mn this could be expected, because of the analogy with the film–film specimens prepared by vacuum evaporation (film–$film_{ev}$). Namely, all the metals mentioned have high melting temperatures (660–1244 °C). The Zn–$Ti_{r.f.}$ couple is a different case. Zinc has a low melting point (419.5 °C). In addition, according to the phase diagram [70], there are many compounds in the Ti–Zn couple which exist down to the room temperature. It was found, however, that

TABLE L X-ray powder results of the compound formed in thin-film Ga–Cr specimens

d (nm)	I/I_0	d (nm)	I/I_0	d (nm)	I/I_0	d (nm)	I/I_0
0.4622	11	0.2557	17	0.2113	32	0.1331	9
0.4287	10	0.2293	69	0.2072	16	0.1328	9
0.3955	20	0.2265	45	0.1983	76	0.1290	6
0.2906	8	0.2214	11	0.1622	15	0.1258	11
0.2814	100	0.2192	43	0.1503	8	0.1173	17
0.2683	7	0.2147	18	0.1410	12	0.1171	13

TABLE LI X-ray powder results of the compound formed in thin-film Bi–Ti specimens [62]

d (nm)	I/I_0	d (nm)	I/I_0	d (nm)	I/I_0	d (nm)	I/I_0
0.4860	13	0.2578	7	0.1737	5	0.1613	6
0.3080	38	0.2515	13	0.1701	6	0.1593	8
0.2918	100	0.2435	46	0.1695	10	0.1563	8
0.2764	84	0.1989	12	0.1672	13	0.1519	5
0.2750	59	0.1771	4	0.1653	13	0.1388	7
0.2690	33	0.1749	9	0.1623	11	0.1337	8

only on annealing the specimen at $\geqslant 100\,^{\circ}C$ did some unidentified phase appear.

A detailed study of the *Bi–Ti* couple (phase diagram [70]) was made using eight specimens with different bismuth content [69]. The results obtained show that in all the specimens, the same compound is formed. The XRD powder results presented in Table LI, do not correspond to the results in the available ASTM standard, so that the compound could not be identified. The authors have supposed that the compound formed is a low-temperature phase of one of the known compounds, (Ti–Bi) LT.

The compound formed is unstable. In the specimen containing lower compound content (shorter time of titanium evaporation), the compound disappears after several months. When the titanium content was considerably higher, more than 2.5 y elapsed before the compound disappeared.

The *Cd–Ti* couple (phase diagram [70, 71]) was the subject of a detailed study, using four specimens with different cadmium concentrations [69]. A new phase was found. It was distinctly oriented and only one or two distinct maxima appeared in the XRD diagram. The precise diffractometric measurements provided the results presented in Table LII. Two investigated Cd bulk–$Ti_{r.f.}$ specimens gave similar results.

TABLE LII The data for identification of the compounds in the thin-film Cd–$Ti_{r.f.}$ couple (Cd thickness 1 μm) [62]

Sputtering time of Ti (min)	Obtained X-ray maxima, d (nm)	Identified compounds[a]
2	0.2480	CdTi
4	0.2467	CdTi
6	0.2465	CdTi
	0.2446	$CdTi_2$
8	0.2455	CdTi
	0.2443	$CdTi_2$

[a] CdTi (ASTM 15-349); $CdTi_2$ (ASTM 15-351).

The *Ga–Ti* couple (phase diagram [70]) was the subject of a detailed study in which 20 specimens with different gallium content were used [69]. Only one compound was found, the XRD results of which are presented in Table LIII. They do not correspond to any of the available ASTM standards for the Ga–Ti system and therefore could not be identified.

In order to identify the compound, the specimens were subjected to a vacuum annealing at 55–120 °C. It was found that after annealing at 120°C, the

TABLE LIII X-ray powder results of the compound formed in thin Ga–Ti specimens [62]

d (nm)	I/I_0	d (nm)	I/I_0	d (nm)	I/I_0	d (nm)	I/I_0
0.4820	15	0.2132	100	0.1443	4	0.1122	2
0.3290	40	0.1880	26	0.1417	3	0.0941	2
0.2788	15	0.1824	4	0.1395	14	0.0909	2
0.2417	5	0.1791	2	0.1285	2	0.0806	2
0.2373	5	0.1749	2	0.1274	3	0.0775	2
0.2333	63	0.1692	3	0.1198	2		
0.2287	3	0.1645	2	0.1186	8		
0.2249	5	0.1610	2	0.1167	4		

compound disappeared; it was transformed to Ti_3Ga. The conclusion derived by the authors was that the compound formed in the $GaTi_{r.f.}$ couple is the low-temperature phase of the Ti_3Ga compound, i.e. α-Ti_3Ga. The transformation temperature is about 120 °C.

A detailed study of the *In–Ti* couple (phase diagram [70]) was made using six specimens with different indium contents [69]. The investigation has shown that some compound is formed, identified to be Ti_3In_4 (ASTM 18–625).

A study in which four specimens with indium bulk were used gave identical results.

The *Pb–Ti* couple (phase diagram [70]) was the subject of a detailed study in which 17 specimens with different lead concentrations were used [69]. Only one compound was found, but it could not be identified on the basis of the available ASTM standards.

Because Pb_4Ti and Pb_2Ti are obviously high-temperature phases, the authors have supposed that the compound in question is probably a low-temperature phase of one of these two compounds.

A detailed study of the *Sn–Ti* couple (phase diagram [70]) was made using seven specimens of the film–$film_{r.f.}$ type with different concentrations, and 11 specimens of the bulk–$film_{r.f.}$ type with different concentrations [69]. A parallel study of both specimen types was made. It was found that one compound is formed. Its powder diffraction results are presented in Table LIV.

The powder diagram obtained does not correspond to any of the available ASTM standards. The authors suppose that the compound in question is probably a low-temperature phase of some of the known Sn–Ti compounds, possibly α–Ti_6Sn_5.

The *Te–Ti* couple (phase diagram [70, 72]) was the subject of a detailed study in which eight specimens with different tellurium concentrations were used [69]. It was found that the same compound is formed in all the cases. The compound was identified as $TiTe_2$ (ASTM 6–0421).

None of the available phase diagrams for the *Te–Ti* system contains a graphical representation from which it could be possible to see in which temperature range $TiTe_2$ is stable, i.e. what the transformation temperature of this compound is, to another high-temperature one. By annealing the specimens in vacuum at different temperatures it was found that $TiTe_2$ remained unchanged at 180 °C.

By following the behaviour of the $TiTe_2$ specimens, it was found that the compound formed is unstable at room temperature. According to the power diagram of the specimen with 0.2 μm thick tellurium, it disappeared within less than 11 mon, although in the specimens with a tellurium film 1 μm thick, the process of the disappearance was not completed after 10 y and the compound is still visible. The instability of the $TiTe_2$ compound could possibly be connected with the observation [72], according to which the Ti–Te compounds are very reactive and reach equilibrium with difficulty.

2.4. Formation of compounds on the contact of semiconducting single-crystal bulk compound with a thin metal film

Semiconducting single-crystal bulk compounds are often used in microelectronics and sensor techniques. InSb and GaAs are among the most often used, but GaSe is also used. Such semiconductors or semiconducting sensors are incorporated into electronic circuits. Contacts made of different metals or alloys are therefore made on them. Sometimes these contacts consist of several different metal layers, some of them being conducting, and others barrier and protective. Silver, gold, copper, aluminium, titanium and some other metals and their alloys are often used for such purpose.

Bearing in mind their application, in the present text, phenomena occurring at room temperature on the contact of the mentioned semiconducting compounds with the metal (Me) layers deposited on them, will be considered. In particular, formation of compounds and their transformation during ageing will be studied.

2.4.1. *InSb–Me contacts*

Phenomena in the InSb–Ag, InSb–Au and InSb–Cu couples, in which compound formation takes place at room temperature, have been the subject of an experimental study. The InSb–Al and InSb–Ti couples, in which no compound formation was found under the same conditions, have also been studied.

2.4.2. *InSb–Ag*

Specimens were prepared using thermal evaporation in vacuum and by r.f. sputtering of silver on a InSb single-crystal bulk [62]. The results are presented in Table LV.

TABLE LIV X-ray powder results of the compound formed in thin-film Sn–Ti specimens [62]

d (nm)	I/I_0	d (nm)	I/I_0	d (nm)	I/I_0	d (nm)	I/I_0
0.3175	24	0.2475	43	0.1797	6	0.1288	8
0.3142	15	0.2433	29	0.1637	8	0.1203	14
0.2940	79	0.2275	30	0.1623	9	0.1198	16
0.2858	63	0.2228	21	0.1608	5	0.1196	9
0.2755	28	0.2207	91	0.1590	10	0.1077	9
0.2684	100	0.1925	5	0.1575	15	0.1067	6
0.2564	15	0.1866	3	0.1539	10		
0.2515	85	0.1852	3	0.1429	20		

TABLE LV Conditions under which compound formation takes place on contact of the InSb single crystal with the deposited silver film

Deposition method	Deposited film		Compound formed
	Thickness (nm)	R.f. power (kW)	
Thermal evaporation	100		0
R.f. sputtering	75	0.6	0
	100	1.0	Ag_3In
	250	1.0	Ag_3In

The table shows that no compound formation takes place by the evaporation and r.f. sputtering using lower power. Only by r.f. sputtering using a higher power for 1–6 min is Ag_3In (ASTM 29–0677) formed.

In thin Ag–In couples (see Section 2.1) Ag_2In or $LTAgIn_2$ are formed at room temperature, depending on the specimen composition. Owing to an increased kinetic energy of silver particles by the r.f. sputtering, the high-temperature Ag_3In phase is formed. The XRD diffractograms of these specimens were again taken after 5.5–6 y and no substantial change could be detected.

2.4.3. InSb–Au

Specimens were prepared by vacuum thermal evaporation and by r.f. sputtering of gold on InSb single-crystal bulk [62]. Specimens were also prepared by first depositing a chromium film on InSb using r.f. sputtering, and then depositing a gold film by the same method.

Thicknesses of the evaporated gold films were 50 and 100 nm, and the thicknesses of the r.f. sputtered films were of the same order (the thickest film, prepared with 1.5 kW/1 min, was 120 nm). The gold films with chromium underlayers had thicknesses in the range 150–600 nm. However, r.f. sputtering power is more important than the film thickness.

The results are presented in Table LVI. The chromium underlayer did not influence the compound formation and these results are not presented in Table LVI.

In the specimens prepared with an evaporated gold film, compound could be detected by the X-ray method used soon after their preparation. The long ageing led to the formation of both $AuSb_2$ and indium compounds. The very slow process was not completed even after 6 y. It can be seen that $AuSb_2$ is formed in the specimens obtained with the lowest r.f. power (0.6 kW). This is the compound with the lowest melting point (460 °C). With higher r.f. power (0.8 kW), indium compounds are also formed (AuIn, m.p. 509.6 °C and Au_4In, m.p. 649.25 °C). Further increase in r.f. power (1 kW), leads to their increasing fraction in the mixture of the compounds formed, while at the highest power (1.5 kW), only indium compounds are obtained.

TABLE LVI Formation and transformation of compounds on InSb–Au contact

Film deposition procedure	R.f. sputtering		Compounds formed		Remarks
	Time	Power (kW)	2 7 d after deposition	After long ageing	
Thermal evaporation			0	$AuSb_2$ Au_4In AuIn	Measured after 8 y
R.f. sputtering	2 × 30 s	0.6	$AuSb_2$	$AuSb_2$ Au_4In[a] AuIn[a]	Reaction continues during ageing; after 5.5 y the intensity of the $AuSb_2$ reflection is considerably higher
	1 × 1 min	0.6	$AuSb_2$	$AuSb_2$ Au_4In AuIn	$AuSb_2$ reflection intensities are considerably higher than in the 2 × 30 s specimen
	2 × 30 s	0.8	$AuSb_2$ Au_4In AuIn	$AuSb_2$ Au_4In AuIn	Compound reflection intensities in the 2 × 30 s specimen
	1 × 1 min	0.8	$AuSb_2$ Au_4In AuIn	$AuSb_2$ Au_4In AuIn	are lower and increase with time more than in the 1 × 1 min specimen
	1 × 1 min	1.0	$AuSb_2$ Au_4In AuIn	$AuSb_2$ Au_4In AuIn	No change during ageing. Sb and In compounds present in approximately equal amounts
	1 × 1 min	1.5	Au_4In AuIn	Au_4In AuIn	No change during ageing

[a]Trace.

In the specimens prepared with lower r.f. sputtering power, the reaction continues during ageing. In the specimens prepared with higher r.f. sputtering power (1.0–1.5 kW) the reaction is completed during the sputtering. One more characteristic feature has been observed. When gold is sputtered at lower power (0.6 and 0.8 kW) it is significant whether the sputtering is done continuously or it is interrupted.

The difference is presumably provoked by the kinetic energy of the sputtered particles, and not by a temperature increase, because the substrate is water-cooled before and during the 1 min sputtering. Depending on the intended use of the specimen, the first or the second way of sputtering should be used. If the sputtering is made using higher power (1.0–1.5 kW), the reaction is completed during the sputtering, so that the mentioned alternative does not exist.

2.4.4. InSb–Cu

The specimens are prepared by thermal evaporation and by r.f. sputtering of copper film on InSb, bulk indium and antimony. The obtained results [73] are presented in Table LVII.

The table shows that there is no compound formation on InSb if a copper sputtering power of 0.6 kW is used, while a higher power (0.7–1.0 kW) leads to the formation of Cu_2Sb and CuIn. During the following 2 mon, no change was observed. Examination of the same specimens after 5.5–6 y [62] showed, however, that certain changes occur. The Cu_2Sb and CuIn compounds were formed in the specimens sputtered with 0.6 kW power. Thus, the composition of the specimen is equal to the composition of specimens sputtered with higher power, but immediately after sputtering. In the specimens sputtered using higher power, no changes were observed after 5.5–6 y.

It seems that the reaction process was nevertheless initiated in the specimen sputtered with 0.6 kW, but it was insufficient to be observed by XRD, similar to the thermally evaporated film. The process took place during ageing and the obtained X-ray reflections are quite distinct, as in the specimens sputtered with higher power. In the latter, the process stopped when the sputtering was interrupted.

Copper thermally evaporated in vacuum on bulk indium gives CuIn, but on bulk antimony or InSb there is no compound formation.

TABLE LVII Conditions of compound formation during r.f. sputtering of copper on bulk polycrystal indium or antimony and bulk single-crystal InSb

Sputtering conditions (kW/min)	Cu film thickness (nm)	Compounds formed on		
		Polycrystal		Single-crystal InSb
		In	Sb	
0.6/1.5	60	CuIn	0	0
0.7/1.5	80	CuIn	0	Cu_2Sb CuIn
0.8/1.5	120	CuIn	0	Cu_2Sb CuIn
1.0/1.5	160	Cu_4In	0	Cu_2Sb CuIn
1.0/2.0	200		Cu_2Sb[a]	Cu_2Sb CuIn
1.0/3.0	320		Cu_2Sb[a]	Cu_2Sb CuIn

[a] After 6–35 d a trace of Cu_3Sb appears [62].

2.4.5. InSb–Al and InSbTi

Only specimens with r.f. sputtered aluminium films have been prepared in the InSb–Al couple. The r.f. sputtering power of 1–2 kW and a sputtering time of 1–6 min have produced aluminium films 80–750 nm thick.

The formation of AlSb could not be definitely proved, either in as-prepared or in the 6.5 y old samples. A barely visible AlSb was obtained by sputtering aluminium on antimony (Table XLVII). No compound formation was found in either the as-deposited or 5 y old specimens prepared by sputtering titanium on InSb with 1 kW power for 10 min.

2.4.6. GaAs–Me and GaSe–Me contacts

Phenomena occurring in the GaAs and GaSe single-crystal bulk with gold, silver and copper films deposited on them have been studied experimentally [62]. The metal films have been prepared by vacuum thermal evaporation and by r.f. sputtering.

The results are presented in Table LVIII. It can be seen from the table that under given experimental conditions, there is no compound formation, except in one case, in either the as-deposited or 6.5 y old specimens.

The GaAs single crystal was found to react with the gold film only at 450 °C, producing Au_7Ga_2 [74].

3. Kinetics of compound formation

The mass diffused at a determined temperature is proportional to time and increases with temperature. The path length, (X), of the diffusing atoms is proportional to square root of time, (t), $X \approx (Dt)^{1/2}$ [75, 76], where D is the diffusion coefficient (cm^2s^{-1}). The diffusion coefficient is a characteristic constant for every diffusion couple at a determined temperature and for a given grain structure. This means of calculating the diffusion coefficient takes into account only diffusion in one direction thickening of the layer perpendicular to the interface. Therefore, the calculated D values are not quantitative but they represent a valuable approximation within one order of magnitude. This equation is also used to calculate the diffusion coefficient in thin-film metal couples at room temperature and serves as an indicator of the reaction rate. However, different researchers use different equations: $D = X^2/t$ [10, 26, 64], $D = X^2/2t$ [21, 41], $D = X^2/4t$ [77], or $D = X^2/16t$ [78].

Depending on the availability of equipment, quantitative measurements of the diffusion path, X, and time, t, are performed by different methods. There are also different opinions on the "diffusion path". Some

TABLE LVIII State of the semiconductor single-crystal–metal film contacts

Single crystal	Metal film	Film deposition procedure	Thickness and/or power/time	Period of measurement	Results and remarks
GaAs	Au	Thermal evaporation	50 and 100 nm	2 d–6 y	No compound; no change on ageing
	Au	R.f. sputtering	300 nm (1 kW/3 min)	7 d–6 y	No compound; no change on ageing
	Cr + Au	R.f. sputtering	Cr = 40 nm Au = 300 nm (1 kW/3 min)	7 d–6 y	No compound; no change on ageing Cr underlayer produced no visible change
	Ag	Thermal evaporation	100 nm	2 d–6 y	No compound; no change on ageing
	Ag	R.f. sputtering	1 kW/2.5 min or 6.0 min or 10.5 min	1 d–6 y	No compound; no change on ageing
	Cu	R.f. sputtering	1 kW/3 min or 6 min	5 d–6 y	No compound; no change on ageing
	Cu	R.f. sputtering	1 kW/10 min		An unidentified compound is formed
GaSe	Au	R.f. sputtering	1 kW/1 min	2 d–6 y	No compound; no change on ageing
	Ag	R.f. sputtering	0.6 kW/1.5 min	2 d–6 y	No compound; no change on ageing

researchers take the thickness of the compound formed [22]. Others consider that it is represented by the layer thickness of one metal diffusing into the other [26, 79, 80]. The third group of researchers take the sum of both metal layers taking part in the reaction, i.e. the sum of products of the layer thickness, d, and density, ρ, of the starting metals, A and B, divided by the density of the compound formed, C: $(d_A\rho_A + d_B\rho_B)/\rho_C$ [21]. The last manner of calculation is feasible only if the density of the formed compound is known, which usually is not the case. Anyway, the layer thickness of the compound formed is, at most, equal to the sum of the layer thicknesses of the starting metals, and at least equal to the layer thickness of one of the starting metals.

Two essential methods, direct and indirect, are used to follow the reaction progress.

(i) *The direct method.* In this method, the layer thickness of the compound formed is measured at different times. The Rutherford back-scattering spectroscopy (RBS) is used to measure directly the layer thickness [35, 36, 41, 81–84].

(ii) *The indirect method.* A change of some physical property as a result of the compound formation is followed as a function of time. Thus, change of electrical resistance of a metal couple as a consequence of the compound formation is followed at a fixed temperature as a function of time [85–88]. Another method used is to follow the decrease of reflection intensity of the golden layer, being the result of the formation of a compound with a layer of lead [26] or aluminium [10].

The X-ray diffraction falls into the indirect methods. A change in X-ray diffraction peaks due to the starting metals and compounds formed is followed as a function of time [21, 64, 79, 80, 89–91].

3.1. Room-temperature interdiffusion coefficients for vacuum-evaporated metal couples

This section contains room-temperature interdiffusion coefficients for 26 thin-film metal couples, each consisting of a high-melting metal (Ag, Au, Cu, Pd) and a low-melting one (Al, Bi, Cd, Ga, In, Pb, Sn, Te, Zn), vacuum evaporated at room temperature. One or more compounds are formed in the couples.

XRD has been used to follow the reaction of compound formation. A decrease of the X-ray peak height of the starting metals and increase of the peak height of the compound formed have been followed as a function of time. The X-ray peak height has been measured in two ways:

(a) by pulse counting at a given angle, θ, for 1 min. The counting had been repeated for the same θ in determined time intervals until the pulse number fell to the background level (for starting metals), or until the maximum value was reached (for the compound formed);

(b) the height of the X-ray peaks on the diffractogram for a specimen obtained at different times (several days, months or years), was measured using a ruler.

In the majority of cases, a decrease in the X-ray peak height due to the high-melting metal was followed. For the couples in which this was not possible, a decrease of peak height due to the low-melting metal was followed. In all the specimens studied, thicknesses of starting metals were adjusted so as to obtain the stoichiometric ratio corresponding to the compound formed.

The dependence of the X-ray peak intensity (pulse number or mm) on square root of time ($\text{min}^{1/2}$) was obtained from the experimental data. In all cases,

a linear dependence was obtained, indicating that the process of compound formation is a diffusion-controlled one.

A simple relation was used to calculate the interdiffusion coefficient: $D = X^2/t$, where X is the diffusion path (cm) and t is time (s). The initial thickness of the high-melting metal was taken to represent the diffusion path, X, and the time needed to complete the reaction was taken to represent the diffusion time, t.

In the case of very rapid processes, the X-ray peaks due to the starting metals could not be detected.

For several couples it was not possible to follow a decrease in the X-ray peaks of both the high-melting and the low-melting metals. Therefore, a disappearance of the colour of gold (or copper) was taken as the indicator of the completion of the reaction. The gold (copper) thickness was taken to represent the diffusion path, and the time until the disappearance of the metal colour as the corresponding time.

In this manner, the interdiffusion coefficients, D, were calculated for the couples in which one compound/couple is formed, as well as the interdiffusion coefficients, D_1, of the first-formed compounds in the couples in which more than one compound/couple is formed. For the couples in which two or three compounds are formed, the thickness of the first-formed compound was used as the path, X, in order to calculate the interdiffusion coefficients, D_2 and D_3 of the second-formed and third-formed compounds, respectively. A detailed description of such a calculation is given in the text concerning the Ag–In, Ag–Te, Au–In and Au–Zn couples.

The interdiffusion coefficient values represent numerical values of the rate of compound formation for the couples studied. These calculated coefficients can be considered only as convenient approximations [91].

Subsequent text contains data relative to the individual couples. The following data are given for each couple: the compounds formed; the procedure used to measure the X-ray peak intensities; the diagram representing the dependence of the X-ray peak intensities on time, or data for the disappearance of the colour of gold (copper), the calculated values of D, D_1, D_2, D_3, and in the cases where different literature data exist on the interdiffusion coefficients, they are presented and commented upon.

3.1.1. Ag–metal couples

3.1.1.1. Ag–Cd. In the Ag–Cd couple three compounds are formed: $AgCd_3$, AgCd and Ag_5Cd_8. Progress of the $AgCd_3$ formation was followed on the specimen containing 75% Cd, in which only this compound was formed. Because the most intensive X-ray peak due to silver, at $\theta = 19.22°$, overlaps one of the $AgCd_3$ peaks, it could not be used, and therefore one of the cadmium peaks was measured (Fig. 1). The time until all cadmium had reacted was taken from the diagram. Because the starting metal thicknesses were adjusted in order to correspond to the stoichiometric

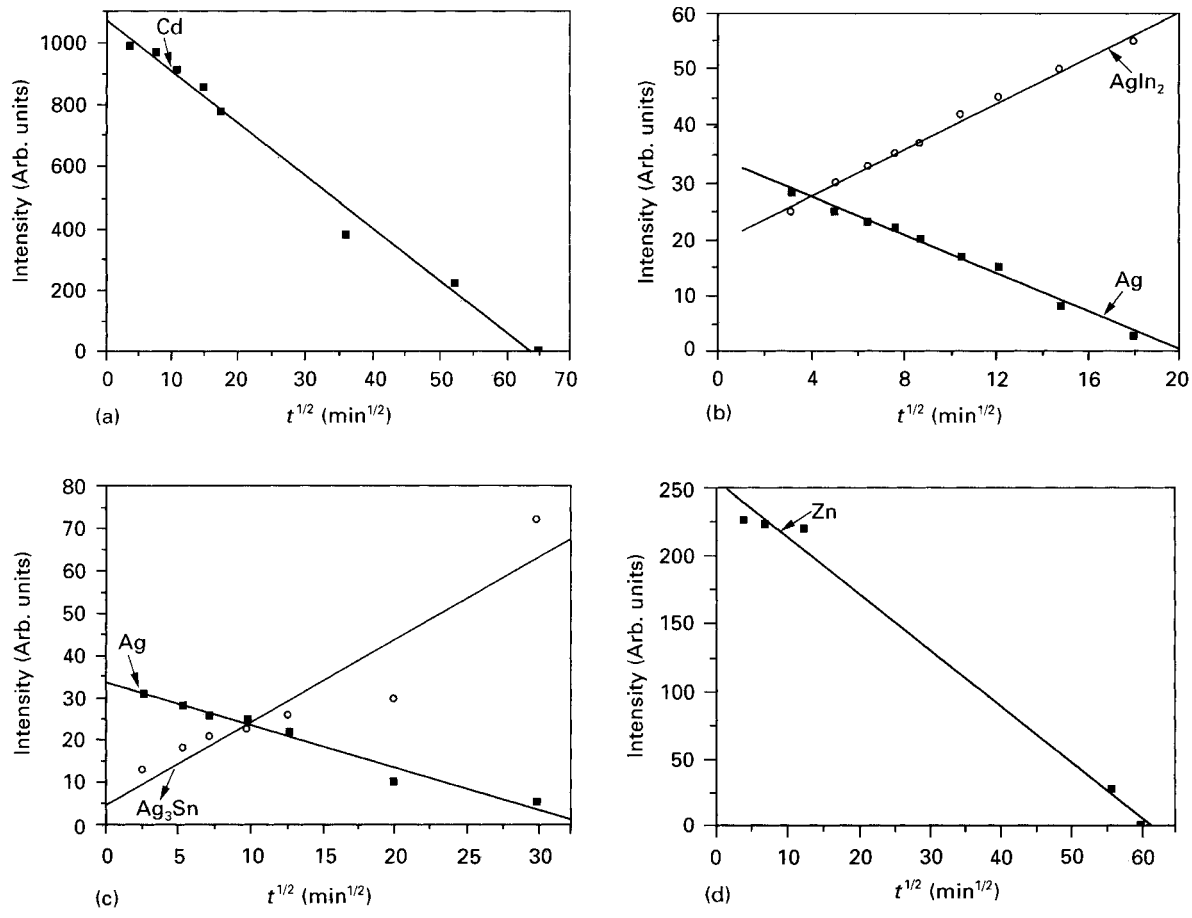

Figure 1 X-ray intensities of different metals and compounds in the Ag–Me couples, versus the square root of ageing time. (a) Ag(60 nm)–Cd(110 nm), (b) Ag(50 nm)–In(181 nm), (c) Ag(50 nm)–Sn (110 nm), (d) Ag(50 nm)–Zn(250 nm).

ratio of $AgCd_3$, the reaction time of silver is equal to that of cadmium. Taking the starting silver thickness, the value $D = 1.4 \times 10^{-16}$ cm^2 s^{-1} was obtained [5].

Progress of the reactions of AgCd and Ag_5Cd_8 formation could not be followed, because the transformation of $AgCd_3$ to these two compounds proceeds partially and simultaneously.

3.1.1.2. Ag–Ga. In the Ag–Ga couple, only one compound, Ag_3Ga, is formed. The Ag_3Ga formation is so rapid that the variation in intensity of the silver diffraction maxima could not be followed.

In the X-ray diffractogram of the sample composed of silver and gallium 73 and 119 nm thick, respectively, taken 2 min after deposition, silver could not be identified. The gallium layer is amorphous and therefore cannot be identified. Only the diffraction maxima corresponding to the Ag_3Ga compound were found. From the diffusion path (silver layer 73 nm thick) and time needed to complete the reaction (2 min), the value $D = 4.4 \times 10^{-13}$ cm^2 s^{-1} was obtained [80].

3.1.1.3. Ag–In. In the Ag–In couple, two compounds, $AgIn_2$ and Ag_2In, are formed. In the sample containing 68 wt% In, $AgIn_2$ only was formed. The rate of its formation was studied by following the decrease in the silver (1 1 1) diffraction maxima (Fig. 1). From the diffusion path (silver layer 50 nm) and time needed to complete the reaction of the silver layer (400 min), the value $D_1 = 1.1 \times 10^{-15}$ cm^2 s^{-1} is obtained [80].

The diffusion coefficient of the other compound, Ag_2In, was calculated as follows. In the specimen containing 34 wt% Zn, two compounds were formed. At the beginning of the reaction the entire amount of indium (80 nm) was consumed in about 625 min, producing $AgIn_2$. The compound formed began to react after that time with the excess silver to form Ag_2In. This reaction was completed after 8100 min when the X-ray peak due to $AgIn_2$ completely disappeared. Supposing that the thickness of the first-formed compound ($AgIn_2$) was equal to the starting indium thickness (80 nm), and that the compound reacted completely to form Ag_2In, this thickness could be taken to represent the diffusion path, X, and 8100 min would be the diffusion time. The diffusion coefficient value for Ag_2In calculated from these data is $D_2 = 1.3 \times 10^{-16}$ cm^2 s^{-1}.

Keppner *et al.* [22] studied the kinetics of $AgIn_2$ formation by measuring the thickness, d_{comp}, of the compound formed as a function of time, $t^{1/2}$, at a fixed temperature. The interdiffusion coefficient at room temperature (300 K) thus obtained amounts to about 10^{-12} cm^2 s^{-1} for $AgIn_2$. This value is considerably higher than that obtained from Marinković and Simić's results, the difference presumably being a consequence of the different experimental and calculation methods.

The formation of $AgIn_2$ phase has been found to be diffusion controlled, the activation energy being about 0.43 eV [24].

3.1.1.4. Ag–Sn. In the Ag–Sn couple, only one compound, Ag_3Sn, is formed. The rate of formation of the Ag_3Sn was followed from the decrease in the silver (1 1 1) diffraction peak intensities. The intersection of the straight line (Fig. 1) representing the decrease of the silver diffraction peaks with the X-axis, indicates the time when the complete quantity of silver has reacted (1225 min). The interdiffusion coefficient, determining the rate of Ag_3Sn formation was calculated from these data, $D = 3.4 \times 10^{-16}$ cm^2 s^{-1} [90]. Sen *et al.* [86] state that the reaction in the Ag–Sn sample composed of silver and tin layers 100 and 95 nm thick, respectively, was completed in a few days (100 h), as can be determined from the diagram presented. From these data, using the equation $D = X^2/t$, one can calculate the interdiffusion coefficient value of 2.7×10^{-16} cm^2 s^{-1}, which is close to the value obtained by Markinković and Simić.

3.1.1.5. Ag–Te. Two compounds, Ag_2Te and Ag_5Te_3, are formed in the Ag–Te couple. The progress of compound formation was studied on the sample containing silver and tellurium having thicknesses of 52 and 294 nm, respectively. In the X-ray diffractogram of the sample taken 3 min after deposition, only the diffraction peaks of Ag_2Te and tellurium were identified, those of silver being absent, which shows that the silver layer has reacted completely in less than 3 min to form Ag_2Te. The interdiffusion coefficient calculated from these data amounts to $D_1 = 1.5 \times 10^{-13}$ cm^2 s^{-1}, which determines the rate of Ag_2Te formation. The X-ray diffractograms of the sample taken during the following days show a gradual decrease in intensity of the Ag_2Te and tellurium diffraction peaks, as well as the appearance followed by an increase in the Ag_5Te_3 peaks. The complete absence of the diffraction peaks due to Ag_2Te in the X-ray diffractogram taken 25 d after deposition, shows that this compound has reacted completely. The following procedure was used to estimate the interdiffusion coefficient value. The thickness of the first-formed compound is at least equal to the initial silver thickness (52 nm). Because this compound reacts completely in 25 d, this time was taken as the diffusion time and the value of $D_2 = 1.2 \times 10^{-17}$ cm^2 s^{-1} was obtained [80].

It was found that the rate of Ag_2Te formation during sputtering or thermal evaporation of tellurium on the silver layer was equal to the rate of tellurium deposition [86]. The rate of tellurium sputtering was 40 nm s^{-1} and that of thermal evaporation was 5 nm s^{-1}. From these values, the interdiffusion coefficients, 1.6×10^{-11} cm^2 s^{-1} and 2.5×10^{-13} cm^2 s^{-1}, respectively, can be calculated. The latter value is in agreement with experimental results obtained by Marinković and Simić for Ag–Te layers prepared by thermal evaporation [80]. A higher rate of compound formation in thin-film couples formed by sputtering was also observed in other systems [48].

3.1.1.6. Ag–Zn. Three compounds, $AgZn_3$, AgZn and Ag_5Zn_8, are formed in this couple. Progress of the $AgZn_3$ formation was studied by following the decrease of the zinc diffraction peak intensity (Fig. 1). Because the thicknesses of the two metal layers were adjusted to correspond to the stoichiometric value of

$AgZn_3$, it is considered that the reaction times of both metals were equal. Taking the starting silver thickness and time from the diagram (Fig. 1), the interdiffusion coefficient value of $1.1 \times 10^{-16}\,cm^2\,s^{-1}$ has been obtained [5].

The progress of AgZn and Ag_5Zn_8 formation could not be followed because the transformation of $AgZn_3$ to these two compounds proceeds partially and simultaneously.

Bandyopadhyay *et al.* [87] studied the kinetics of β-AgZn formation between room temperature and 300 °C, in thin-film Ag–Zn couples 200 and 300 nm thick, respectively. The room-temperature diffusion coefficient value, $D = 1.4 \times 10^{-17}\,cm^2\,s^{-1}$, has been obtained. The same authors found that the diffusion of silver into tin is several times that of silver into zinc. This behaviour is in accord with the results of Marinković and Simić for Ag–Sn [80] and Ag–Zn [5].

3.1.2. Au–Me couples

3.1.2.1. Au–Al. Two compounds, Au_2Al and $AuAl_2$ are formed in the Au–Al couple, the first within several days and the second after 3 y. The diffraction peaks of gold (1 1 1) aluminium (1 1 1) and Au_2Al (5 1 0) are all located at the $\theta = 19.15°$. Therefore, it was not possible to follow the reaction rate via the decrease in the diffraction peak intensities, but visually by following the disappearance of gold colour. For the sample with gold and aluminium layer thicknesses of 62 and 30 nm, respectively, the gold colour disappeared within 20 d. From these data, the interdiffusion coefficient $D_1 = 2.2 \times 10^{-17}\,cm^2\,s^{-1}$, determining the rate of Au_2Al formation, has been calculated. In another sample with gold and aluminium layer thicknesses of 39 and 33 nm, respectively, the gold colour disappeared after 3 y, when $AuAl_2$ was formed. A rough estimation gives the interdiffusion coefficient $D_2 = 1.6 \times 10^{-19}\,cm^2\,s^{-1}$ [79].

3.1.2.2. Au–Cd. Two compounds, $AuCd_3$ and AuCd, are formed in the Au–Cd couple. The diffraction peaks due to gold, cadmium and $AuCd_3$ have the same angular position, $\theta = 19.15°$. Therefore, the disappearance of the gold colour was used to follow the reaction rate. The sample with a gold layer 31 nm thick loses its colour within 1.5 h, giving rise to $AuCd_3$ only. From these data, the interdiffusion coefficient $D_1 = 1.7 \times 10^{-15}\,cm^2\,s^{-1}$ was estimated. In another sample, the cadmium layer 77 nm thick reacts completely within several hours with part of the gold to form $AuCd_3$ and then excess of gold reacts with the first-formed compound, which is thereby transformed into AuCd within 8 d. The interdiffusion coefficient $D_2 = 8.5 \times 10^{-17}\,cm^2\,s^{-1}$, which determines approximately the rate of AuCd formation, has been estimated from these data [79].

3.1.2.3. Au–Ga. Four compounds, $AuGa_2$, AuGa, Au_2Ga and Au_7Ga_2, are formed in the Au–Ga couple. In the sample containing 70 wt% Ga, gold has reacted completely with gallium during layer preparation, the loss of the golden colour showing that the reaction is completed. Thereby only one compound, $AuGa_2$, is formed. The interdiffusion coefficient was calculated from the gold layer thickness (100 nm) and the time of evaporation (1 min). The value $D = 1.6 \times 10^{-12}\,cm^2\,s^{-1}$, determining the rate of formation of $AuGa_2$, has been obtained from these data [79].

Interdiffusion coefficients for the remaining three compounds could not be determined, because in the samples containing 10–50 wt% Ga, the formation of different compounds proceeds simultaneously and too rapidly to be followed by the X-ray method.

3.1.2.4. Au–In. In the Au–In couple, four compounds are formed: $AuIn_2$, AuIn, Au_7In_3 and Au_4In. The progress of the compound formation was studied by following the decrease in the gold (1 1 1) diffraction peak intensity. The time required for the 67 nm thick gold layer to react completely is 529 min (Fig. 2). The interdiffusion coefficient, D_1, determining the rate of the $AuIn_2$ compound formation was thus calculated to be $1.4 \times 10^{-15}\,cm^2\,s^{-1}$. In another sample having gold and indium layer thicknesses of 100 and 50 nm, respectively, indium reacts with part of the gold in 180 min, again producing $AuIn_2$. The excess gold reacts with $AuIn_2$ to form AuIn compound within 5 d. If the entire indium layer has reacted to form $AuIn_2$ which was then transformed into AuIn, it can be considered that the $AuIn_2$ thickness is equal to the initial indium thickness, *i.e.* 50 nm. From these data, an approximate value follows of the interdiffusion coefficient, $D_2 = 5.0 \times 10^{-17}\,cm^2\,s^{-1}$, which determines the rate of AuIn formation. In the sample having gold and indium thicknesses of 80 and 16 nm, respectively, the reaction proceeds in the same manner as in the previous case; however, because the sample contains more gold, the reaction continues by the transformation of AuIn through Au_7In_3 into Au_4In. This transformation is completed within 4 mon, giving the final Au_4In product. From these data, an approximate value follows of the interdiffusion coefficient, $D_3 = 2.4 \times 10^{-19}\,cm^2s^{-1}$, which determines the rate of Au_4In formation [79].

3.1.2.5. Au–Pb. Three compounds are formed in the Au–Pb couple: $AuPb_3$, $AuPb_2$, and Au_2Pb. The progress of compound formation was studied by following the decrease in the gold (1 1 1) diffraction maxima (Fig. 2). In this sample, gold has reacted completely within 161 min. From these data, $D_1 = 3.7 \times 10^{-15}\,cm^2\,s^{-1}$ follows, determining the rate of $AuPb_3$ formation.

In another sample consisting of gold and lead layers with thicknesses of 74 and 67 nm, respectively, lead has reacted with part of the gold within 4 h, producing $AuPb_2$. From these data $D_1 = 3.1 \times 10^{-15}\,cm^2\,s^{-1}$ folows, determining the rate of $AuPb_2$ formation. The obtained value of interdiffusion coefficient corresponds to that calculated by Weaver and Brown [26] from the rate of decrease in the mirror reflection of gold. In the above-mentioned sample, the reaction continues by the reaction of excess gold with $AuPb_2$ to form Au_2Pb within 27 d. Because the thickness of $AuPb_2$ is at least equal to the initial lead layer

thickness, an approximate value of the interdiffusion coefficient can be obtained from these data, $D_2 = 1.9 \times 10^{-17}$ cm^2 s^{-1}, which determines the rate of Au_2Pb formation [79].

3.1.2.6. Au–Sb. Only one compound, $AuSb_2$, is formed in the Au–Sb couple. The $AuSb_2$ (2 0 0) and gold (1 1 1) X-ray peaks appear at the same angle ($\theta = 19.15°$) so that the increase in the former masks the decrease in the latter. The reaction rate was determined therefore from the decrease in the antimony (1 0 2) peak intensity (Fig. 2). The straight line obtained by plotting the antimony (1 0 2) peak intensity versus $t^{1/2}$ intersects the abscissa at 97 d. Because the gold and antimony thicknesses have been chosen to correspond to the stoichiometric value of $AuSb_2$, it can be considered that the time in which the entire gold has reacted will be the same. Taking the gold thickness to represent the diffusion path and time from the diagram, a value of $D = 4.0 \times 10^{-18}$ cm^2 s^{-1} determining the rate of $AuSb_2$ formation has been calculated [90].

3.1.2.7. Au–Sn. Four compounds are formed in the Au–Sn couple: $AuSn_2$, $AuSn_4$, AuSn and Au_5Sn. The reaction rate has been investigated for the sample in which only $AuSn_2$ is formed (53 wt% Sn). The experimental results show that the diffraction maximum of gold drops to the background level within 100 min (Fig. 2). This yields an interdiffusion coefficient value $D = 7.4 \times 10^{-15}$ cm^2 s^{-1}, which determines the rate of $AuSn_2$ formation [79].

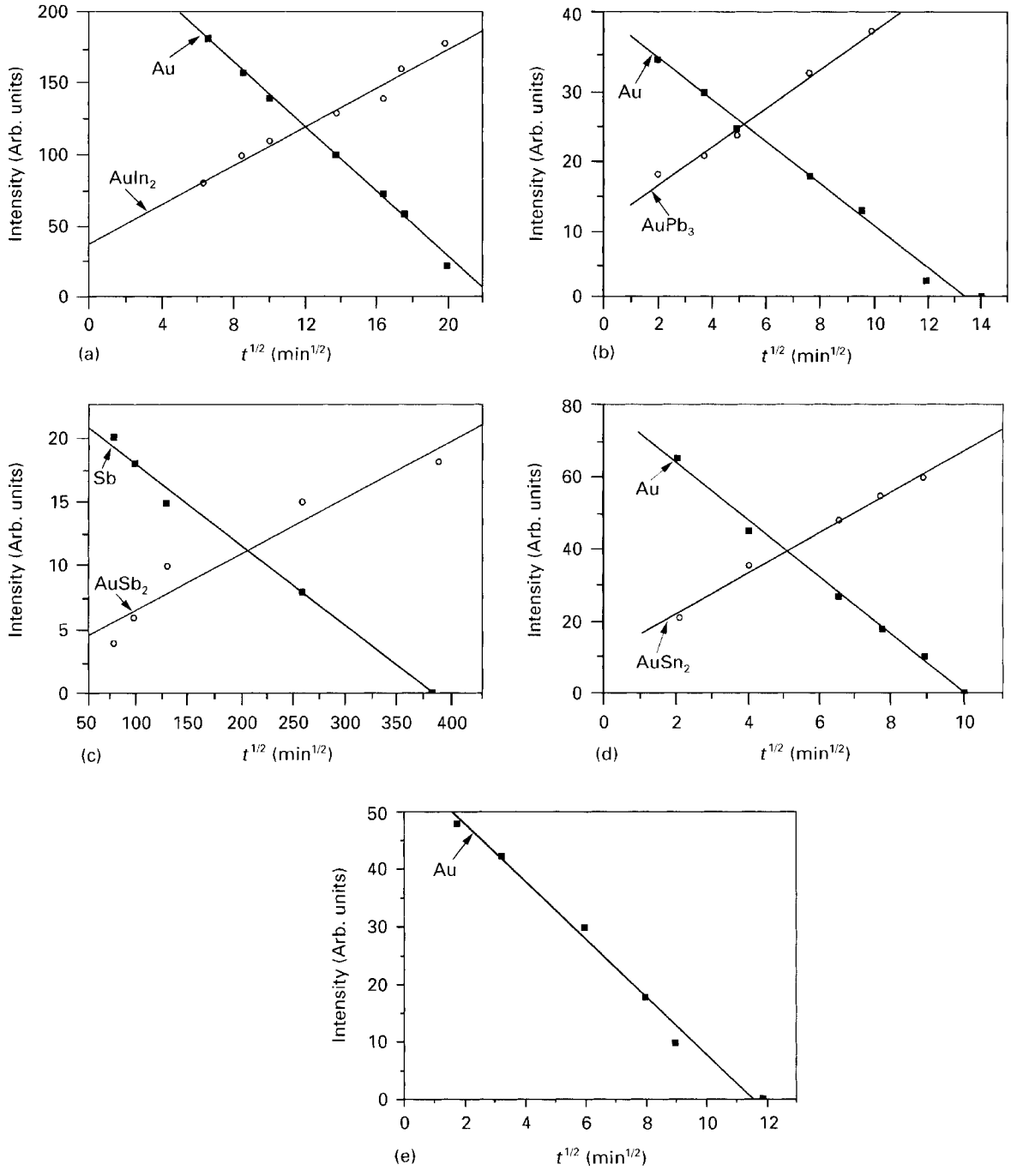

Figure 2 X-ray intensities of different metals and compounds in the Au Me couples versus the square root of ageing time. (a) Au(67 nm)–In (188 nm), (b) Au(60 nm)–Pb(430 nm), (c) Au(60 nm)–Sb(210 nm), (d) Au(67 nm) Sn(183 nm), (e) Au(60 nm)–Zn(300 nm).

3.1.2.8. Au–Zn. Three compounds are formed in the Au–Zn couple: $AuZn_3$, AuZn and Au_3Zn. The rate of $AuZn_3$ formation was investigated following the decrease of the gold (1 1 1) diffraction peak intensity (Fig. 2). From these data the interdiffusion coefficient value, $D_1 = 4.3 \times 10^{-15}$ cm^2 s^{-1}, has been obtained [62].

The approximate rates of formation for the other compounds have been determined by analysing the XRD patterns of the sample containing 10 wt% Zn (gold and zinc thicknesses of 80 and 24 nm, respectively). The reaction leading to $AuZn_3$ formation is completed within a few hours. It can be supposed that the compound thickness is at least equal to the initial thickness of the zinc layer, *i.e.* 24 nm. This compound then reacts with the excess gold to produce AuZn, the reaction being completed in 4 d. The interdiffusion coefficient value, $D_2 = 1.6 \times 10^{-17}$ cm^2 s^{-1}, determining the rate of AuZn formation, has been obtained from these data [79]. It takes 8 y for the AuZn contained in the sample to react completely with the excess gold to form Au_3Zn. From the AuZn layer thickness, taken to be at 24 nm, and time of 8 y, the interdiffusion coefficient determining the rate of Au_3Zn formation is obtained: $D_3 = 2.0 \times 10^{-20}$ cm^{-2} s^{-1} [79].

3.1.3. Cu–metal couple

3.1.3.1. Cu–Cd. Two compounds, Cu_4Cd_3 and $CuCd_3$, are formed in this couple. The copper diffraction peak at $\theta = 21.75°$ overlaps one of the Cu_4C_3 peaks and therefore it was not possible to follow intensity decrease of the copper peak, so that the reaction was followed visually. In the specimen Cu(50 nm)–Cd (70 nm), *i.e.* containing 57% Cd, which is the stoichiometric value of Cu_4Cd_3, 10 d after the specimen preparation, copper was no longer discernible and cadmium could not be detected by XRD. Taking the copper layer thickness to represent the diffusion path, the interdiffusion coefficient, $D = 2.0 \times 10^{-17}$ cm^2 s^{-1} has been calculated [90].

3.1.3.2. Cu–Ga. Only one compound, CuGa, is formed in this couple. The progress of compound formation was studied by following the copper X-ray peak intensity decrease and the increase of the CuGa peak intensity (Fig. 3). It can be seen that copper has reacted completely in 108 min. Taking the copper layer thickness as the diffusion path and the time from the diagram, the interdiffusion coefficient, $D = 3.1 \times 10^{-15}$ cm^2 s^{-1} was calculated [90].

3.1.3.3. Cu–In. Only one compound, CuIn, is formed in this couple. Progress of compound formation was studied by following the indium diffraction peak intensity. The copper diffraction peak could not be followed because it overlaps with one of the compound peaks. In the specimen Cu(45 nm)–In(145 nm) (Fig. 3), indium has reacted completely in 45 min and the copper colour is no longer visible. Taking the copper layer thickness as the diffusion path and time from the diagram, the interdiffusion coefficient $D = 7.5 \times 10^{-15}$ cm^2 s^{-1} was calculated [90].

3.1.3.4. Cu–Sb. Only Cu_2Sb is formed in this couple. The formation of the compound is very slow, so that first traces of its X-ray peaks become noticeable a month after the evaporation. The copper X-ray peak at $\theta = 21.75°$ overlaps with one of the compound peaks, so that the reaction progress could be studied only by following a decrease of the antimony peaks. The dependence represented in Fig. 3 has been obtained by measuring the antimony diffraction peaks in the diffractograms taken after 8 mon and after 8 y. It appears that antimony would react with copper completely within about 36 y. Taking the copper thickness and time from the diagram, the interdiffusion coefficient value $D = 1.2 \times 10^{-20}$ cm^2 s^{-1} was obtained [90].

3.1.3.5. Cu–Sn. Only Cu_5Sn_5 is formed in this couple. Progress of the reaction has been studied by following the tin X-ray peak intensity decrease (Fig. 3). Copper was not used for the same reason as in the Cu–In couple. Tin has completely reacted in 6.7 d and copper could not be seen. Taking the copper thickness (62 nm) and time from the diagram, the interdiffusion coefficient value $D = 6.6 \times 10^{-17}$ cm^2 s^{-1} has been calculated [90].

3.1.3.6. Cu–Te Three compounds are formed in this couple: Cu_3Te, Cu_7Te_5 and CuTe. In the X-ray diffractogram of the specimen Cu(80 nm)–Te(115 nm) taken 12 min after the specimen preparation, only the peaks due to Cu_7Te_5 and no diffraction peaks due to copper and tellurium were visible. Taking the copper thickness to represent the diffusion path, the interdiffusion coefficient value $D = 8.8 \times 10^{-14}$ cm^2 s^{-1} was calculated from these data [90].

3.1.3.7. Cu–Zn. Only one compound, $CuZn_4$, is formed in this couple. Progress of the compound formation has been studied by following the zinc X-ray peak intensity (Fig. 3). In the investigated specimen, zinc has reacted with copper completely within 20 d. It was not possible to follow a decrease of the copper X-ray peaks for the same reasons as in the Cu–In couple. Taking the starting copper thickness, the interdiffusion coefficient value $D = 3.8 \times 10^{-18}$ cm^2 s^{-1} was calculated [90].

3.1.4. Pd–metal couples

3.1.4.1. Pd–Bi. Only one compound, $PdBi_2$, is formed in this couple. Progress of the $PdBi_2$ formation was studied by following the decrease of a bismuths diffraction peak as a function of time (Fig. 4). Palladium reflects weakly and it is therefore difficult to follow the intensity decrease of its diffraction peaks. Taking the palladium thickness as the diffusion path, and the time from the diagram, the interdiffusion coefficient value, $D = 3.8 \times 10^{-17}$ cm^2 s^{-1}, has been obtained [90].

3.1.4.2. Pd–Ga. The $PdGa_5$ compound is the only one formed in this couple. The gallium layer is

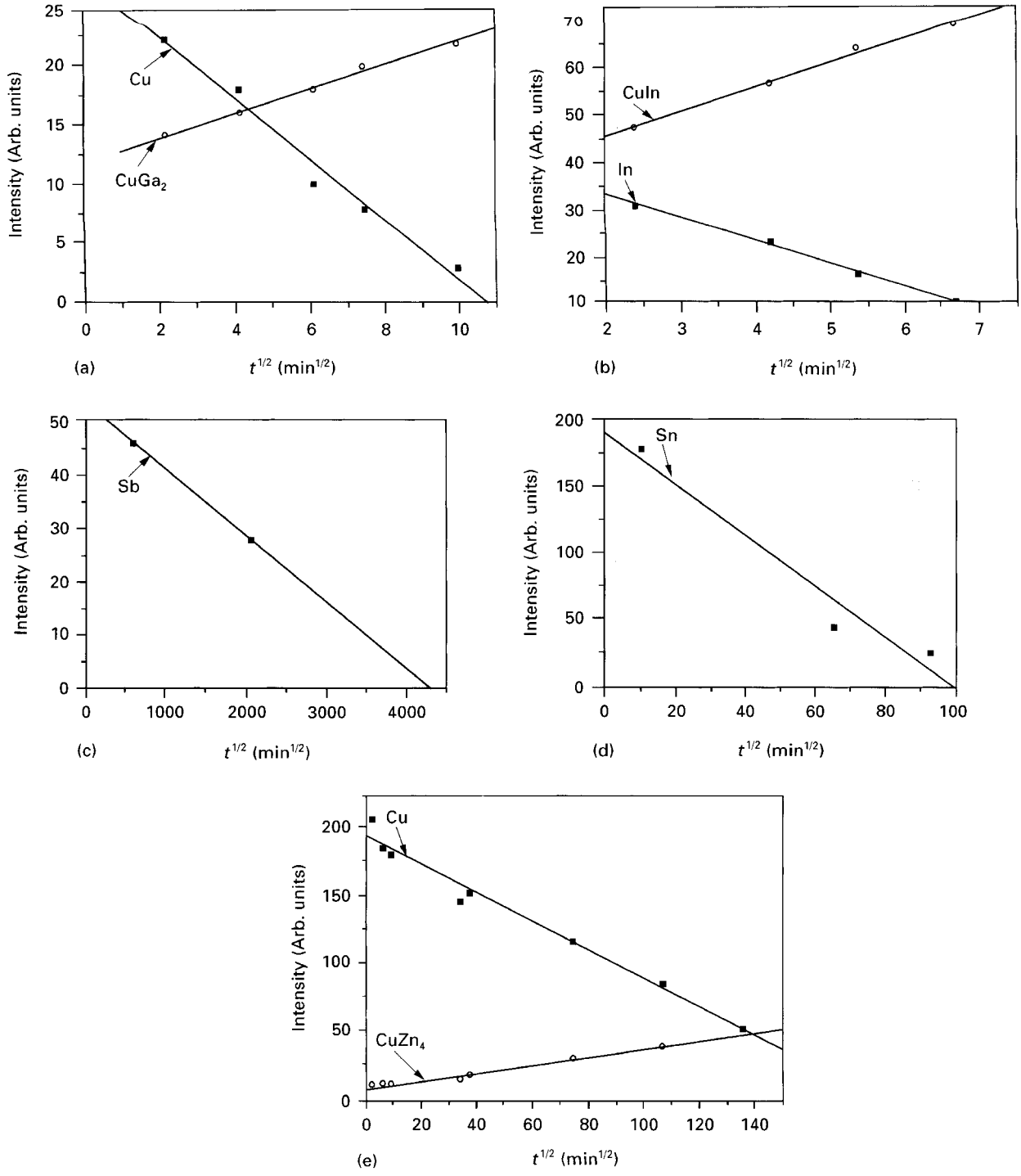

Figure 3 X-ray intensities of different metals and compounds in the Cu–Me couples versus the square root of ageing time. (a) Cu(45 nm)–Ga(144 nm), (b) Cu(45 nm)–In(145 nm), (c) Cu(38 nm)–Sb (152 nm), (d) Cu(62 nm)–Sn(124 nm), (e) Cu(26 nm) Zn(159 nm).

amorphous and palladium is weakly reflecting, and therefore the progress of the compound formation was studied by following the increase in the compound X-ray peak intensities in the specimen Pd(108 nm)–Ga(280 nm). The time at which the increase has stopped is taken to represent the time of the reaction completion (8 d). The starting palladium thickness was taken as the path, X. The interdiffusion coefficient value $D = 1.6 \times 10^{-16}$ cm^2 s^{-1} was obtained from these data [90].

3.1.4.3. Pd–In. Only one compound, $PdIn_3$, is formed in this couple. Palladium is weakly reflecting, so that the reaction progress was studied by following the decrease in the indium X-ray peak intensity (Fig. 4). Taking the starting palladium thickness as the diffusion path, and the time from the diagram, the interdiffusion coefficient value $D = 1.9 \times 10^{-17}$ cm^2 s^{-1} was obtained [90].

3.1.4.4. Pd–Pb. The $PdPb_2$ compound is the only one formed in this couple. For the same reason as in the Pd–In couple, the reaction progress was studied by following the lead X-ray peak intensity (Fig. 4), and the interdiffusion coefficient $D = 8.0 \times 10^{-17}$ cm^2 s^{-1} was determined in the same manner [90].

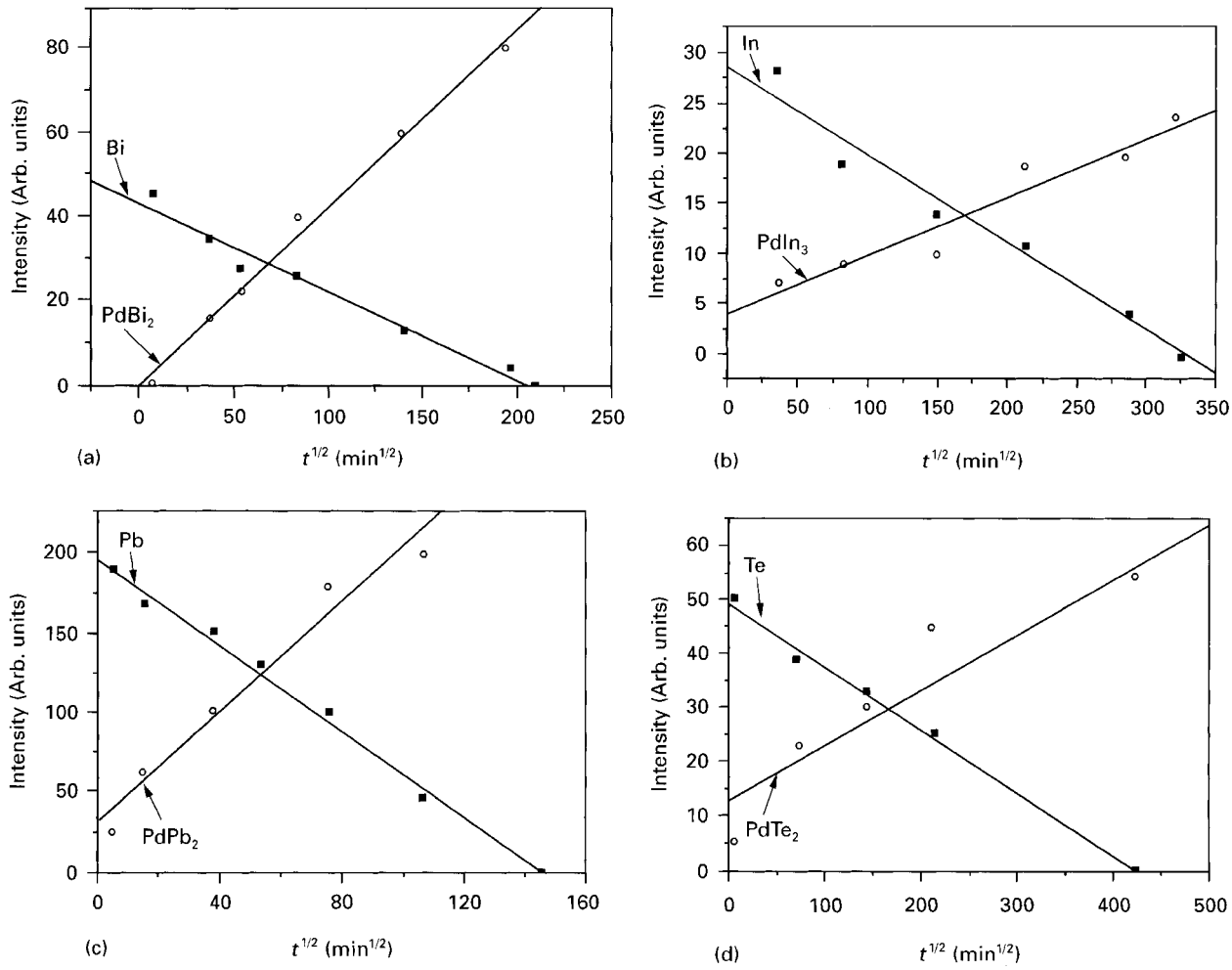

Figure 4 X-ray intensities of different metals and compounds in the Pd–Me couples versus the square root of ageing time. (a) Pd(100 nm)–Bi(456 nm), (b) Pb(112 nm)–In(187 nm), (c) Pd(100 nm)–Pb (418 nm), (d) Pd(95 nm)–Te (486 nm).

3.1.4.5. Pd–Te. Only one compound, Pd–Te_2, is formed in this couple. For the same reason as in the Pd–In couple, the reaction progress was studied by following the tellurium X-ray peak intensity (Fig. 4), and the interdiffusion coefficient $D = 8.5 \times 10^{-18}$ cm^2 s^{-1} was determined in the same manner [90].

3.2. Comparative analysis of interdiffusion coefficients

On the basis of the experimental results for 26 investigated couples, Table LIX has been made.

The results are grouped for the Ag–Me, Au–Me, Cu–Me, and Pd–Me systems, the low-melting metals (Me) being arranged by the increasing melting points. For the Au–Me, Ag–Me, Cu–Me and Pd–Me systems, linear relationships between interdiffusion coefficient and melting point of the low-melting metal have been found. This is shown in Fig. 5, in which naperian logarithm of diffusion coefficient of the first-formed compound, ($\ln D$), is related to melting point, (T_m) of the metal reacting with gold silver, copper and palladium, respectively. A linear least squares fit gives the relations

$$D = 2.36 \times 10^{-11} \exp(-0.0160 T_m) \quad (30)$$

for Au–Me

$$D = 3.20 \times 10^{-13} \exp(-0.0085 T_m) \quad (31)$$

for Ag–Me

$$D = 7.34 \times 10^{-13} \exp(-0.0015 T_m) \quad (32)$$

for Cu–Me

$$D = 5.59 \times 10^{-16} \exp(-0.0048 T_m) \quad (33)$$

for Pd–Me

From the results presented, it can be seen that the lower the melting point of the low-melting metal, the higher is the interdiffusion coefficient. i.e. the faster the diffusion. This is in agreement with findings of Bokshtein [92], according to which the activation energy of self-diffusion, (Q), in metals is proportional to their melting point, (T_m) : $Q = 34\ T_m$. It follows from this relation that for the metals having lower melting points, self-diffusion at room temperature requires lower activation energy than for the higher-melting metals.

In the couples where two or three compounds are formed, the interdiffusion coefficient of the first-formed compound (D_1) , is about two orders of

TABLE LIX Interdiffusion coefficients, (D), in metal–metal thin-film couples at room temperature

Metal couple, A–B	Melting temperature (°C) [4]		Compound formed	Melting/transformation temperature of compound formed (°C) [4]	Interdiffusion coefficient[a] (cm^2s^{-1})
	A	B			
Ag–Ga	961.9	29.4	Ag_3Ga	425	$D = 4.4 \times 10^{-13}$
Ag–In		156.6	$AgIn_2$	166	$D_1 = 1.1 \times 10^{-15}$
			Ag_2In	315	$D_2 = 1.3 \times 10^{-16}$
Ag–Sn		231.8	Ag_3Sn	480	$D = 3.4 \times 10^{-16}$
Ag–Cd		320.9	$AgCd_3$	590	$D = 1.4 \times 10^{-16}$
Ag–Zn		419.6	$AgZn_3$	631	$D = 1.1 \times 10^{-16}$
Ag–Te		452	αAg_2Te	145	$D_1 = 1.5 \times 10^{-13}$
			αAg_5Te_3	295	$D_2 = 1.2 \times 10^{-17}$
Au–Ga	1064.4	29.4	$AuGa_2$	491.3	$D = 1.6 \times 10^{-12}$
Au–In		156.6	$AuIn_2$	540.7	$D_1 = 1.4 \times 10^{-15}$
			AuIn	509.6	$D_2 = 5.0 \times 10^{-17}$
			Au_4In	649.25	$D_3 = 2.4 \times 10^{-19}$
Au–Sn		231.8	$AuSn_2$	309	$D = 7.4 \times 10^{-15}$
Au–Cd		320.9	$AuCd_3$	270	$D_1 = 1.7 \times 10^{-15}$
			AuCd	505	$D_2 = 8.5 \times 10^{-17}$
Au–Pb		327	$AuPb_3$	221.5	$D_1 = 3.7 \times 10^{-15}$
			$AuPb_2$	253	$D_1 = 3.1 \times 10^{-15}$
			Au_2Pb	434	$D_2 = 1.9 \times 10^{-17}$
Au–Zn		419.6	$LTAuZn_3$	225	$D_1 = 4.3 \times 10^{-15}$
			AuZn	725	$D_2 = 1.6 \times 10^{-17}$
			α_2Au_3Zn	270	$D_3 = 2.0 \times 10^{-20}$
Au–Sb		630.5	$AuSb_2$	460	$D = 4.0 \times 10^{-18}$
Au–Al		660.4	αAu_2Al	575	$D_1 = 2.2 \times 10^{-17}$
			$AuAl_2$	1060	$D_2 = 1.6 \times 10^{-19}$
Cu–Ga	1083.4	29.4	$CuGa_2$	254	$D = 3.1 \times 10^{-15}$
Cu–In		156.6	CuIn	310	$D = 7.5 \times 10^{-15}$
Cu–Sn		231.8	Cu_6Sn_5	189	$D = 6.6 \times 10^{-17}$
Cu–Cd		320.9	Cu_4Cd_3	547	$D = 2.0 \times 10^{-17}$
Cu–Zn		419.6	$CuZn_4$	~ 600	$D = 3.8 \times 10^{-18}$
Cu–Te		452	Cu_7Te_5	360	$D = 8.8 \times 10^{-14}$
Cu–Sb		630	Cu_2Sb	586	$D = 1.2 \times 10^{-20}$
Pd–Ga	1554	29.4	$PdGa_5$	200	$D = 1.6 \times 10^{-16}$
Pd–In		156.6	$PdIn_3$	664	$D = 1.9 \times 10^{-17}$
Pd–Bi		271	$\alpha PdBi_2$	380	$D = 3.8 \times 10^{-17}$
Pd–Pb		327	$PdPb_2$	454	$D = 8.0 \times 10^{-17}$
Pd–Te		452	$PdTe_2$	752	$D = 8.5 \times 10^{-18}$

[a] In the couples in which more than one compound is formed, D_1, D_2, D_3 are interdiffusion coefficients of the first, second and third compound formed, respectively.

magnitude larger than that of the second-formed compound, (D_2), which is, in turn, two orders of magnitude larger than that of the third-formed compound, (D_3).

The first compound is formed directly from the starting metals, the second one is formed by the reaction of the first compound with the excess of the high-melting metal, and the third compound is formed by the reaction of the second one with the excess of the high-melting metal. The exceptions are the Au–Al couple in which the first-formed compound reacts with the excess of aluminium and not of gold, and the Au–Sn couple in which both reaction types can take place, depending on the constituent concentrations. The interdiffusion coefficient values are in accord with the order in which the compounds are formed: the interdiffusion coefficient of the first-formed compound is the highest, and then follow the coefficients of the second and third compound.

For all the couples in which two or three compounds are formed, the first-formed compound has a lower melting point than the second one, and the melting point of the second compound is lower than that of the third one. An exception is Au_3Zn which is formed as the third compound, although its melting point is lower than that of the second one (AuZn). The reason is that the first-formed compound ($AuZn_3$) reacts with the excess gold to produce AuZn, which by reacting with gold produces Au_3Zn. Because Au_3Zn is formed as the third compound, its interdiffusion coefficient is the lowest one. In order to show reactivity of the low-melting metals with the high-melting metals studied. Table LX presents the values of the interdiffusion coefficient, (D_1), of; (i) gallium and indium with all the four high-melting metals; (ii) tin, cadmium, zinc and tellurium with three of them; and (iii) antimony and lead with two high-melting metals. It can be seen from Table LX that the interdiffusion coefficient value of a given metal is the highest in the couple with gold, and then follow the couples with silver, copper and palladium. An exception is indium, for which the interdiffusion coefficients of the couples with gold, silver and copper are of the same order. It follows that gold is the most reactive, i.e. its reaction rate is the highest, and then follow silver, copper and palladium.

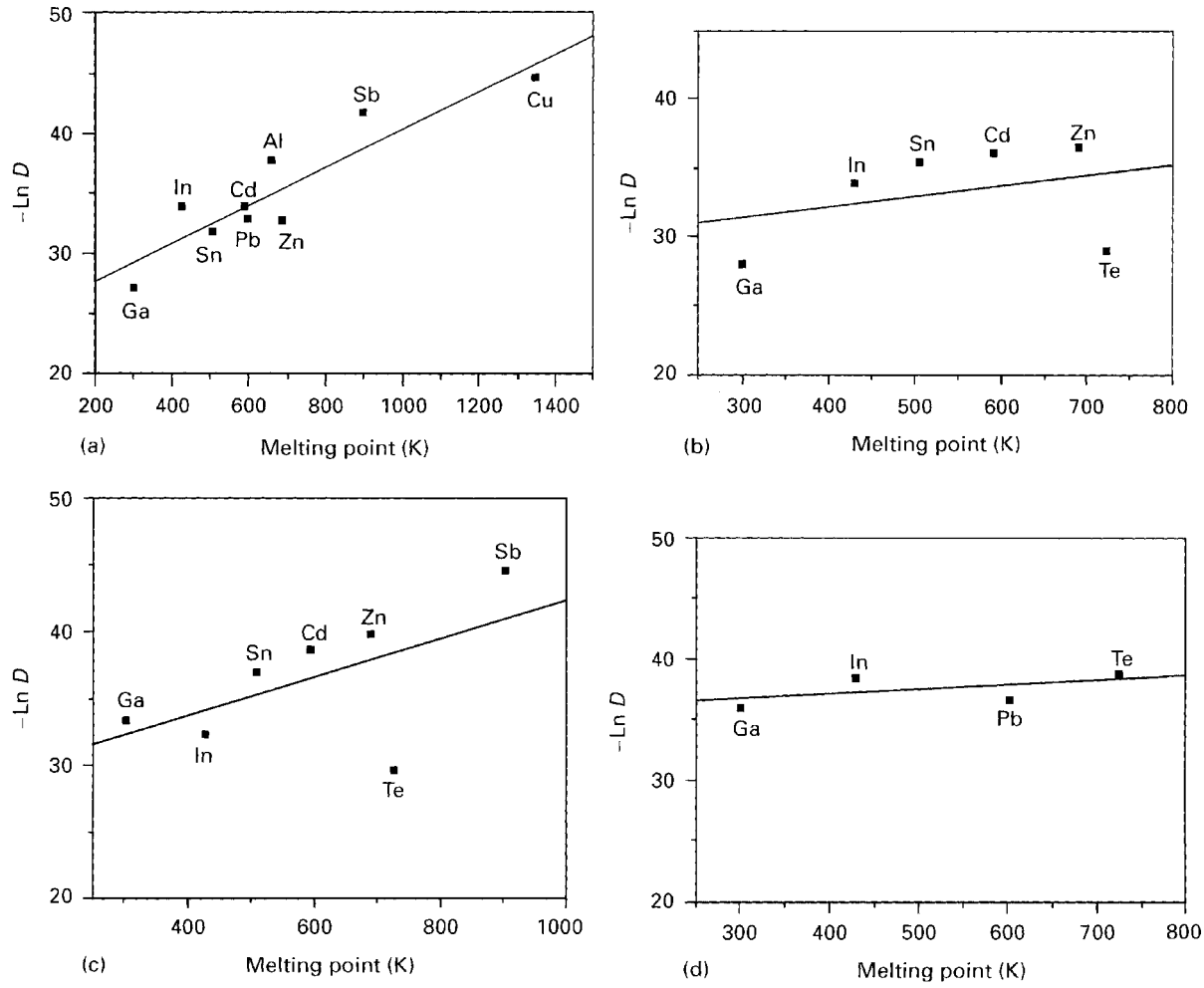

Figure 5 Diffusion coefficient, D ($cm^2 s^{-1}$) versus melting temperature T_m (K) of metals reacting with (a) gold, (b) silver, (c) copper and (d) palladium in thin-film couples.

TABLE LX Interdiffusion coefficients, D_1, ($cm^2 s^{-1}$) in metal-metal thin-film couples at room temperature

	D ($cm^2 s^{-1}$)			
	Au	Ag	Cu	Pd
Ga	1.6×10^{-12}	4.4×10^{-13}	3.1×10^{-15}	1.6×10^{-16}
In	1.4×10^{-15}	1.1×10^{-15}	7.5×10^{-15}	1.9×10^{-17}
Sn	7.4×10^{-15}	3.4×10^{-16}	6.6×10^{-17}	
Cd	1.7×10^{-15}	1.5×10^{-16}	2.0×10^{-17}	
Pb	3.7×10^{-15}			8.0×10^{-17}
Zn	4.3×10^{-15}	1.1×10^{-16}	3.8×10^{-18}	
Te		1.5×10^{-13}	8.8×10^{-14}	8.5×10^{-18}
Sb	4.0×10^{-18}		1.2×10^{-20}	

Gold is most reactive also from the viewpoint of the number of the low-melting metals with which it reacts (9) and the number of the compounds formed (24). Then follow silver (6 couples, 13 compounds), copper (7 couples, 10 compounds) and palladium (5 couples, 6 compounds).

4. Reaction progress and rules regulating compound formation

On the basis of experimental results obtained during the 1970s/1980s in studying behaviour of thin-film metal couples at room temperature (see Section 2), a certain picture could be formed about the compound formation processes in the couples.

It is a well-known fact that the properties and performance of polycrystalline materials including polycrystalline thin films, are strongly affected by the grain structure. Therefore, the process is considered here starting from the microstructure of the metal films in the couple. Polycrystalline thin films contain a large number of microcrystalline grains with corresponding grain boundaries. The higher the melting point of the metal, the smaller are the grains in the evaporated thin film, the larger their number in a given volume and the larger is the number of grain boundaries; and vice versa. In addition, thin films may contain dislocation densities as high as 10^{10}–10^{11} cm^{-2} [93]. It is well established that dislocations and grain boundaries in metal films act as rapid diffusion short-circuits. In general, the short circuit diffusion proceeds with a lower activation energy than the lattice diffusion. Accordingly, short circuiting tends to become particularly important at relatively low temperatures [93, 94]. It is particularly pronounced at room temperature and therefore the diffusion mass transport at this temperature most often proceeds by such a mechanism.

Many experiments have shown [6, 13, 47] that compounds are most often formed at room temperature

when one of the metals is high melting (fine-grained film), and the other is low melting (coarse-grained film). Because of the lower energy needed (rapid diffusion short circuits), the diffusion mass transport via grain boundaries and dislocations is intense. Diffusion in one direction (for example from a fine-grained film to a coarse-grained one) will be dominant with respect to the opposite direction. The resulting constant flux permits intimate contact of the two metals at the interface. This may lead to diffusion through the crystal grain. A solid solution may be formed by incorporation of one of the metals by substitution or in the interstitial positions of the other metal structure. This may be followed by compound formation, starting perhaps on the contact of crystal grain and grain boundary. An excellent example for compound formation is presented in the article by Nakahara and McCoy [95].

Ma *et al.* [96] show evidence that interdiffusion of aluminium and nickel leading to solid solution precedes the formation of intermetallic crystalline compounds. This step indicates the importance of prenucleation interdiffusion in the selection of the first intermetallic phase that subsequently forms. Furthermore, in the bright-field micrographs they observed the protrusion of $NiAl_3$ into the grain boundaries of aluminium. Barmak *et al.* [97] made similar observations in sputter-deposited Nb/Al multilayers, annealed at 600 K. The evidence presented clearly reveals the formation of $NbAl_3$ along the Nb/Al interface and its protrusion, i.e. preferential formation, along the grain boundaries of aluminium. It can be concluded that niobium (in this instance) is diffusing along the grain boundaries of aluminium as has also been concluded for zirconium in Zr/Al layers [98], thereby highlighting the importance of grain-boundary diffusion in thin-film reactions.

These recent experimental results indicate that the earlier created picture of the reaction processes in thin-film metal couples was not incorrect.

The results of investigation of the reaction processes in thin-film metal couples obtained until some ten years ago, including those presented in this monograph, were interpreted by the so-called one-step models. These models and descriptions focus primarily on the growth stage and to a much lesser extent on the nucleation phase. Therefore, they could not always explain the entire process which is obviously more complex. Thus, papers appeared contributing to the knowledge of the real complexity of the processes.

Coffey *et al.* [99] supplied experimental evidence for nucleation during thin-film reactions. The results of a study of the Nb/Al and Ni/amorphous Si couples obtained by means of differential scanning calorimetry (DSC) and differential thermal analysis (DTA) suggested a two-step growth process. The authors have developed a model in which the first step is taken to be the nucleation and two-dimensional growth to coalescence of the product phase (compound) in the plane of the initial interface. The second step is assumed to be the thickening of the product layer by the growth perpendicular to the interface plane. The success of this simple model in describing the principal features of the experimental results for different metal couples suggested that nucleation is an important aspect of phase formation in thin-film reactions.

The early stage of solid-state reactions in thin-film couples was investigated at elevated temperatures and also for other couples. Thus the Ni–Al couple was investigated by Ma *et al.* [96], Michaelsen *et al.* [100] and Barmak *et al.* [101], the V/amorphous Si couple was the subject of a study made by Clevenger *et al.* [102], and the Ni/Zr couple was studied by Newcomb and Tu [103]. The results obtained indicated that there is a number of systems in which nucleation and growth take place prior to thickening of the product phase.

In the model by Coffey *et al.* [99] nucleation and growth parallel to the interface are combined with the growth normal to it in order to describe the rate of volume fraction transformed. The model was quite successful in describing the essential behaviour of Nb/Al and Ni/amorphous Si films [99], and, after minor modifications, that of Ni/Al [96] and V/amorphous Si [102].

It has been noted that such a description of reactive phase formation bears a great resemblance to the film formation from the vapour phase [104, 105].

The model was based on the measurements at elevated temperatures. The question is whether it is applicable to the reactions at room temperature. The appearance of isolated randomly formed islands observed in early reaction stages at room temperature [62], indicates such a possibility. However, no paper confirming it has yet been published. The most important methods used for investigation at elevated temperatures cannot be employed to study the room-temperature reactions, while the methods used so far at room temperature were not able to register two stages in the compound formation. In order to use TEM, which is the method most often used to study these processes, considerable adaptations are needed in sample preparation and in the measurement procedures to enable the two-stage processes to be observed. In addition, TEM does not supply all the necessary information.

New experiments at elevated temperatures will perhaps indicate procedures that might also be used at room temperature. By the measurements both at room and elevated temperatures, several points should be clarified. In the case of the two-stage process schematically outlined for the first phase formation, experiments should test whether it is the same for the formation of the second and following phases. Namely, the interface is different and one of the constituents is a new phase and not the starting element. In addition, the possibility to obtain interdiffusion coefficients should be checked for every stage and for every phase formed in the couple.

4.1. Couples in which compounds are formed

In order to understand the reaction process, we shall analyse in this section only the vacuum-evaporated

metal couples in which compounds can be formed according to the phase diagrams [4]. In some of these couples the compounds can be formed at room temperature, but in others there is no room-temperature compound formation.

In order to prepare the couples, 23 metals were used. According to their melting points, they can be classified into three groups:

(i) metals with high melting point (960–1775 °C) (12);
(ii) metals with medium melting point (630–660 °C) (3); and
(iii) metals with low melting point (29–450 °C) (8).

This classification is justified by the experimentally established relationship between the melting point of the metal and the ability of compound formation at room temperature. It fits well in the classification made earlier [106, 107] on the basis of the relationship between the melting point of the metal and the grain size of the microcrystals in the evaporated thin film. The metals were then divided into three groups: "I – with m.p. above 1900 °C. II – with m.p. between 600 and 1900 °C and III – with m.p. below 650 °C". It was established that grain size of the crystals in the evaporated thin films generally increases with decreasing melting point of the metal. These results indicate that melting points of the metal and grain size of the crystals in the film influence compound formation in the metal couples.

The metals with medium melting point (aluminium, magnesium, antimony) are those capable of compound formation with high-melting metals (Al + Au form Au_2Al and $AuAl_2$) with low-melting metals (Mg + Ga form Mg_2Ga and Mg_2Ga_5), or with both groups of metals (Sb + Au form $AuSb_2$; Sb + Cu form Cu_2Sb, Sb + Pd form PdSb and Sb + Ga form GaSb). Therefore, they may be considered as the "metals in the intermediate region" and a *natural boundary between the low-melting and high-melting metals*. The range of their melting point (630–660 °C, or perhaps melting points from ~600 °C to ~700 °C) can be considered as the "range of intermediate temperatures".

4.1.1. Number and characteristics of compounds formed

Table XLIV shows that room-temperature compound formation takes place in 39 couples. In 23 couples, a single compound is formed, and in the remaining 16 couples more than one (two, three, or four) compounds are formed.

The available experimental materials and the necessary literature data are assembled in two tables: Table LXI refers to the couples with a single compound, and Table LXII refers to those with more than one compound formed at room temperature.

Out of 23 couples in which a single compound/couple is formed, at room temperature, the respective phase diagrams allow, in 17 of the couples, more than one compound (or phase) [4]. In the majority of these 17 couples (Table LXI), compounds formed have the lowest melting point in the couple and at the same time the highest concentration of the low-melting metal in the couple.

TABLE LXI Data relative to couples in which only one compound/couple is formed at room temperature

Couple Metal A–B	Concentration range studied (wt % B)	Compounds formed		
		Formula [4]	m.p. (°C) [4]	
Ag–Ga	18–75	ξ′ (Ag_3Ga)	425	a,b
Ag–Sn	15–75	ε (Ag_3Sn)	480	a,b
Au–Sb	9–86	*$AuSb_2$*	460	
Au–Te		*$AuTe_2$*	464	a,b
Cd–Te	34–70	*αCdTe*	1098	
Cu–Ga	15–68	ν (CuGa)	254	a,b
Cu–In	15–85	CuIn	310	a,b
Cu–Sb	23–75	η $CuSb_2$	586	a
Cu–Sn	20–85	η′ (Cu_6Sn_5)	189	a,b
Cu–Zn	26–83	$CuZn_4$	598	a,b
Ni–Ga	30–90	$NiGa_4$	363	a,b
Ni–Sn	40–73	NiSn Ni_3Sn_4 [8]	795	a,b
Ni–Te	69–81	$NiTe_2$		a
Pb–Te	15–60	*PbTe*	924	
Pd–Bi	37–80	$PdBi_2$	380	a
Pd–Ga	26–60	$PdGa_5$	200	a,b
Pd–In	26–52	$PdIn_3$	664	a,b
Pd–Pb	46–79	$PdPb_2$	474	a
Pd–Sb	40–54	PdSb	805	
Pd–Te	38–71	$PdTe_2$	752	a,b
Pt–Pb	[8]	$PtPb_4$	360	a,b
Pt–Sn	[8]	$PtSn_4$	522	a,b
Sb–Ga	27–47	*αGaSb*	712	

[a] The compound has maximal concentration of low-melting metal in the couple.
[b] The compound has lowest melting point in the couple. The compounds in italics are those only known according to the respective phase diagrams [4]. In the couples studied (except Pd–Bi and Pd–Pb), compounds are formed for all concentrations investigated.

Out of 13 couples with two or three compounds/couples formed at room temperature (Table LXII), the first-formed compound has the lowest melting point in eight couples and the highest concentration of the low-melting metal, also in eight couples.

Table LXI gives in the parentheses the formulae of the compounds designated in the phase diagrams [4] with Greek characters only.

4.1.2. Sequence of compound formation

The time at which evaporation of the upper layer has been stopped is taken as an approximate beginning of the reaction of compound formation in a metal couple.

If only one compound in a couple can be formed, and constituent concentrations are in the stoichiometric ratio, the reaction is finished when both constituents are completely consumed. In such a couple this compound is stable for a very long time.

If a number of compounds in a couple can be formed, the situation is as follows. When one of the constituents is in excess, the process can continue by the reaction of the first-formed compound with this constituent. The reaction can continue until the constituent in excess has been consumed and until the conditions for formation of new compounds exist. The

TABLE LXII Data relative to couples in which more than one compound/couple is formed at room temperature

Couple	Concentration range studied (wt % B)	Compounds formed			
Metal A–B		Formula [4]	m.p. (°C) [4]	Sequence of formation	
(a) Couples with two compounds					
Ag–In	11–80	$LTAgIn_2$	60–120 [6]	1	a, b
		Ag_2In	315	2	
Ag–Te	35–78	αAg_2Te	145	1	b
		αAg_5Te_3 [108]	265	2	
Au–Al	3–58	Au_2Al	575	1	
		$AuAl_2$	1060	2	
Au–Cd	15–71	$\varepsilon'(AuCd_3)$	270	1	a, b
		$\beta(AuCd)$	629	2	
Cu–Cd	25–90	γ (Cu_4Cd_3)	547	1	
		ε ($CuCd_3$)	397	2	
Mg–Ga	45–85	Mg_2Ga_5	203	1	a, b
		Mg_2Ga	441	1	
Ni–In	39–82	$LTNi_2In_3$	?	1	b
Pd–Sn	27–82	$PdSn_4$	295	1	a, b
		$PdSn_3$	345	2	
(b) Couples with three compounds					
Ag–Cd	39–76	ε ($AgCd_3$)	590	1	a
		γ' (Ag_5Cd_8)	640	2	
		β (AgCd)	736	3	
Ag–Zn	38–64	ε ($AgZn_3$)	631	1	a
		β (AgZn)	710	2	
		γ (Ag_5Zn_8)	661	3	
Au–Pb	24–85	$AuPb_3$	221.5	1	a, b
		$AuPb_2$	253	1	
		Au_2Pb	434	2	
Au–Zn	10–83	γ_2 ($AuZn_3$)	520	1	a
		β' (AuZn)	758	2	
		? (Au_3Zn)	?	3	
Cu–Te	20–85	Cu_3Te	317	1	b
		Cu_7Te_5	360	1	
		CuTe	407	2	

Note: In the couples Au–Ga, Au–In and Au–Sn with four compounds/couples formed, all the existing compounds are formed rapidly and practically at the same time. The presence of a number of compounds in the couple speeds up their formation and practically annihilates the influence of melting point on the sequence of their formation.

results of experiments on many couples indicate the following regularities.

(i) An excess of one of the constituents is present and the reaction leading to the compound richer in it can take place at room temperature. This compound can be formed, as well as the following compound still richer in the constituent if this exists. The reaction ends when the constituent has been consumed. Both variants, with an excess of the high-melting or low-melting metal, are possible.

(ii) An excess of one of the constituents is present, but the reaction leading to the compound richer in it cannot take place. The reason is that no such compound exists at all, or it does not exist at room temperature.

After excluding the Mg–Ga couple, in which both compounds formed are unstable and disappear, the remaining 15 couples (Table LXII) can be divided in three groups according to the compounds formed during the first day, for all the constituent contents.

(a) *First-formed compound having a maximum concentration of low melting metal.* An example is the Au–Zn couple, in which the $AuZn_3$ compound is formed first, for any concentration studied (Table XVII). The AuZn compound is formed initially in 2 days only in the specimen containing 27 wt% Zn. However, the appearance of AuZn represents probably part of the transformation process, because this concentration is approximately the stoichiometric value for AuZn. The transformation occurs according to the expression.

$$AuZn_3 + 2\,Au = 3\,AuZn \qquad (34)$$

and over 6 mon AuZn is formed in all the specimens containing less than 50 wt % Zn [5]. By following the transformation process, the formation of the Au_3Zn compound has been observed after 8 y in the specimen containing 10 wt % Zn [29]. The transformation occurs according to the expression

$$AuZn + 2\,Au = Au_3Zn \qquad (35)$$

The X-ray reflections due to gold, AuZn and Au_3Zn are observed in the diffractogram. The reaction is finished, although excess gold is present, because no compound containing more gold than in Au_3Zn is known in the Au–Zn system [53].

Thus, the transformation always takes place if an excess of the noble metal (gold) is present, leading to

the formation of compounds containing a progressively lower content of the low-melting metal. An excess of the low-melting metal (zinc) in the specimens with 56%–83% Zn would not change the situation, because no compound containing more zinc than in $AuZn_3$ is known.

Transformations in the Ag–Cd, Ag–In, Ag–Zn, Au–Cd, Au–Ga, Au–In, Au–Pb and Pd–Sn couples proceed in the same manner. Thus the following remarks are necessary. In the Ag–Zn couple [5], $AgZn_3$ transforms first to AgZn and then the remaining $AgZn_3$ transforms to Ag_5Zn_8. In the Au–In couple, $AuIn_2$ formation is not observed during the first day in the specimens containing 3.4–7 wt% In, because transformation to AuIn has after several hours already taken place in this case.

(b) *First formed compound having a minimum concentration of low-melting metal.* An example is the Ag–Te couple, in which Ag_2Te is formed during the first day (Table VII). In the specimens containing 44 and 54 wt% Te, Ag_5Te_3 formation is a part of the transformation process, which takes place according to the expression

$$5\,Ag_2Te + Te = 2\,Ag_5Te_3 \qquad (36)$$

Thus Ag_5Te_3 is formed over 6 mon in the specimens containing more than 35 wt% Te (35 wt% Te is approximately the stoichiometric value for Ag_2Te). The transformation process is then finished, because there is no compound with higher tellurium content than in Ag_5Te_3.

Transformations in the Au–Al, Cu–Cd, Cu–Te and In–Ni couples proceed in the same manner. It should be mentioned that in the Au–Al couple, aluminium is the low-melting metal (with respect to gold). In the Cu–Te couple, the transformation $Cu_7Te_5 + 2\,Te = 7CuTe$ takes place after several days, while the transformation $Cu_3Te + 2\,Te = 3\,CuTe$ has only been observed more than a decade later.

(c) *Both compound types (a and b) can be formed.* The only example is the Au–Sn couple, in which all four compounds can be formed during the first day (Table XVI). In this case, in the specimens containing an excess of gold. Au_5Sn will be formed. In the specimens containing an excess of tin, $AuSn_2$ and $AuSn_4$ are formed, their relative content depending on the tin concentration. Thus, both the previous cases can appear in this case.

Examination of the specimens containing 45, 53, 58, 73 and 82 wt% Sn was repeated 14 y later. In the specimen containing 45% Sn, the AuSn and $AuSn_2$ compounds have been identified. This happens because the tin concentration is between the stoichiometric values for these two compounds. In the specimen containing 53% Sn, no change with respect to the original state has taken place because this concentration is close to the stoichiometric value for $AuSn_2$ (54.62 wt% Sn). In the specimen containing 58% Sn, $AuSn_4$ has disappeared and $AuSn_2$ has remained, again because this concentration is close to the stoichiometric value for $AuSn_2$. In the specimens containing 73 and 82 wt% Sn, no change occurred. Although the latter specimen contains more tin than the former one, no reaction has occurred because no compound exists with higher tin content than in $AuSn_4$.

4.1.3. Constituent concentration ranges in which compounds are formed

The phase diagrams [4, 45, 53, 109, 110] and the majority of the handbooks contain chemical formulae of the compounds and designation of the phases, but do not always give the concentration ranges in which the compounds are present. The only available handbook containing such data is Smithell's book [1 1 1]. Therefore, this review paper has been used to compare the concentration ranges in which compounds formed in thin-film couples at room temperature appear, with concentration ranges in which the same bulk compounds appear according to the phase diagrams. It should be mentioned, however, that the Smithell's book does not contain data about all the compounds known to date.

It has been observed that the extent of the range in which the compounds are formed becomes changed in some couples during the reaction. The aim of this analysis is to determine the scope of these changes for the couples and compounds formed, as well as to find out how much the width of the range of compound formation at the end of the reaction corresponds to that given in the phase diagrams, i.e. in Smithell's book.

4.1.3.1. Formation of one compound/couple. In 17 couples, only one compound is formed at room temperature (Table LXI), although more compounds exist according to the phase diagram [4]. In 15 out of 17 couples the compound is formed in the whole investigated constituent concentration range (Pd–Bi and Pd–Te are exceptions). The extent of the concentration range does not change during the reaction, even after 10–15 y.

4.1.3.2. Formation of more than one compound/couple. The couples in which four compounds are formed at room temperature, are best suited to follow the scope of the concentration ranges in which the compounds are formed at the beginning and at the end of the reaction. The concentration ranges in which the compounds are formed are indicated by horizontal lines (Fig. 6). For each compound, the situation on the first day and at the end of the reaction is presented, as well as the situation for the same couple corresponding to the bulk (according to Smithell's [1 1 1]). It can be seen from Fig. 6 that the $AuGa_2$ and $AuIn_2$ compounds are formed during the first day in all the specimens, i.e. for any concentration. The remaining compounds are formed in broader concentration ranges than those corresponding to the bulk samples. It can be said that, as in the case of only one compound formed in the couple, all compounds tend to form for all constituent concentrations. Because of the transformation, the concentration range in which each

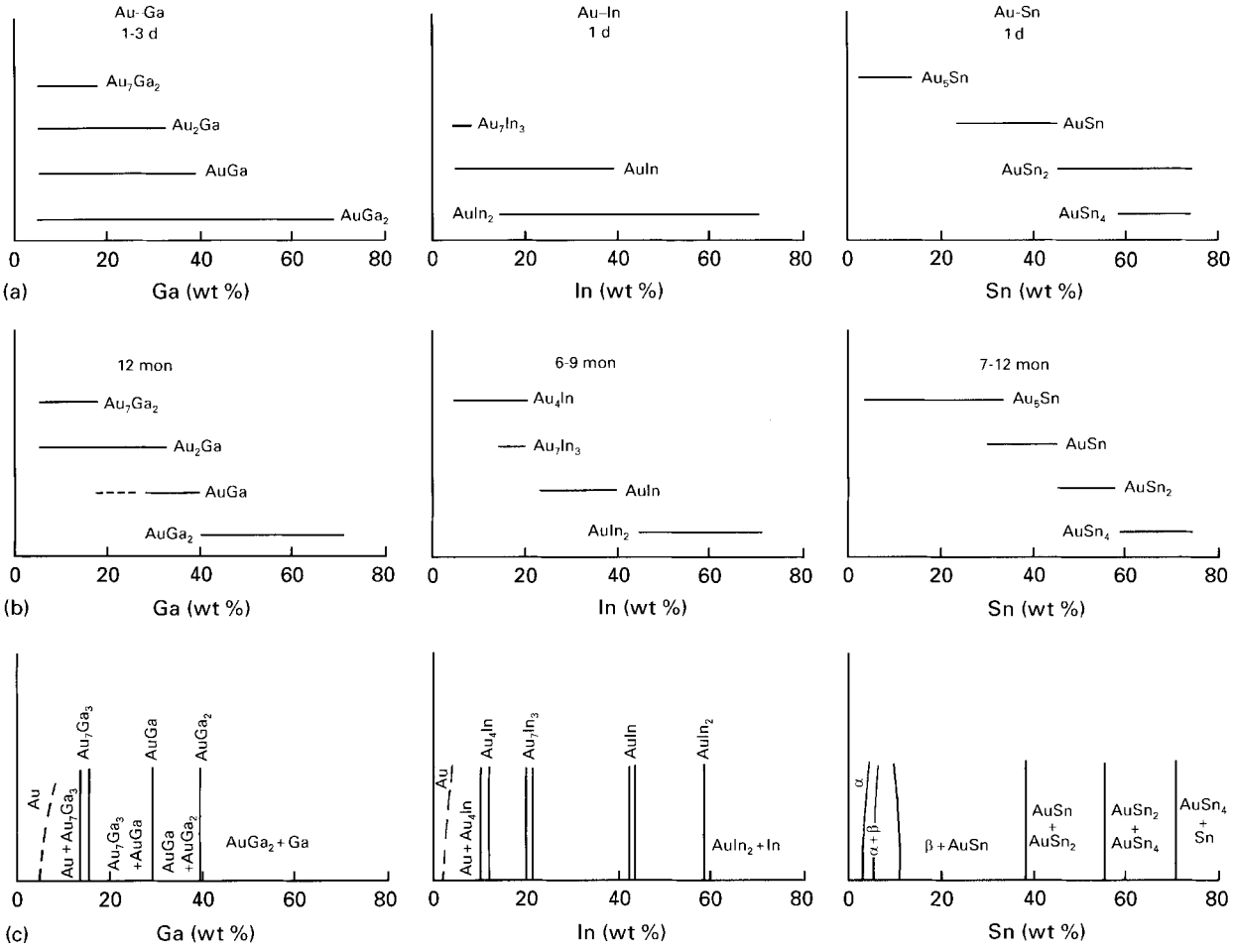

Figure 6 Constituent concentration ranges (wt% B) in which compounds are formed (for the couples in which four compounds are formed) : (a) beginning of the reaction; (b) end of the reaction; and (c) the phase diagram.

compound is formed becomes considerably contracted during the reaction. After the reaction has been completed, overlapping of the concentration ranges for different compounds in the given couple, mostly disappears. For a given couple, concentration ranges in which different compounds are formed form, with a little overlapping, a succession. A rather good agreement is obtained when the concentration ranges in which the compounds are formed at the end of the reaction are compared to the corresponding phase diagrams from Smithell's book. This shows that the state in thin-film specimens after the reaction completion corresponds rather closely to that of the bulk samples molten in a tube.

A similar behaviour is found for the couples Ag–Cd, Ag–Zn, Au–Pb, Au–Zn, Cu–Te in which three compounds/couples are formed. It should be pointed out that the phenomenon found for the couples forming four compounds has also been observed here, although results are not so impressive. The compounds formed during the first days in a wide concentration range, are reduced to a narrower range after the reaction has been completed. With a certain overlap, these ranges touch each other.

In the Ag–In, Ag–Te, Au–Al, Au–Zd, Cu–Cd, Ni–In, Pd–Sn couples, two compounds/ couples are formed. The results obtained are more convincing than for the couples with three compounds.

4.1.4. Rate and total reaction time

The reaction consists of two parts: (a) the formation of the first compound, and (b) the transformation of the first-formed compound to the other compound or compounds (if more than one compound exists in this couple). The reaction can stop for several reasons: because one or both constituents have been consumed, or because a barrier between the compound formed and one of the constituents has developed. The duration of the reaction depends on several factors: the rate of interdiffusion of the constituent metals, the specimen thicknesses and constituent concentrations.

Under the reaction process we shall not consider either the processes due to weathering (formation of compounds under atmospheric action), or the decomposition reactions due to long ageing, followed by amorphization.

The data relevant for discussion of factors cited on the reaction time are:

(i) the time to observe the first-formed compound;

(ii) the time to observe the second-formed compound (first transformation);

(iii) the time consumed before the reaction is finished.

Two tables have been made of the so-far existing experimental data. Table LXIII contains the data for 19 couples in which one compound is formed, and in

Table LXIV the data are presented for 16 couples in which more than one compound is formed. For the Au–Te, Pt–Pb, and Pt–Sn couples, investigated by other authors, as well as for the Pb–Sb couple, the existing data are not sufficient.

4.1.4.1. Time elapsed before first-formed compound was observed. It can be seen from Table LXIII that in the majority of the couples with one compound (10 of 19) this was observed during the first day. In the remaining couples, the compound was observed within 1 wk (four couples), within 2 wks (four couples), or within 7 wks (one couple). As far as the couples with more than one compound are concerned (Table LXIV), the first-formed compound was observed during the first day in 12 couples, and within 1 wk in four couples.

It can be concluded from the above data that formation of the first compound takes place rapidly. It is somewhat more rapid in the couples in which more than one compound is formed (the compounds are formed during the first day in 75% of the couples), than in the couples with one compound (during the first day the compounds are formed in 52.6% of the couples). The couples in which more than one compound is formed are more reactive and the process of the first compound formation is also more rapid.

4.1.4.2. Time elapsed before second and third compound were observed. The transformation process of the first-formed compound into the second one is somewhat slower than the process of the first compound formation. In 10 out of 16 analysed couples (Table LXIV) the transformation takes place within 2 d. In one couple, the transformation is observed after 1 wk and in three couples this occurs after 1–3 mon. Only in the Au–Al couple is formation of the second compound observed after 3 y. For the Au–Sn couple, the time of transformation cannot be defined in this manner. In five couples it is possible to measure time of formation of the third compound. In the couples Ag–Cd, Ag–Zn, Au–In, Au–Pb it extends from 1–4 mon, and in the Au–Zn couple it is identified after 8 y.

4.1.4.3. Time elapsed before reaction is finished. In order to compare time intervals within which the reaction in different couples stops, it is desirable to use the specimens with approximately equal thicknesses. Beside other factors (e.g. the interdiffusion coefficient), the duration of the reaction then depends on the constituent concentrations.

Tables LXIII and LXIV present the longest and the shortest duration of the reaction, as a function of constituent concentrations and stoichiometric values of the compounds formed. For certain constituent

TABLE LXIII Reaction progression in couples with a single compound formed

Couple		Compound formed		Total reaction time		Stoichiometric value of compound formed (wt% B)
Metal A–B	Total thickness (nm)	Formula	Observed (d)	Ended within	For wt% B	
Ag–Ga	172–192	Ag_3Ga	1	< 8.5 mon	17.5–24	17.5
				1 d	39–75	
Ag–Sn	170–210	Ag_3Sn	1	6 mon	15–27	25
				2 d	75	
Au–Sb	100–260	$AuSb_2$	8	> 3 mon	43–86	56
				1.5 mon	17.5–25.7	
Cu–Ga	180–190	CuGa	1	900 d	15–52	52
				2 d	62–68	
Cu–In	176–200	CuIn	1	10 d	70	65
				1 d	15–46	
Cu–Sb	175–220	Cu_2Sb[a]	51	[b]		
Cu–Sn	183–189	Cu_6Sn_5	1	3 mon	50	61
				1 d	85	
				5 d	20	
Cu–Zn	185–187	$CuZn_4$	1	10 d	26–62	83
				1 d	83	
Ni–Ga	147–176	$NiGa_4$	1	3–5 mon	44.3–90	82.6
Ni–Sn	171–183	NiSn	10	> 4 mon	> 50	67
Ni–Te	180–185	$NiTe_2$	9	> 7 mon	68.5–81.3	81.3
Pd–Bi	150–550	$PdBi_2$	2	[c]	37–80	79
Pd–Ga	200–450	$PdGa_5$	1	[c]	26–60	77
Pd–In	130–300	$PdIn_3$	2	~2 mon	26.4–51.8	77
Pd–Pb	195–520	$PdPb_2$	1	1.5–3 mon	> 60	
				1–4 d	< 60	
Pd–Te	185–580	$PdTe_2$	5	[c]		77
Sb–Ga	160–187	GaSb	7	9–11 y	37	37
				2.5 mon	> 50	
Cd–Te	170–200	CdTe	15	⩾ 8 mon	53.2	53.2
Pd–Te	100–200	PdTe	1	[a]		77

[a] The influence of the atmosphere is noticeable in the investigated time.
[b] Reaction ended after 5–8 mon for all antimony concentrations, even with excess of copper and antimony.
[c] Process not ended within the investigated time (about 2–3 mon).

TABLE LXIV Reaction progression in couples with more than one compound/couple formed

Couple		First-formed compound		Second-formed compound		Total reaction time		Stoichiometric value of compound according to sequence of formation (wt% B)			
Metal A–B	Total thickness (nm)	Formula	Observed (d)	Formula	Observed (d)	Ended within	For ~wt% B	I	II	III	IV
Ag–Cd	850–904	$AgCd_3$	1	Ag_5Cd_8	1	> 5 mon 14 d	51 76	76	62	51	
Ag–In	180–215	$LTAgIn_2$	1	Ag_2In	2	⩽ 9 mon ⩽ 5 d	26–35 < 25 > 50	69	34		
Ag–Te	187–197	Ag_2Te	1	Ag_5Te_3	1	6 mon 1 d	44 35,54	37	42		
Ag–Zn	665–1265	$AgZn_3$	1	AgZn	1	> 6 mon	38–64	64	38	50	
Au–Al	75–170	Au_2Al	4	$AuAl_2$	⩽ 3 y	⩽ 3 y ⩾ 2 mon	11–58 3–6	6	22		
Au–Cd	130–217	$AuCd_3$	1	AuCd	8	2.5 mon 1.5 mon	⩾ 51 ⩽ 36	63	37		
Au–Ga	150–760	$AuGa_2$	1	AuGa Au_2Ga Au_7Ga_2	1 1 1	1 y 1 d	5–40 ⩾ 60	42	26	17	12
Au–In	85–400	$AuIn_2$	1	AuIn Au_7In_3	1 1			54	37	20	13
Au–Pb	37–300	$AuPb_3$ $AuPb_2$	1 1	Au_2Pb	30	> 60 d 15–30 d	24–44 67–85	76	68	35	
Au–Sn	215–480	$AuSn_4$ $AuSn_2$ AuSn Au_5Sn	1 1 1 1			~ 12 mon ~ 12 mon 1 d 1 d	24–32 65–73 3–13 37–58	70	55	37	10
Au–Zn	216–350	$AuZn_3$	1	AuZn	2	8 y 2–3 mon	10 15–83	50	25	10	
Cu–Cd	120–220	Cu_4Cd_3	2	$CuCd_3$	30	> 90 d ⩽ 60 d	90 25–85	57	84		
Cu–Te	182–195	Cu_7Te_5 Cu_3Te	1 1	CuTe	2	3 mon ⩽ 13 d	60–85 20–50	40	58	67	
Mg–Ga	175–188	Mg_2Ga	1	Mg_2G_5	1			58	88		
Ni–In	180–184	$LTNi_2In_3$	2	$Ni_{10}In_{27}$	90	⩾ 1 y 3 mon	82 39	75	84		
Pd–Sn	170–800	$PdSn_4$	6	$PdSn_3$	48	> 3 mon	76–82	82	76		

Remarks. Third-formed compound in the couple: in the Ag–Cd couple, AgCd was observed after 40 d; in the Ag–Zn couple, Ag_5Zn_8 was observed after 60 d; in the couple Au–In, Au_4In was observed after 1.5 mon; in the Au–Zn couple, Au_3Zn was observed after 8 y.

concentrations, one or a few days are often a sufficient time interval needed for the reaction completion. However, in a number of cases, several months are necessary. No particular regularity could be observed in this respect.

The time within which the reaction is completed for all the constituent concentrations of a given couple is considerably more interesting. A compound is formed only for the concentration noted. In 10 out of 11 couples in which one compound/couple is formed, the longest reaction time is found for the specimens with a stoichiometric ratio of the constituents. For eight couples, the reaction time could not be established. The reasons are as follows. In five couples the reaction was not finished within the investigated period. In two couples the compound formed only for stoichiometric concentration of constituents, and in one couple the reaction was interrupted by a barrier formation.

In five out of eight couples in which two compounds/couples were formed, the longest reaction time was found for the constituent concentrations representing stoichiometric values of the second compound. For the remaining three couples, the reaction time could not be established.

In four out of five couples in which three compounds/couples were formed, the longest reaction time was found for the specimens with constituent concentrations corresponding to the stoichiometric values of the third compound formed. For the fifth couple, the process lasted for a very long time and it suffered from side phenomena.

Because of the complexity of the process, no such analysis could be made for any of the four couples in which four compounds were formed.

It was found that in about four out of five of the couples, the longest reaction time was needed for the constituent concentrations equal to the stoichiometric values. This happens for the last compound formed in a given couple (i.e. the first formed for the couple in which only one compound is formed, the second one for the couple in which two compounds are formed, and the third one for the couple in which three compounds are formed).

TABLE LXV Thin-film metal couples in which no compound was formed at room temperature

(a) One metal has high m.p., the other has low (or medium) m.p., but potential compound has high m.p.								
Au–Mg,	Co–Al,	Co–Ga,	Co–In,	Co–Mg,	Co–Sb,	Co–Te,	Cr–Al,	Cr–Ga,
Cr–Sb,	Ge–Mg,	Ge–Te,	Mg–Bi,	Mg–Sn,	Mn–Al,	Mn–Bi,	Mn–In,	Mn–Sb,
Mn–Te,	Ni–Al,	Ni–Mg,	Pd–Zn,	Sm–Al,	Sm–In,	Sm–Mg,	Sm–Pb,	Sm–Sb,
Sm–Sn,	Sm–Te,	Sm–Zn						
(b) Both metals have high m.p.								
Ag–Sm,	Au–Cu,	Au–Ge,	Au–Mn,	Au–Sm,	Co–Cr,	Co–Ge,	Co–Sm,	Cr–Ge,
Cr–Mn,	Cu–Ge,	Cu–Mn,	Cu–Sm,	Ge–Mn,	Ge–Ni,	Ge–Sm,	Mn–Ni,	Mn–Sm,
Ni–Sm								
(c) Both metals have medium m.p.								
Al–Mg,	Al–Sb,	Mg–Sb						
(d) Both metals have low m.p.								
Bi–In,	Bi–Te,	Ga–Te,	In–Sn,	In–Te,	Sn–Te,	Te–Zn.		
(e) One metal has medium m.p., the other has low m.p., and potential compound has low m.p.								
Al–Te,	Al–Zn,	Cd–Sb,	In–Sb,	Mg–Cd,	Mg–In,	Mg–Pb,	Mg–Te,	Mg–Zn,
Sb–Sn,	Sb–Te,	Sb–Zn						
(f) One metal has high m.p., the other has low (or medium) m.p., and potential compound has low m.p.								
Ag–Al,	Ag–Mg,	Ag–Sb,	Au–Bi,	Co–Sn,	Co–Zn,	Cr–Sn,	Cr–Te,	Cr–Zn,
Cu–Al,	Cu–Mg,	Mn–Ga,	Mn–Sn,	Mn–Zn,	Ni–Bi,	Ni–Cd,	Ni–Sb,	Ni–Zn,
Pd–Cd,	Sm–Cd,	Sm–Ga						

4.2. Couples in which no compound formation takes place

The results of experimental investigations are assembled in the Table LXV.

4.3. Formulation of rules

4.3.1. Analysis of results obtained

It was found experimentally that at temperatures above room temperature, one or more compounds were formed in a number of metal–metal couples. On the basis of reliable data. Walser and Bené [67] formulated a rule concerning the first-formed compound in the silicon–transition metal interfaces: "the first compound nucleated in planar binary reaction couples is the most stable congruently melting compound adjacent to the lowest-temperature eutectic on the bulk equilibrium phase diagram". Later Bené [112] extended this rule to thin-film metal–metal couples.

Experimental data from some published articles indicate that in thin-film metal–metal couples, compounds with higher concentrations of low-melting metal are formed at lower temperatures, while compounds with a lower concentration of these metals are formed at higher temperatures. There are a number of examples. In the thin-film Cu–In couple, CuIn is formed at room temperature [50], $Cu_{11}In_9$ at 200 °C [51], while Cu_9In_4 and Cu_7In_4 are formed at 400 °C [50]. In the Cu–Al couple, $CuAl_2$ is already formed at 200 °C [113]. In the couples of gold with titanium, zirconium and niobium at about 400 °C, Au_4Ti, Au_4Zr, and Au_2Nb, are formed respectively, but at higher temperatures the compounds with lower concentrations of the lower-melting metal (gold in this case) are formed [114]. In the Cr–Al couple, $CrAl_7$ is formed at 300–450 °C [115], in the Pt–Al couple Pt_2Al_3 is formed at 225–550 °C [116], but in the Pd–Al couple Pd_2Al_3 is formed at 200–450 °C [117]. Li *et al.* [118] found that in the Cu–Mg couple $CuMg_2$ is formed at 275 °C, but Cu_2Mg is formed at 400 °C; in the Cu–Pt couple Cu_3Pt is formed, and Cu_3Pd is formed in the Cu–Pd couple. The first-formed compound is again that containing the highest concentration of the lower-melting metal (in the first case it is magnesium, but in the second and third one, it is copper), D'Heurle and Ghez [119] formulated a rule which explains such a behaviour: in systems where one of the reactants, A, has a much higher diffusion coefficient (in the pure state) than the other, the first phase to grow should be a phase rich in A. This rule will be most valid as the differences in diffusion coefficients or, for that matter, melting points, between A and B are great.

Some authors [120, 121] related compound formation to effective heat of formation model. On this basis they even predicted which compound will be the first-formed one: "the first-compound phase to form during metal–metal interaction is the phase with the most negative effective heat of formation ($\Delta H'$) at the concentration of the lowest temperature eutectic (liquidus) of the binary system" [120]. Pretorius *et al.* [120] confirmed that rule for a large number of thin-film metal couples at elevated temperatures. One can see that in all cited couples, the first-formed (or the only-formed) compound has the highest concentration of the lower-melting metal in the corresponding couple.

The rules regulating compound formation at room temperature were not formulated until now, because of the lack of published data. Partial findings nevertheless exist. Tu and Rosenberg [8] found that in the couples of platinum, palladium or copper with tin or lead, compounds with the highest concentrations of the low-melting metals (tin, lead) were formed. Simić and Marinković found that in the couples Ag–Me [6], Au–Me [29] and Cu–Me [47] the compound formed had the lowest melting point (m.p.) in the corresponding couple.

Now we have sufficient data about formation (and the absence of formation) of compounds at room temperature. These results are collected in tables LXI,

LXII and LXV. From 131 examined couples, compounds were formed in 39, while no compound formation was detected in the remaining 92 couples. The compounds were formed mainly in the couples in which one metal is high-melting and the other is low-melting.

A considerable influence on compound formation is also exerted by the melting point of the compound. The majority of compounds formed do not have a high melting point. This is a consequence of the fact that a high compound melting point will almost always correspond to low diffusion coefficients of the metals involved and sluggish compound formation rates [90, 119].

On the basis of the experimental results mentioned, it can be concluded that, for optimum compound formation, the following conditions should be fulfilled: one metal with a high melting point, the other with a low melting point (one of the metals in the couple can also be medium melting), and the compound formed not with a high melting point. These conditions are fulfilled in 33 out of 39 couples in which compounds are formed at room temperature. The exceptions are four couples (Ga–Sb, Ni–Sn, Pd–Sb, Pd–Te) in which the compounds formed have high melting points. In addition, in two couples (Cd–Te, Pb–Te) with both low-melting metals, the compounds formed (CdTe, PbTe) have high melting points. These compounds are semiconductors.

In 33 out of 39 couples (four out of 5) all conditions for compound formation are fulfilled, and compounds have been formed. In 59 out of 92 couples (two out of three) all conditions for no compound formation are fulfilled, and no compound has been formed. In 33 out of 92 couples without any compound formed, for some potential compounds there are no existing data about melting point, or these compounds are not stable at room temperature [4].

4.3.2. Formulated rules

On the basis of the experimental results and analysis presented, the following rules can be formulated.

In thin evaporated film metal couples at room temperature:

(i) compounds are formed if one metal in the couple has a high melting point, the other metal has a low melting point, while the compounds formed do not have high melting points (one metal in the couple may have a medium melting point);

(ii) no compound formation occurs in the above case if potential compounds have a high melting point;

(iii) no compound is formed if both metals in the couple have melting points in the same temperature range;

(iv) the compound formed (or the first-formed one when more than one compound is formed) will be the one with lowest melting point or with the highest concentration of the low-melting metal in the respective couple.

5. Action of atmosphere on metals and metal couples

5.1. Action of atmosphere on evaporated thin metal films

The action of atmosphere on evaporated thin films of 20 metals were investigated. These were Ag, Al, Au, Bi, Cd, Co, Cr, Cu, In, Ga, Ge, Mg, Mn, Ni, Pb, Sb, Sm, Sn, Te and Zn. The films, 120 nm thick, were prepared at room temperature by evaporating the metals in vacuum on glass substrates. The films were stored under normal laboratory conditions. The behaviour of the films was followed by the XRD for 15 y. All the films, except gallium, were found to be polycrystalline.

Prolonged ageing results in the formation of oxides, carbonates, and hydroxides in 10 of the 20 investigated metal films (Table LXVI). Some of the products of oxidation that could not be identified by means of the available ASTM cards, are designated by (X).

It is of utmost importance whether the products of oxidation appear on a metal film, thus changing its characteristics, while the question of whether one or more oxides are formed is less significant.

5.2. Action of atmosphere on thin film metal couples

5.2.1. Evaporated thin film metal couples in which no compounds are formed

The action of the atmosphere was followed during prolonged ageing on 91 thin-film couples prepared by combining the 20 investigated metals. The total thickness (of both films) in the couples was approximately the same for all constituent concentrations. This means that the higher the metal concentration, the higher the film thickness; and vice versa.

The changes were followed over the course of 15 y. No reaction between the two metals in these couples took place and consequently no compounds were formed, although such compounds exist according to the

TABLE LXVI Influence of atmosphere on evaporated thin metal films after 15 y of ageing. X, unidentified compound

Metal film	Products of oxidation	ASTM data [3]	Metal film	Products of oxidation	ASTM data [3]
Ag	Ag_2O	12 0793	Mg	Mg(X)	
Bi	Bi_2O_3	29–0236	Mn	MnO(OH)	18–0804
Cd	Cd(X)		Pb	$PbCO_3$	5–0417
				Pb(X)	
Cu	Cu_2O	5–0667	Sb	Sb_2O_3	5 0534
	$CuCO_3$	27–0150			
In	In_2O_3	22 0336	Sm	$Sm(OH)_3$	6–117

TABLE LXVII Evaporated thin film metal couples in which no compounds are formed

Ag Al,	Al–Co,	Al–Cr,	Al Mn,	Al–Ni,	Al–Sb,	Al Te,	Al Zn,	Au–Bi,
Au–Cu,	Au–Ge,	Au Mn,	Bi Ni,	Co–Cr,	Co Ga,	Co Ge,	Co In,	Co Mg,
Co Sb,	Co Sn,	Co Te,	Co–Zn,	Cr–Ga,	Cr Ge,	Cr Mn,	Cr–Sb,	Cr Sn,
Cr–Te,	Cr Zn,	Cu Ge,	Ga–Mn,	Ga Te,	Ge Ni,	Ge–Te,	In–Sn,	Mn Te,
Mn–Zn,	Ni–Sb,	Ni–Zn,	Sb Sn,	Sb Te,	Sb–Zn,	Sn–Te,	Te Zn.	

phase diagrams, except for the Ag–Cu couple [4]. In 44 couples, products of oxidation did not appear. The couples are presented in Table LXVII.

In 47 couples, products of oxidation appeared on one or on both metals. These couples are presented in Table LXVIII.

The observation times for the metal couples were the same as those for the individual metals (Table LXVI). Therefore, it was not difficult to observe that the metals behave identically toward the atmosphere when they are alone or in couples (the same products of oxidation were formed on the same metal).

Therefore, the results presented in Tables LXVI and LXVIII may be useful to those investigating or applying thin metal films at room temperature or close to it. There are three possible combinations of two metal layers. Of the 91 couples, 24 couples belong to state (a), 44 to state (b) and 23 to state (c).

State (a)– the products of oxidation are formed on both metals, if these are alone. The products of oxidation were formed on both metals in 9 couples, from 24 possible; the products of oxidation were formed only on one of the two metals in 15 couples. When products of oxidation were formed only on one metal film, this was the bottom one in 11 couples, and the top one in four couples.

State (b)– the products of oxidation are formed only on one of the metals, if this is alone. The products of oxidation were formed on one of the metals in 23 couples. In 21 couples, no products of oxidation were formed, although it could be expected.

State (c)– no products of oxidation are formed on any of the metals, if these are alone, and they were not found.

It can be seen from state (a) that the products of oxidation were mostly formed on the bottom layer (11 couples compared to four on the top layer). The reason favouring such behaviour could be supposed. Inherent to thin films are numerous defects. The upper layer can therefore be regarded as a sieve for the atmospheric gases. These diffuse through it towards the bottom layer in which they become absorbed. There is a very small probability that the unabsorbed gases will escape from the bottom layer back to the atmosphere. However, the action of the atmosphere on the upper layer has a rather two-way character. One part of the atmospheric gases which enter the layer can escape. Therefore, the bottom layer is more susceptible to the action of the atmosphere than the top one.

When, for a given couple, there were several specimens with different constituent concentrations (states a and b) it happened that for some concentrations the products of oxidation were formed, but not for others. For example, in the Ag–Sb couple with 13% Sb, Sb_2O_3 was identified, but it was not detected in the specimens containing 25% and 65% Sb. In the Au–Mg couple, Mg(X) was found in the specimen with 11% Mg, only a trace of it could be found in the specimen with 20% Mg, while no products of oxidation were detected in the specimen containing 27% Mg. These two examples show that the thinner the top layer, the more easily the products of oxidation are formed on it.

The same can be proved for the products of oxidation formed on the bottom film. In the Cd–Sb, Mg–In and Mn–Sn couples, in which the sum of the top and bottom films, as usual, was approximately constant*, the products of oxidation formed on the bottom film were detected only when the top layer was thicker, i.e. when the bottom film was thinner (Table LXVIII).

A similar situation is true for the In–Sb and Mn–Ge couples. In these couples, the products of oxidation appear for all concentrations, but the relative intensity of the X-ray reflections is different for different concentrations. Thus, in the In–Sb couple with 51% Sb, the relative intensity of the In_2O_3 reflection is 52, but it amounts to 100 in the specimen containing 64% Sb. In the Mn–Ge couple, the relative intensity of the MnO (OH) maximum increases with increasing germanium content, i.e. with decreasing manganese film thickness (it amounts to 9% for 29% Ge, 15% for 35% Ge, 30% for 44% Ge and 100% for 46% Ge).

5.2.2. Evaporated thin-film metal couples in which compounds are formed

To date, 39 couples were examined in which compounds were formed at room temperature (Table XLIV). The action of the atmosphere during prolonged ageing was studied on 29 couples. The remaining ten couples were studied for too short a time (seven Pd–Me couples up to 4 y [46], two Pt–Me couples for 2 3 wks [8] and the Au–Te couple for 1 y [43]). In 15 out of 29 couples, there was no appearance of products oxidation in 10–15 y investigation. In seven of these 15 couples (Al–Au, Au–Ga, Au–Sn, Au–Zn, Ga–Ni, Ni–Sn, Te–Ni) the products of oxidation could not appear because they were composed from the metals stable to the action of the atmosphere. In another seven couples (Ag–Ga, Ag–Sn, Ag–Te, Au–In, Cu–Zn, Ga–Sb, In–Ni), products of oxidation could appear on one metal, and in the

*The total thickness (of both films) in the couples was approximately the same, and therefore a higher concentration of one metal means a higher thickness of the respective film; and vice versa.

TABLE LXVIII Influence of atmosphere on evaporated thin-film metal couples in which no compounds are formed (the metal concentrations are rounded up within 1 wt %)

Metal film in couple		Wt% of top film	Products of oxidation identified after	
Bottom	Top		1 y	10–15 y
Ag	Cu	25	0	Ag_2O
Ag	Mg	7,18,40,60	0	Mg(X)
Ag	Sb	13	0	Sb_2O_3
		25,65	0	0
Ag	Sm	36,51	0	$Sm(OH)_3$
Cu	Al	17,29,46	0	Cu_2O
Al	Mg	50	0	Mg(X)
Al	Sm	58,85	0	$Sm(OH)_3$
Au	Mg	11	0	Mg(X)
		20	0	Mg(X) (trace)
		27	0	0
Au	Sm	21,43,66	0	$Sm(OH)_3$
In	Bi	48	0	Bi_2O_3, In_2O_3
		65	Bi_2O_3 (trace); In_2O_3 (trace)	Bi_2O_3, In_2O_3
Mg	Bi	58	0	Mg(X)
Mn	Bi	79	MnO(OH)	MnO(OH)
Bi	Te	18,25,48	0	Bi_2O_3
Mg	Cd	60	Cd(X)	Cd(X),Mg(X)
		82	Cd(X)	Cd(X),Mg(X)
Ni	Cd	67,89	Cd(X)	Cd(X)
Cd	Sb	42	0	0
		52,75	0	Cd(X)
Sm	Cd	42,74	$Sm(OH)_3$	$Sm(OH)_3$, Cd(X)
Sm	Co	44	0	$Sm(OH)_3$
Cu	Mg	46,76	0	Cu_2O, $CuCO_3$ (trace), Mg(X)
Cu	Mn	22	0	Cu_2O (trace)
Cu	Sm	42,70,91	0	$Sm(OH)_3$
Sm	Ga	14,47	0	$Sm(OH)_3$
Mg	Ge	60	0	Mg(X)
Mn	Ge	29,35,44,46	0	MnO(OH)
Sm	Ge	51	0	$Sm(OH)_3$
Mg	In	41	0	0
		65	0	Mg(X)
Mn	In	31, 51	MnO(OH)	MnO(OH)
In	Sb	51	0	In_2O_3
		64	In_2O_3(trace)	In_2O_3
In	Sm	26	0	In_2O_3
In	Te	36,53	0	In_2O_3
Mg	Ni	55,83	0	Mg(X)
Mg	Pb	81	0	Mg(X), $PbCO_3$
Mg	Sb	77	0	Mg(X)
Mg	Sm	86	0	Mg(X), $Sm(OH)_3$
Mg	Sn	79	0	Mg(X)
Mg	Te	75	0	Mg(X) (trace)
Mg	Zn	45,84	0	Mg(X)
Mn	Ni	48	MnO(OH) (trace)	MnO(OH)
Mn	Sb	42,62	MnO(OH)	MnO(OH), Sb_2O_3
Mn	Sm	58	0	MnO(OH), $Sm(OH)_3$
		91	0	MnO(OH) (trace), $Sm(OH)_3$
Mn	Sn	42	0	0
		52,81	MnO(OH)	MnO(OH)
Sm	Ni	44	0	$Sm(OH)_3$
Sm	Pb	80	$Sm(OH)_3$ (trace); $PbCO_3$ (trace)	$Sm(OH)_3$, $PbCO_3$
Sm	Sb	11	$Sm(OH)_3$	$Sm(OH)_3$
Sm	Sn	70	0	$Sm(OH)_3$
Sm	Te	44,58	0	$Sm(OH)_3$ (after $\geqslant$ 2y)
Zn	Sm	70	0	$Sm(OH)_3$

couple Ag–In on both metals, but it did not occur. Table LXIX contains the results of investigation of 14 remaining couples after long ageing. As can be seen, the 14 couples, composed of the metals on which the products of oxidation could appear, these appeared within 1 mon in two couples, within 1 y in six couples and within the period of maximum investigation length (10–15 y) in all 14 couples.

In five couples, in which the products of oxidation could appear on both metals, this occurred in one couple (Cu–In), but only on one of the metals in the three couples (Ag–Cd, Cu–Cd, Cu–Sb) and neither

TABLE LXIX Influence of atmosphere on evaporated thin-film metal couples in which compounds are formed

Metal film in couple		Wt% of top film[a]	Products of oxidation identified after	
Bottom	Top		1 y	10–15 y
Ag	Cd	34,52	0	Cd(X)
Ag	Zn	35	0	Ag_2O
		48,67	0	0
Au	Cd	36,84	0	Cd(X)
Au	Pb	34,44,68	$PbCO_3$[b]	$PbCO_3$
Au	Sb	26,56,75	0	Sb_2O_3
Cd	Cu	75	0	Cd(X)
Cd	Te	34,58,70	Cd(X)	Cd(X)
Cu	Ga	15	Cu_2O (trace)	Cu_2O
		25	0	Cu_2O
Cu	In	15	0	Cu_2O
		25,85	0	In_2O_3
Cu	Sb	23	0	Sb_2O_3
		50	Sb_2O_3 (trace)	Sb_2O_3
Cu	Sn	20	Cu_2O	Cu_2O
		50	0	Cu_2O
Cu	Te	20	0	Cu_2O
		67	0	0
Ga	Mg	26,41	0	Mg(X)
Pb	Te	38,60	Pb(X)[b]	$PbCO_3$[b]

[a]The metal concentrations are rounded up within 1 wt%.
[b]Appeared after 2–3 wks.

metal in one couple (Ag–In). In ten couples, in which the products of oxidation could be formed on one of the metals, this actually occurred.

As can be seen from Tables LXVIII and LXIX, the products of oxidation appeared in thin metal couples, both with and without the compounds formed. The products of oxidation are formed in gradually *increasing number of couples in the course of time.*

In the initial period of ageing (up to 1 y) no regularity can be perceived for the couples both without and with the compounds formed. During this period, the products of oxidation appear in a small number of couples and it does not seem possible to anticipate in which couple this will occur.

In the final phase (after 10–15 y), the situation is quite different. In the couples without compounds, the products of oxidation appear on seven of the possible ten metals. Three groups of metal films can be distinguished. In the first group, oxides appear in virtually all investigated couples (on cadmium and lead in 100% on magnesium and samarium in 94%). In the second group of metals, the oxides appear in about half of the couples studied (on copper in 67%, on indium and manganese in 50%). In the third group, the oxide appearance is more an exception than the rule (on silver in 13% on antimony in 15% and on bismuth in 29%).

In the couples with compounds, the products of oxidation appear on five of the possible seven metals. The situation is analogous to that for the same five metals in the couples without compounds.

The number of couples with oxides with respect to the number of couples studied, can be examined on some examples. The increase in the number of the couples with oxides will be followed in the initial and the final period on bismuth and magnesium, i.e. on metals with a small and large percentage of the couples with oxides, respectively. The number of the couples with oxides on bismuth has increased from one in the initial to two in the final phase (of the six possible), i.e. from 14% to 29%. For magnesium, an increase from 0 to 15 (of the 16 possible) was found, i.e. from 0% to 94%.

The situation in the final phase for all the couples studied is as follows. In the couples without compounds, on seven of the possible ten metals (70%) and on those with the compounds in five of the possible seven (72%), oxides appear on more than a half of the couples studied. In other words, in nearly three-quarters of the metals on which the oxides could appear, these appeared in at least one-half, but often in much more, of the couples studied. This is a very high increase of the product of oxidation formation. It follows from the above that if, on a constituent metal in a couple, the products of oxidation can appear, the couple without the products of oxidation is, after long ageing, more an exception than the rule. *The products of oxidation will appear sooner or later.*

After long ageing, there is no great difference in the number of couples with the oxides formed, irrespective of whether the compounds have been formed in the couple, although the film configurations in these two couple classes (with and without compounds) is different. When there are no compounds, the metal films are distinct entities joined to each other via a common surface. When there are compounds formed on the film interface, the specimen is practically a single layer.

5.3. Action of atmosphere on bulk–thin film couples

The results relative to the compound formation in the bulk high-melting metal–low-melting metal film and bulk low-melting metal–high-melting metal film couples are presented in Section 2.2, Table XLV. In the present section, the influence of atmosphere is analysed in the same couples during ageing up to 13y: 21 specimens, in which products of oxidation can appear were investigated. The thickness of the evaporated films was 50–100nm. After about 13 y, products of oxidation appeared only on seven couples (33%) of the investigated specimens (on cadmium and lead bulk and on cadmium, antimony, copper and lead films).

5.4. Action of atmosphere on metal couples with top-sputtered film

In addition to specimens with an evaporated top film, specimens (film–film and bulk–film) with top-sputtered film were also examined. Only couples with possible oxides were studied.

The specimens of this type were prepared by sputtering: silver on aluminium antimony and tin films, aluminium on antimony film and copper on aluminium, gold, cadmium, gallium, germanium, antimony, tin and zinc films. The thicknesses of the evaporated bottom films were 100nm or 1 μm, and those of sputtered films 50–100nm. Out of these 12 specimens,

products of oxidation appeared on three, i.e. on 25% of the investigated couples.

The specimens of the bulk–film type were prepared by sputtering the top film: silver on bulk aluminium, indium and tin, gold on bulk cadmium and indium and copper on bulk aluminium, gold, cadmium, germanium, indium, tin and zinc. A total of 13 specimens with sputtered top film was studied. Thickness of the sputtered films were from 50 to 100nm.

After 11 y ageing, out of 13 specimens, oxides appeared only on three (23%). The products of oxidation appeared on copper, cadmium and tin-films, and on cadmium and antimony bulk.

5.5. Comparison of sensitivity of different specimen types to the influence of atmosphere

In thin-film couples, products of oxidation appear on the same metals as when these metals are alone, irrespective of whether or not compounds are formed in these couples.

The oxide formation on thin films is a relatively slow process. It is most rapid on lead film (they appear after a month) and slowest on silver film (after several years). On other metal films, the oxides appear after about a year.

In the bulk–film specimens, oxide formation occurs more slowly, irrespective of whether the film is evaporated or sputtered. This is in agreement with an earlier observation, according to which compound formation in the bulk–film couples proceeds more slowly than that in the film–film couples. In all these cases, the reason is a compact bulk constituent.

More sensitive to atmospheric action are film–film evaporated specimens (89 with possible: 70 with appeared oxides –67.4%). Less sensitive are bulk–film specimens (21: 7 – 33%), and specimens with top-sputtered film (25: 6 – 24%).

6. Stability of compounds during ageing

6.1. Decomposition of the compounds with simultaneous amorphization of one of the constituents

Considerable changes may take place in the compounds formed in thin-film metal couples during their ageing at room temperature. These were observed for 15 y following 21 of the couples in the Au–Me, Ag–Me, Cu–Me and Cd–Me systems [54]. For some of the couples, the reflections of the compounds formed disappear from the XRD powder patterns, but at the same time the reflections corresponding to one of the constituents (the noble metal) become considerably intensified. Thus, it is essential that the specimens were prepared in the same evaporation equipment and examined by the same X-ray diffractometer during the entire period of the study. The X-ray diffractograms of every sample were taken at definite time intervals, usually 5–20 times during 10–15 y. The total number of investigated samples amounts to nearly 200, with more than 1300 diffractograms taken and analysed.

6.1.1. The available experimental data

As an example of how the changes were followed in the investigated couples during long ageing, Table LXX shows a detailed description of the process in the Ag–Ga couple. It can be seen that the changes caused by long ageing depend on the low-melting metal (gallium) content and the ageing time. The X-ray peak intensity of the compound reflections decreases and that of the noble metal (silver) increases. At the end, only silver can be observed (Fig. 7). With increasing concentration of the low-melting constituent in the couple, a longer time is needed to complete the reaction. Thus, the specimens containing 49% and 75% Ga remained stable even after 11–13y, i.e. no reaction started within this time.

TABLE LXX Compound transformation in Ag–Ga couples during ageing

Ga (wt%)	State after ageing			
	0.33 y	3 y	9 y	11–13 y
17.5	Ag Ag_3Ga	Ag↑[a] Ag_3Ga↓[b]		Ag
21.9	Ag_3Ga		Ag↑[a] Ag_3Ga↓[b]	
24.0	Ag Ag_3Ga	Ag Ag_3Ga		Ag↑[a] Ag_3Ga↓[b]
39.0	Ag_3Ga	Ag_3Ga		
49.0	Ag_3Ga	Ag_3Ga		Ag_3Ga
75.0	Ag_3Ga	Ag_3Ga		Ag_3Ga

[a]↑Increases.
[b]↓decreases.

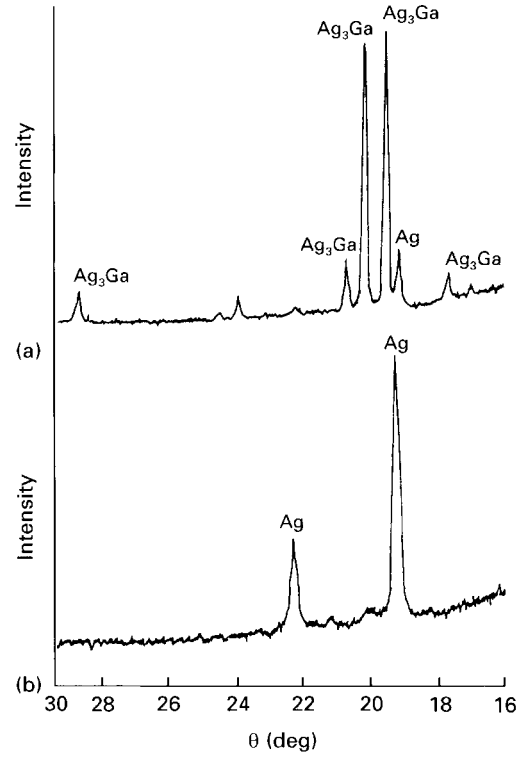

Figure 7 X-ray diffraction patterns of the Ag–Ga sample with original structure Ag(130 nm)–Ga(49 nm) (17.5% Ga), taken at (a) 8.5 mon; (b) 12 y after evaporation.

For each couple studied in the Ag–Me, Au–Me and Cu–Me systems, data tables were prepared, similar to Table LXX. However, there is no need to present these tables. Instead, Table LXXI is presented. In addition to the necessary literature data, the table contains condensed results obtained by studying the three mentioned systems, with a total of 18 couples. It can be seen that in the couple with no solid solubility range of the non-noble metal in the noble one (Ag–Te, Au–Al, Au–Ga, Au–Sb, Cu–Sb, Cu–Sn, Cu–Te), the compounds formed are stable during long ageing.

In the couple with an existing solid solubility range (Ag–Ga, Ag–In, Ag–Sn, Ag–Zn, Au–Zn, Cu–Ga, Cu–Zn), the compounds formed are completely decomposed and the X-ray peaks of the compounds and non-noble metal disappear in the samples with lower Me concentration. In the Au–Pb and Cu–In couples, products of oxidation are formed, while the Au–Sn couple had to be excluded from the analysis, because the specimens with low tin content were not preserved. The Au–In couple is an exception.

Several couples should be commented on in particular. In the case of the Ag–Zn couple, the situation is considerably more complex. The compounds formed in this couple were unstable in an extended concentration range. Partial or complete decomposition of the compounds was found to take place in 10 out of 11 analysed samples with different concentrations. In the samples containing $\leqslant 35\%$ Zn, silver disappeared partly at the beginning of the reaction, giving rise to compound formation. In the subsequent period, during which the compounds gradually decomposed and finally disappeared, the silver X-ray peak increased.

A complete disappearance of the silver X-ray peak during the process of compound formation (1–4 mon) has taken place in the samples containing more than 35% Zn. However, silver again appeared during the disappearance of the X-ray peaks of the compounds, its concentration increasing with time. The higher the original silver concentration, the more silver was observed in the sample at the end of the reaction.

Table LXXII shows the change in the X-ray peak intensity of silver in the samples containing eight different zinc concentrations.

The Au–Zn couple is a suitable illustration of the result that the rate of the compound decomposition depends on the concentration of the dissolved constituent (Zn). In the sample containing 4% Zn (within the solid solubility range), the decomposition of the compound takes place within 4 mon. In the sample containing 10% Zn (beyond the solid solubility range), years are needed for the process, and traces of the compound remain visible even after 12–14y.

The Cu–Zn couple has a wide solid solubility range and is characterized by a high rate of the compound decomposition. In the samples containing 26%, 49% and 62.5 % Zn, the decomposition begins after 1–1.5 %mon and is completed after 3.5–4 mon for 26% and 49% Zn, and after more than 1y for 62.5% Zn. In the Cd–Me samples (Me = Ag, Au, Cu), exposure to the atmosphere acts on cadmium to form some oxides and carbonates (parasitic compounds), thereby leading to decomposition of the originally formed intermetallic compounds. The parasitic compounds are polycrystalline (Au–Cd) or amorphous (Cu–Cd), or three processes take place simultaneously (Ag–Cd). These three couples are therefore unsuitable for the analysis.

TABLE LXXI Stability of compounds in Ag–Me, Au Me and Cu Me couples during ageing

Couple	Solubility limit of Me in Ag, Au, or Cu [4]		Supposed solid solubility at room temperature (wt% Me) [4]	Sample age (y)	Presence of compound at given composition (wt% Me)	
	(wt%)	t(°C)			No	Yes
Ag–Ga	8.0	200	4–5	13	17.5	24.0–75.0
Ag–In	20.0	300	19	11	11.2–26	34.7–80.0
Ag–Sn	10.2	200	9.5	13	15.0	27.0–75.0
Ag–Te	[a]		[a]	11		35.0 78.0
Ag–Zn	25.6	200	17	12	17.0–35.0	35.0–77.0
Au–Al	0.9	300	0	13		3.4–58.0
Au–Ga	3.1	270	~1	14		5.1 70.0
Au–In	6.3	400	~6	14		3.6–76.0
Au–Pb	0	500	0	10		24.0–83.0
Au–Sb	0	200	0	13		8.7[b]
						17.7–86.0
Au–Sn	3.5	350	~2	14		24.0 73.0
Au–Zn	13.0	600	5	12–14	4.4	10.0[c]
						14.9 83.0
Cu–Ga	20.0	200	19.5	13	15.0	25.0–68.0
Cu–In	2.2	300	[a]	11		
Cu–Sb	2.0	200	[a]	11		22.9 75.0
Cu–Sn	1.3	200	[a]	11		20.0–85.0
Cu–Te	0.003	600	[a]	11		20.0–85.0
Cu–Zn	35.2	250	31.0	11	26.0–62.5	83.0

[a] Negligible.
[b] In the sample containing 8.7% Sb there was no compound formation.
[c] Traces only.

TABLE LXXII Change in X-ray silver peak intensity in diffractograms of Ag–Zn samples during ageing

Zn (wt%)	Time after evaporation		
	1 d[a]	4 mon	12 y
17	100	95	98
35	100	85	80
48	100	0	25
53	100	0	25
55	100	0	20
65	100	0	20
67	100	0	8
77	100	0	0

[a] Intensity of the X-ray peak on the first day is taken as 100.

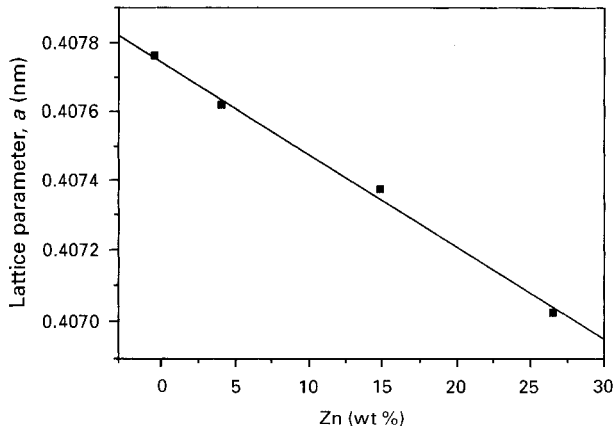

Figure 8 Lattice parameter of gold versus wt% Zn in the Au–Zn thin-film sample at room temperature.

By following the compound decomposition by the X-ray method, the existence of the noble metals in the samples and an intensity increase of their reflections with time was found. However, no low-melting metals were found in the samples. In order to determine whether the solid solutions of the low-melting metals in the noble metals exist in these cases, the Ag–In, Ag–Sn, Ag–Zn, Au–Cd, Au–In, Au–Sn and Au–Zn couples were studied. The solid solutions were found to exist only in the Au–Zn and Au–Sn couples.

Fig. 8 shows the experimentally determined lattice constant change as a function of zinc content of the sample at room temperature [62]. Taking the data from Pearson's book [109], it was calculated that for the sample containing 26 wt% Zn, the concentration of zinc dissolved in gold would be 2.5 wt%. In the same way it was found that in the thin-film Au–Sn couple there was about 0.5 wt% Sn in the solid solution in gold at room temperature.

The Ag–In, Ag–Sn, and Ag–Zn samples have been analysed by electron spectroscopy for chemical analysis (ESCA). The analysis has shown that indium and tin are in the form of In_2O_3 and SnO_2, respectively, while zinc is present but it is not clear in which form. Because these phases could not be identified by X-ray diffraction, they are presumably in a non-crystalline (amorphous) state.

6.1.2. Analysis of the available data and hypothesis on the course of the process

From the results obtained, the following conclusions concerning decomposition of the compounds in thin-film metal couples at room temperature were derived.

1. If, for a given metal couple, a solid solubility range exists, the compounds formed decompose in the course of ageing.

2. If there is no solid solubility range, the compounds remain stable for the same period of ageing.

Excluding the Au–Pb and Cu–In couples (strong influence of the atmosphere), as well as the Au–Sn couple (samples with low tin content missing), the remaining 15 analysed couples have been compared and the results are as follows. In metal couples (Ag–Ga, Ag–In, Ag–Sn, Ag–Zn, Au–Zn, Cu–Ga, Cu–Zn), in which a range of solid solubility exists decomposition by ageing takes place. In metal couples (Ag–Te, Au–Al, Au–Ga, Au–Sb, Cu–Sb, Cu–Sn, Cu–Te) in which there is no solid solubility range, the compounds remain stable for the same testing of time. Of the 15 couples, only the Au–In couple is an exception.

The decomposition process is not affected by the fact that, in some couples (Au–Sn, Au–Zn), a solid solution is also formed, because in these couples most of the tin or zinc is not in the solid solution. The following process of transformation of the samples during long ageing may be supposed on the basis of the available results [54]. The compounds formed within the solid solubility range cannot be stable for a long time. During the course of their ageing, the compounds are decomposed into the constituent elements. The noble metal (silver, gold, copper) remains in a crystalline state, while the other constituent (a low-melting metal) passes into a non-crystalline state. Once begun, the decomposition of the compound extends from the solid solubility range into the ranges in which there is no solid solubility. From the examples such as Ag–Zn and Cu–Zn, it can be seen that, given a long enough time, the process will be spread over the entire sample independently of the constituent concentrations. Because the decomposition process does not take place in the couples in which there is no solid solubility range, in these couples there is no reason for instability.

7. Comparative analysis of compound formation and stability in different types of specimens

The results obtained by studying specimens of the film–film, bulk–film and semiconductor–film types, in which the film was thermally evaporated or radio frequency (r.f.) sputtered, are presented in the preceding text. Similarities and differences have been observed in the obtained results. It has been shown that these depend on both the specimen types (film–film or bulk–film) and procedure used to deposit the upper film (evaporation or r.f. sputtering). The similarities and differences observed will be compared and

analysed for systems Ag–Me, Al–Me, Au–Me and Cu–Me.

The results to be compared, both for fresh and very old specimens, are presented in Table LXXIII. In the table, five specimen types have been compared: two vacuum-evaporated films, bulk–vacuum evaporated film (specimens are in two variants, differing in the metal being in the bulk form), two films with the upper one r.f. sputtered, and bulk–r.f. sputtered film.

Table LXXIII is complex in construction, but simple to use. For every couple, a maximum of ten data are presented. The upper line contains the data concerning five types quoted of the as-deposited specimens for each couple, and in the lower line are the corresponding data for the same specimens after long ageing. In this manner all the existing data concerning the given couple are presented in the same place, which allows their intercomparison for scientific and practical purposes.

In the text, first the reactions in the as-deposited, and then in very long-aged specimens, of the same type are discussed.

7.1. As-deposited specimens

According to "disposition" for compound formation, the couples show two extremities. The first extremity presents couples Al–Ag, Al–Cu and Au–Cu, in which compounds do not form at all. The second extremity presents couples of silver with gallium, indium, tin and

TABLE LXXIII Comparative data of the compounds formed in different types of as-deposited and long-aged specimens

Metal couple A–B	Specimen type Evaporated			Sputtered	
	Film A–film B, Aged 30 d / 10–15 y	Bulk A–film B, Aged 30–90 d / 13 y	Bulk B–film A, Aged 30–90 d / 13 y	Film B–film A, Aged 5 d / 11 y	Bulk B–film A, Aged 5 d / 11 y
Ag–Al	0			0	0
	0			0	0
Ag–Cd	$AgCd_3$ Ag_5Cd_3 AgCd				
	ATM				
Ag–Ga	Ag_3Ga	Ag_3Ga	Ag_3Ga		
	D-A	Ag_3Ga			
Ag–In	$LTAgIn_2$ Ag_2In	Ag_2In	$LTAgIn_2$		$LTAgIn_2$
	D-A	D-A	$LTAgIn_2^a$		$LTAgIn_2$
Ag–Sb	0			Ag_3Sb	Ag_3Sb
	ATM			Ag_3Sb^b	Ag_3Sb^b
Ag–Sn	Ag_3Sn	Ag_3Sn	Ag_3Sn	Ag_3Sn	Ag_3Sn
	D-A	D-A	Ag_3Sn	Ag_3Sn^b	
Ag–Te	Ag_5Te_3 Ag_2Te	Ag_2Te	Ag_5Te_3		Ag_5Te_3
	Ag_5Te_3 Ag_2Te	Ag_2Te	$Ag_5Te_3^a$		Ag_5Te_3
Ag–Zn	$AgZn_3$ Ag_5Zn_8 AgZn	$AgZn_3$ Ag_5Zn_8	$AgZn_3$ Ag_5Zn_8 AgZn		
	D-A	Ag_5Zn_8 AgZn	$AgZn_3$ Ag_5Zn_8 AgZn		
Al–Sb	0			$AlSb^c$	$AlSb^c$
	0			$AlSb^c$	
Au–Al	Au_2Al	0	0		Au_2Al $AuAl_2$
	Au_2Al $AuAl_2$	0[a]	0		Au_2Al $AuAl_2$

TABLE LXXIII (*Continued*)

Metal couple A–B	Specimen type Evaporated			Sputtered	
	Film A–film B, Aged 30 d	Bulk A–film B, Aged 30–90 d	Bulk B–film A, Aged 30–90 d	Film B–film A, Aged 5 d	Bulk B–film A, Aged 5 d
	10–15 *y*	13 y	13 y	11 y	11 y
Au–Cd	$AuCd_3$	$AuCd_3$	$AuCd_3$ AuCd		$AuCd_3$ AuCd
	ATM	$AuCd_3^a$	$AuCd_3^a$ $AuCd^a$		$AuCd_3$ AuCd
Au–Ga	$AuGa_2$ AuGa Au_2Ga Au_7Ga_2	$AuGa_2$ AuGa Au_2Ga	$AuGa_2$		
	$AuGa_2$ AuGa Au_2Ga Au_7Ga_2	$AuGa^a$ Au_2Ga Au_7Ga_2			
Au–In	$AuIn_2$ AuIn Au_7In_3 Au_4In	$AuIn_2$ AuIn	$AuIn_2$		$AuIn_2$
	$AuIn_2$ AuIn Au_7In_3 Au_4In		$AuIn_2$		$AuIn_2$
Au–Pb	$AuPb_3$ $AuPb_2$ Au_2Pb	$AuPb_3$ $AuPb_2$	$AuPb_3$		
	ATM	ATM	ATM		
Au–Sb	$AuSb_2$	$AuSb_2$	0		$AuSb_2$
	ATM	$AuSb_2^a$	0^a		
Au–Sn	$AuSn_4$ $AuSn_2$ AuSn Au_5Sn	AuSn	$AuSn_4$ $AuSn_2$ AuSn		
	$AuSn_4$ $AuSn_2$ AuSn Au_5Sn	$AuSn^a$	$AuSn_4$ $AuSn_2$ AuSn		
Au–Zn	$AuZn_3$ AuZn	$AuZn_3$ AuZn	0		$AuZn_3$
	$AuZn_3$ AuZn Au_3Zn^d	$AuZn_3$ AuZn	0		$AuZn_3$
Cu–Al	0			0	0
	ATM			0	0
Cu–Au	0			0	0
	0			0	0
Cu–Cd	Cu_4Cd_3 $CuCd_3$	Cu_4Cd_3	0	Cu_4Cd_3	Cu_4Cd_3
	ATM	Cu_4Cd_3	Cu_4Cd_3	Cu_4Cd_3	Cu_4Cd_3
Cu–Ga	CuGa	CuGa	CuGa	CuGa Cu_9Ga_4	
	D-A	D-A		CuGa Cu_9Ga_4	

TABLE LXXIII (*Continued*)

Metal couple A–B	Specimen type Evaporated			Sputtered	
	Film A–film B, Aged 30 d / 10–15 y	Bulk A–film B, Aged 30–90 d / 13 y	Bulk B–film A, Aged 30–90 d / 13 y	Film B–film A, Aged 5 d / 11 y	Bulk B–film A, Aged 5 d / 11 y
Cu–Ge	0			Cu_3Ge Cu_5Ge	Cu_3Ge Cu_5Ge
	0			Cu_3Ge Cu_5Ge	Cu_3Ge Cu_5Ge
Cu–In	CuIn	CuIn	CuIn		CuIn
	ATM	CuIn	CuIn		Cu_4In CuIn
Cu–Sb	Cu_2Sb	0	0	Cu_2Sb	Cu_2Sb Cu_3Sb[a]
	ATM	0	0[a]	Cu_2Sb	
Cu–Sn	Cu_6Sn_5	Cu_6Sn_5	Cu_6Sn_5	Cu_6Sn_5 Cu_3Sn	Cu_6Sn_5 Cu_3Sn[a]
	Cu_6Sn_5	Cu_6Sn_5	Cu_6Sn_5	Cu_6Sn_5 Cu_3Sn	Cu_6Sn_5 Cu_3Sn[c]
Cu–Te	Cu_3Te Cu_7Te_5 CuTe	0	Cu_7Te_5 CuTe		Cu_7Te_5
	Cu_7Te_5 CuTe	0	CuTe[a]		
Cu–Zn	$CuZn_4$	$CuZn_4$	0	$CuZn_4$ Cu_5Zn_8	$CuZn_4$
	D-A		0	$CuZn_4$ Cu_5Zn_8	$CuZn_4$

Notes: ATM, substantial change in the specimen provoked by the atmosphere; D-A, decomposition of a compound followed by amorphization of one of the constituents.

[a] After 5–8 y.

[b] After 6.5 y.

[c] Trace.

[d] Two types of changes take place in addition to the transformation, decomposition of the compounds with amorphization has been observed.

tellurium, then couples of gold with cadmium, indium, lead, antimony and tin, and couples of copper with cadmium, gallium, indium and tin, in which compounds have formed practically in all types of specimen.

In the first group are the couples with both constituents with high melting point, and in the second group (mainly) the couples in which one constituent has a high and another a low melting temperature. The rest of the couples present transition between these two extremities.

From Table LXXIII, one can see several points.

(a) In the specimens of the film–evaporated film type, fewer compounds are formed than in the specimens of the film–sputtered film type. For example, in the specimens of couples Ag–Sb, Al–Sb, and Cu–Ge, film–evaporated film type compounds are not formed, but in the specimens of the film–sputtered film type of the same couples, corresponding compounds formed (Ag_3Sb, AlSb, Cu_3Ge, Cu_5Ge). The second example shows the couples Cu–Ga, Cu–Sn and Cu–Zn. In the evaporated specimens of these couples forms one compound per couple (CuGa, Cu_6Sn_5, $CuZn_4$), while in the sputtered specimens, beside those listed, another compound per couple has formed (Cu_9Ga_4, Cu_3Sn, Cu_5Zn_8).

(b) In the bulk–evaporated film type specimens fewer compounds were formed than in the bulk–sputtered film type specimens. For example, in the specimens of bulk Al–Au film, Sb bulk–Au film, Sb bulk–Cu film and Zn bulk–Au film, compounds do not form. In the specimens of the same couples when film was sputtered, corresponding compounds were formed (Au_2Al + $AuAl_2$, $AuSb_2$, Cu_2Sb, Cu_3Sb trag, $AuZn_3$). In the In bulk–Cu film specimens, when films are evaporated, one compound formed per couple (CuIn, Cu_6Sn_5), while when the films are sputtered,

two compounds per couple formed (CuIn + Cu_4In and Cu_6Sn_5 + Cu_3Sn, respectively).

(c) When compounds are formed in the film–evaporated film type specimens, they will also form in the film–sputtered film type specimens of the same couple.

(d) When compounds are formed in the bulk–evaporated film type specimens, they will also form in the bulk–sputtered film type specimens of the same couple.

(e) When compounds are formed in the bulk–sputtered film type specimens, they will also form in the film–sputtered film type specimens of the same couple.

7.2. Long-aged specimens

During the course of long ageing, three groups of essential changes have been observed.

In the first group, a transformation occurs (Section 2). Two types of change are noticed:

(i) The last transformations of compounds were observed after many years (evaporated thin-film couples Au–Al and Au–Zn, after 3 and 8 y, respectively). This is also valid for Cd bulk–Cu film evaporated couples in which compound formation was observed after 5–8 y.

(ii) In the couples with one bulk constituent, compounds are formed, during the course of ageing, with successively more and more metal in the bulk. These couples are: Ag bulk–Zn film evaporated, Au bulk–Ga film evaporated, In bulk–Cu film sputtered and Te bulk–Cu film evaporated.

In the second group, a spontaneous decomposition of a compound takes place, whereby one component becomes amorphous (Section 6). This was observed in the evaporated specimens of the film–film (Ag–Ga, Ag–In, Ag–Sn, Ag–Zn, Au–Zn, Cu–Ga and Cu–Zn) and bulk–film evaporated (Ag bulk–In, Ag bulk–Sn and Cu bulk–Zn) types. In all couples, a solid solubility range exists. This phenomenon was not registered in couples with top-sputtered film.

In the third group, a substantial change due to weathering takes place (Section 5). It can be seen that in 23 specimens, all the types of products of oxidation appeared under the influence of atmosphere. In 11 specimens only (one-half of the specimens with products of oxidation), substantial changes take place; that means that the compounds formed are destroyed. Nine out of 11 specimens were film–film evaporated, but two were the bulk–film evaporated type. In both these specimens, one constituent was lead, a very sensitive metal to atmospheric influence.

8. Significance of results presented from the standpoint of application

The present review contains many experimental results of the investigations performed in the last decades. Beside purely scientific, many of these results have a definite practical significance. Namely, they can serve as a basis for development and production of the pertaining components and devices. The question is posed, therefore, as to the principal achievements of the investigations performed from the standpoint of their application.

The most important results from this standpoint are as follows.

1. The rules relative to compound formation, as well as those concerning their stability during long ageing, have been formulated.

2. Experimental data have been established to complement the low-temperature range of the existing phase diagrams.

3. Experimental results and technological practice have been established. It may help to select the appropriate couples for contacts (and other applications) in designing microelectronic devices, and other components and devices.

For physicists–technicians, accomplishing the systems mentioned, this has the following implications. Knowledge of the rules relative to the compound formation (and non-formation) allows the first selection of the metal couples available for application. The complemented phase diagrams serve for a further selection and narrowing down of the number of couples for a final choice. Finally, the experimental data and technological practice serve to estimate each couple from the viewpoint of its application, taking into account the requirements of the device in question. Knowledge of the reaction kinetics in the metal couples, as well as the processes taking place during long ageing, are decisive in the choice of the optimum couple.

If sufficiently complete data do not yet exist for some couples, the results and procedures presented permit them to be obtained.

8.1. Principal formulated rules

This review contains numerous formulated rules, but some of them can be selected as the most important for application.

The rule concerning compound formation and the rule pertaining to the situation in which compounds are not formed. Simply stated, the compound is formed in the couple if one metal has a high melting point, the other has a low melting point, and the potential compound has a melting point which is not high. If, the couple with a high m.p. metal–low m.p. metal potential compound has a high melting point, or if both metals in the couple have melting points in the same temperature region, compounds are not formed.

The system designer can decide whether to choose the couple in which no compound will be formed or the couple whose characteristics after compound formation may better satisfy the requirements.

The rule concerning the rate of compound formation. In a binary system high-melting metal–low-melting metals, the interdiffusion coefficient is higher when the melting point of the low-melting metal is lower. The interdiffusion coefficient value reflects the rate of compound formation in the couple studied. For the Ag–Me, Au–Me, Cu–Me and Pd–Me systems, it was proved that the dependence is linear (Fig. 5).

If the designer has chosen in contact couple in which the compound formation takes place, he can estimate the time needed to complete the reaction and for necessary ageing, i.e. how long it is necessary to wait until the couple is ready for use.

The rule concerning the compound decompositon. If, for a given metal couple, a solid solubility range exists, the compound formed decomposes during the course of ageing; if there is no solid solubility range, the compound remains stable for the same period of ageing.

The devices with incorporated contact couples have a long life, often a whole decade. In such a case, the incorporated contacts must not be made of the couple in which the compounds are formed, if the solid solubility ranges exist in this couple. Such couples could be used for the contacts only if the devices have a relatively short life.

8.2. Supplement of low-temperature ranges of existing phase diagrams

Numerous phase diagrams do not contain the low-temperature part, even those for which the compounds are known to exist at lower temperatures [4]. Thus, in many phase diagrams, there are no data for the existence of compounds below 200 or 300 °C, and more often below 100 °C. The least known is the situation at room temperature.

To the authors' knowledge, the data obtained at room temperature have not been used to complement the existing phase diagrams. An exception is the monograph by Okamoto and Massalski [12], in which such data have been analysed in preparing the Au–Me phase diagrams. The difficulties obviously exist in the processing of the available experimental data and their incorporation into existing phase diagrams, and there are also different concepts regarding the point. However, the effort would be rewarded, because the most deficient regions of the phase diagrams would be thus complemented, often for the least-studied couples. The collected data presented here offer material for complementing the low-temperature ranges of the existing phase diagrams.

Of 39 couples in which the compounds are formed at room temperature, data deserving to be introduced into the phase diagrams were obtained in 21 couples. There are 13 couples in which results concerning 23 compounds formed at room temperature do not produce any changes in the existing phase diagrams. A suitable example which illustrates the procedure of introducing the data in the phase diagram is the Ag–In couple. The available experimental data for this couple are as follows [6].

(i) A compound identified as the low-temperature phase $AgIn_2$ (LT $AgIn_2$ = α-$AgIn_2$) is formed at room temperature in the thin-film specimen. The authors' own bulk standards containing the stoichiometric concentrations for $AgIn_2$, homogenized at 125 and 180 °C for 48 h, have identical X-ray patterns (β-$AgIn_2$), but differ from that of the compound prepared at room temperature. By annealing the thin-film specimen at 60–120 °C, an X-ray pattern identical to the bulk standard was obtained. It was concluded, therefore, that the transformation temperature for the α-$AgIn_2$ → β-$AgIn_2$ is between 60 and 120 °C.

(ii) In the thin-film specimens containing more than 50 wt% Ag, the Ag_2In (γ) compound is formed; it was identified by means of the authors' own bulk standard for Ag_2In, homogenized at 180 °C/48 h.

(iii) The Ag_3In (ξ) compound was not formed in the thin-film specimens. The authors' own bulk standard containing stoichiometric concentrations for the compound, homogenized at 180 °C/48 h, is identical to the ASTM card 15-163 for Ag_3In.

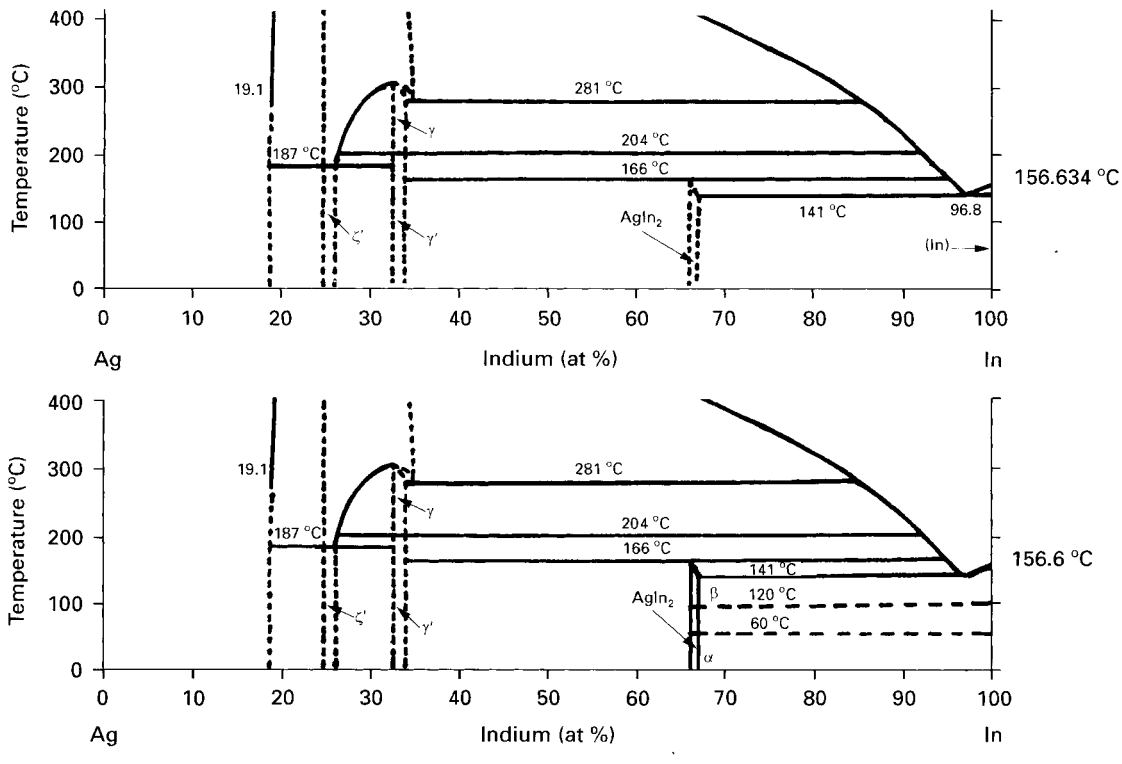

Figure 9 Example of inserting the obtained experimental results into an existing phase diagram.

TABLE LXXIV Experimental results to be introduced in the low-temperature range of the phase diagrams

Couple metal A–B	Compounds formed			Proposed supplements	
	Formula	Identification ASTM standard	Other source	In temperature range (~°C)[a]	In concentration range (~At %B)
Ag–Cd	β′(AgCd)	28–197		180–20	50
	γ(Ag$_5$Cd$_8$)	14–14		180–20	62
	ε(AgCd$_3$)	28–199		180–20	70
Ag–Ga	ξ′(Ag$_3$Ga)		[6]	200–20	25
Ag–Te	α(Ag$_2$Te)	12–695	[108]	145–20	33
	α(Ag$_5$Te$_3$)	16–372		100–20	37–40
Ag–Zn	ξ(C-AgZn)	29–1156		180–20	52
	β(H-AgZn)	29–1155		180–20	52
	γ(Ag$_5$Zn$_8$)	29–956		180–20	62
	ε(AgZn$_3$)	25–1325		180–20	75
Al–Au	α, β-Au$_2$Al		[12]	200–20	67
	AuAl$_2$	17–0877		200–20	33
Au–Pb	AuPb$_3$	11–573		52–20	75
Au–Sb	AuSb$_2$	8–460		200–20	67
Au–Sn	η(AuSn$_4$)		[32]	50–20	80
Au–Te	AuTe$_2$ [44]		[44]	200–20	67
Cd–Cu	γ(Cu$_4$Cd$_3$)	20–188		200–20	55
	ε(CuCd$_3$)	16–17		200–20	20–70
Cu–Ga	ν(CuGa)	3–1048		200–20	50–67
Cu–In	CuIn	35–1150		200–20	42–50
Cu–Sb	η(Cu$_2$Sb)	3–1024		200–20	33
Cu–Sn	η′(Cu$_6$Sn$_5$)	2–0693		100–20	45
Cu–Zn	ε(CuZn$_4$)		[47]	200–20	80
Ga–Mg	Mg$_2$Ga	22–260		200–20	67
In–Ni	LTNi$_2$In$_3$		[56]	200–20	40
Pb–Te	PbTe	8–28		200–20	50
Pd–Te	PdTe$_2$	29–0970		200–20	67
Pt–Sn	PtSn$_4$		[8]	100–20	90

[a] The upper temperature limit to which the phase diagrams should be extended is defined precisely only for the compounds for which their own standards, annealed to 200 °C, exist. For other compounds, this has been estimated as follows. The compounds formed at room temperature have been identified by means of the ASTM standards, which had supposedly been used to identify the compounds presented in the phase diagrams [4]. The existence of the lowest temperatures given in the phase diagrams has so far been reported for these compounds.

Notes: Ag–Cd: Because of undefined concentration ranges of formation, for each of the three Ag–Cd compounds, a full line should be drawn, nearer to the stoichiometric value of the compounds.

Ag–Ga: own standard, annealed at 200 °C, close to the ASTM card 28–0432, is identical to the thin film (TF) specimens at room temperature.

Ag–Te: the α – β Ag$_2$Te transformation temperature is at 145 °C [4]. In the latest phase diagram [108], the Ag$_5$Te$_3$ formula has been used.

Ag–Zn: because of unidentified concentration ranges of formation, for each Ag–Zn compound, a full line should be drawn nearer to the stoichiometric value of the compound.

Al–Au: own standard, annealed at 200 °C is identical to the TF specimens at room temperature. According to [53] t_{min} = 300 °C; according to [4] t_{min} = 400 °C.

Au–Sn: own standard, annealed at 200 °C, is identical to the ASTM card 28–0441 and TF specimen at room temperature.

Cd–Cu: the same remarks apply as for the Ag–Cd and Ag–Zn couples.

Cu–Ga: before the exact value (at % Ga) has been defined for Cu–Ga, full lines should be drawn for the existing ν phase.

Cu–In: the same remarks apply for Cu–Ga. Own TF standard prepared at room temperature is now the ASTM card 35–1150.

Cu–Zn: own standards are identical to the TF specimens at room temperature; they are now the CuZn$_5$ ASTM cards: 36–1151 (bulk) and 35–1152 (TF).

In–Ni: own TF standard (20 °C); this standard is now the ASTM card 36–1147; the LTNi$_2$In$_3$ to Ni$_2$In$_3$ transformation temperature is not known.

Fig. 9a presents the existing phase diagram [4] for Ag–In. In Fig. 9b the same diagram is presented into which the described experimental data for AgIn$_2$ have been introduced.

It should be pointed out that the transformation temperature α → β AgIn$_2$ (although not determined with sufficient precision) represents a new fact, which does not exist in the Ag–In phase diagram. This stimulates new investigations to establish possible transformations in the temperature range from 0 °C to about 200 °C in other couples as well.

Table LXXIV contains the data for the remaining 20 couples in which many compounds are formed. New data exist for each of these compounds and they should be introduced into the existing phase diagrams. For the most part, these are taken from the published and unpublished papers of the present authors.

As in the example of the Ag–In couple (Fig. 9), similar supplements are proposed for the phase diagrams of the couples denoted in Table LXXIII. The introduction of full lines is proposed from the lowest temperature registered so far, up to room temperature

(~20 °C). When the ranges of the compound formation are not clearly defined (e.g. for Ag–Cd, Ag–Ga, Ag–Zn, Cu–Cd, ...), it is perhaps adequate to draw only one full line, close to the stoichiometric value of the compound, as is given for the Ag–Sn (ε) and Au–Cd (ε′) couples [4].

8.3. Selection of contact couples with optimum characteristics

In the modern microelectronic, optoelectronic, sensor and similar devices, contacts play a significant role. We shall take sensors as an example. The contacts should be chosen so that their characteristics remain stable during their multiyear exploitation and that they are not sensitive to the atmosphere. The sensor element is a part of the contact couple. An electroconductive layer is deposited on it and a thin conductive wire is welded on the layer. The semiconducting sensor element (e.g. PbS or InSb) consists either of a thin-film or bulk. Thus, the couples of the film–film or bulk–film type are produced in these cases (first, the sensor element–Me contact film, and second, the Me contact film–bulk the conductive wire). If these couples are not chosen so that their characteristics optimally match each other, the device into which the couples are incorporated may stop functioning after some time.

An electronic device [122] is a good example. The device worked at room temperature, but some of its components became heated up to 50 °C. A weakening and finally breakage of the contact was observed between the thin aluminium film and a thin gold wire (a contact film–bulk). The electronic circuit was interrupted because of the formation of intermetallic compounds, the electrical and mechanical characteristics of which were different from those of gold and aluminium. On the basis of the data presented in Section 2.1, it can be supposed that the Au_2Al and $AuAl_2$ compounds were formed, two of the five compounds which can be formed in this couple. The temperature must have been somewhat elevated too. Two additional problems occurring because of changes in the metal couples led to a breakdown of functioning of the optical devices – optical grating [11] and golden mirror [10, 26].

Another example is as follows. It was found that the contact between silver coating and tellurium film was broken in about a day [123]. This happened because of Ag_2Te and Ag_5Te_3 compound formation (Section 2.1). More subtle changes in contacts are also possible, which do not cause a break in the (micro) electronic devices, but modify their characteristics, which may be even more serious. In order to avoid such problems, the contacts having optimum characteristics from the physical, electronic, technological and any other standpoint, should be chosen in each particular case. The data presented in this review make it possible in many cases. Table LXXV shows in which couple combinations, formed from the 20 metals mentioned, will the products of oxidation appear. The table presents separately the couples in which products of oxidation are formed and those with no products of oxidation formation. The selection of contacts having optimum characteristics is much more difficult than may look at first sight. We shall therefore

TABLE LXXV Data for quick selection of thin-film couples for contacts [62] (The layer above the line is the upper one)

Metal film on which products of oxidation can be formed	In couple in which products of oxidation are	
	Not formed	Formed
Ag	Al Ag	Mg, Sb, Sm Ag
Bi	Bi Au, Ni	Bi Te In, Mg, Mn Bi
Cd		Cd Sb Mg, Ni, Sb, Sm Cd
Cu	Cu Ge Au Cu	Al, Mg, Mn, Sm Cu
In	Co, Sn In	Sb, Sm, Te In In Mg, Mn
Mg	Mg Co,Te	Ge, Ni, Pb, Sb, Sm, Sn, Te, Zn Mg Mg Al,Au
Mn	Mn Cr, Zn Al, Au, Ga, Te Mn	Ge, Ni, Sb, Sm, Sn Mn
Pb		Pb Sm
Sb	Sb Al, Co, Cr, Ni, Sm, Te, Zn Te Sb	Sb Sm
Sm		Sm Al, Au, Cd, Co, Ga, Te, Zn Co, Ga, Ni, Sn Sm

TABLE LXXVI Sequence of activities in selection of contact layers

Sequence of procedures	Tables showing				
	Film–film$_{ev}$	Bulk–film$_{ev}$	Film–film$_{r.f.}$	Bulk–film$_{r.f.}$	Semiconducting compounds–film$_{ev}$ or film$_{r.f.}$
Compound formation	XLIV	XLV	XLVII–XLIX	XLVII, XLVIII	LV–LVIII
Influence of atmosphere	LXVII, LXVIII				
Stability during long ageing	LXXI, LXXII	XLV	XLVII–XLIX	XLVII XLIX	LVI, LVIII
Comparison of all five specimen types	LXXIII	LXXIII	LXXIII	LXXIII	

mention a few data and technological experiences which may help, or at least induce one to consider how to orient oneself in this rather complex field.

Table LXXVI contains a sequence of tests that should be performed in order to diminish the number of couples from which a final choice would be made. Thereby it should be determined, according to the specified demand, which type of specimen is needed. For every part of the examination, tables and sections in the review are indicated in which the necessary data are to be found.

9. Concluding remarks and trends of further research

The authors hope that this review will be:

(a) a competent and complete source of information concerning room-temperature reactions in thin metal film couples and changes caused by prolonged ageing;

(b) a guide to select contact couples with the optimum characteristics for microelectronics and sensor technique projects, and

(c) a stimulus for other researchers to continue, extend and deepen investigations of thin metal films at room temperature, as well as in a broader temperature range.

On the basis of the results presented in this review, trends of further investigations can be anticipated as follows.

9.1. Complementing existing data

Investigation of phenomena of compound formation in so-far unexplored couples, in particular those important from the viewpoint of their application, will be continued. In addition, it should be useful to complement such investigations for those couples for which the results are not complete or are insufficiently reliable. It is especially interesting to study the behaviour of couples in which no compounds were formed when the specimens had been prepared by vacuum evaporation. For this purpose, the specimens should be prepared using r.f. sputtering, an ion beam or electron gun.

The already published data should be complemented in an appropriate way by the so-far unknown interdiffusion coefficients for both the couples in which compounds are formed and for those in which no compound formation was detected. It should thereby instil an increase in the accuracy of results by applying improved methods.

9.2. Solving so far partly solved or only noticed problems

Complementing the low-temperature regions of the existing phase diagrams, as proposed in this review, is only a small part of the requirements. Nevertheless, the data presented here often do not cover the whole missing region of the phase diagram. It would be most useful to combine such an investigation with checking whether compound transformations take place in the low-temperature region (from room-temperature upwards) and what the transformation temperatures are for the LT to HT (MT) phase transition.

The existence of solid solutions at room temperature has only been noticed so far. Obviously, systematic investigation of their existence and quantitative determination, wherever possible, are forthcoming, both for the couples in which compounds are formed and for those in which no compound formation was detected.

It is of particular significance for practical application to know the stability of characteristics of metal couples, which depends on their chemical stability. It is therefore essential to follow long-term chemical changes in the couples caused by influence of the atmosphere. Because it is usually impossible to wait for such a long time, it is necessary to simulate conditions (elevated temperature, increased concentration of the atmospheric agents, etc.) under which the changes would take place in a considerably shorter time. The phenomenon of decomposition of the compounds formed into constituent metals, taking place during prolonged ageing, whereby one of the constituents remains crystalline and the other becomes amorphous, is among such changes. A systematic investigation using "accelerated" procedures would probably contribute to establish whether this phenomenon has a broader significance, from both theoretical and practical viewpoints.

The rules concerning compound formation and decomposition, demand further research with the aim of

verifying their validity within the range investigated so far, and a possible extension of this range.

9.3. Generalization of experimental results

A more extensive analysis of the room-temperature contact phenomena in metal couples is obviously necessary, together with inevitable generalizations.

By comparing the results obtained at room temperature with those obtained at elevated temperatures, and comparing the results obtained from the thin-film specimens with those obtained from the bulk ones, common features in their behaviour and pertaining rules should be sought.

A more extensive analysis of the comparative results obtained from different specimen types and different film deposition methods might provide, beside practical, certain results of a fundamental character. It might also lead to certain new theoretical explanations of the experimental results obtained.

References

1. W. C. ROBERTS-AUSTEN, *Phil. Trans. R. Soc. Lond. A* **187** (1896) 404.
2. M. FARADAY, *Phil. Trans.* **147** (1857) 145.
3. Joint Committee on Powder Diffraction Standards, ASTM Powder Diffraction File (American Society for Testing and Materials, Swarthmore, PA).
4. T. MASSALSKI (ed.), "*Binary Alloy Phase Diagrams*". (American Society for Metals, Metals Park, OH, 1986, 1990).
5. V. SIMIĆ and Ž. MARINKOVIĆ, *Thin Solid Films* **209** (1992) 44.
6. *Idem, ibid.* **61** (1979) 149.
7. Y. FUJIKI, *J. Phys. Soc. Jpn* **14** (1959) 913.
8. K. N. TU and R. ROSENBERG, *Jpn. J. Appl. Phys. Suppl.* 2. Part 1 (1974) 633.
9. I. KARAKAYA and W. T. THOMPSON, *Bull. Alloy Phase Diagr.* **8** (1987) 340.
10. C. WEAVER and L. C. BROWN, *Philos. Mag.* **7** (1962) 1.
11. W. R. HUNTER, T. L. MIKES and G. HASS, *Appl. Opt.* **11** (1972) 1594.
12. H. OKAMOTO and T. B. MASSALSKI (eds.), "*Phase Diagrams of Binary Gold Alloys*", (American Society of Metals, Metals Park, OH, 1987).
13. Ž. MARINKOVIĆ and V. SIMIĆ, *Thin Solid Films* **75** (1981) 229.
14. *Idem*, in "*Proceedings of the 7th International Vacuum Congress* and 3rd *International Conference on Solid Surfaces*", Vienna (1977) p. 2111.
15. V. SIMIĆ and Ž. MARINKOVIĆ, *Thin Solid Films* **34** (1976) 179.
16. M. PUSELJ and K. SCHUBERT, *J. Less-Common Metals* **38** (1974) 83.
17. I. P. GREBENNIK and A. G. TONKOPRYAD, *Fiz. Metall. Metalloved* **36** (1973) 524.
18. T. G. FINSTAD, T. ANDREASSEN and T. OLSEN, *Thin Solid Films* **29** (1975) 145.
19. V. SIMIĆ and Ž. MARINKOVIĆ, *Thin Solid Films* **41** (1977) 57.
20. M. PUSELJ and K. SCHUBERT, *J. Less-Common Metals* **41** (1975) 33.
21. J. M. VANDENBERG and R. A. HAMM, in "*Proceedings of the Symposium on Thin Film Interfaces and Interactions*", edited by J. E. E. Baglin and J. M. Poate, Princeton, NJ, 1980, p. 283.
22. W. KEPPNER, R. WESCHE, T. KLAS, J. VOIGT and G. SCHATZ, *Thin Solid Films* **143** (1986) 201.
23. J. BJÖNTEGARD, L. BUENE, T. FINSTAD, O. LÖNSJÖ and T. OLSEN, *ibid.* **101** (1983) 253.
24. R. ROY and S. K. SEN, *ibid.* **197** (1990) 303.
25. L. B. LEDER, *Cryogenics* **8** (1968) 364.
26. C. WEAVER and L. C. BROWN, *Philos. Mag.* **8** (1963) 1379.
27. H. SCHOPPER, *Z. Phys.* **143** (1955) 93.
28. C. PARISET and M. GALTIER, *Thin Solid Films* **29** (1975) 325.
29. Ž. MARINKOVIĆ and V. SIMIĆ, *J. Less-Common Metals.* **115** (1986) 225.
30. V. SIMIĆ and Ž. MARINKOVIĆ, *ibid.* **53** (1977) 287.
31. L. BUENE, T. FINSTAD, K. RIMSTAD, O. LÖNSJÖ and T. OLSEN, *Thin Solid Films* **34** (1976) 149.
32. V. SIMIĆ and Ž. MARINKOVIĆ, *J. Less-Common Metals* **51** (1977) 177.
33. K. SCHUBERT, H. BREIMER and R. GOHLE, *Z. Metallkde* **50** (1959) 146.
34. I. I. MIRKIN, "*Handbook of X-ray Analysis of Polycrystalline Materials*", (GIFML, Moscow, 1961) (in Russian).
35. L. BUENE, *Thin Solid Films* **43** (1977) 285.
36. *Idem, ibid.* **47** (1977) 159.
37. L. BUENE, H. FALKENBERG-ARELL and J. TAFTÖ, *ibid.* **65** (1980) 247.
38. L. BUENE, H. FALKENBERG-ARELL, J. GJÖNNES and J. TAFTÖ, *ibid.* **67** (1980) 95.
39. D. GREGERSEN, L. BUENE, T. FINSTAD, O. LÖNSJÖ and T. OLSEN, *ibid.* **78** (1981) 95.
40. S. NAKAHARA, R. J. McCOY, L. BUENE and M. VANDENBERG, *ibid.* **84** (1981) 185.
41. B. HUGSTED, L. BUENE, T. FINSTAD, O. LÖNSJÖ and T. OLSEN, *ibid.* **98** (1982) 81.
42. S. K. SHARMA, M. P. SINGH and G. L. MALHOTRA, *Phys. Status Solidi* (a) **128** (1991) 407.
43. J. C. BERNÈDE, Y. TREGOUET and M. NACIRI, *Thin Solid Films* **62** (1979) 29.
44. J. C. BERNÈDE, *ibid.* **115** (1984) L49.
45. R. P. ELLIOTT, "*Constitution of Binary Alloys*", First Supplement (McGraw-Hill, New York, 1965).
46. V. SIMIĆ and Ž. MARINKOVIĆ, *Mater. Chem. Phys.* **47** (1996) 246.
47. *Idem, J. Less-Common Metals* **72** (1980) 133.
48. *Idem, ibid.* **116** (1986) L7.
49. Ž. MARINKOVIĆ and V. SIMIĆ, *Thin Solid Films* **82** (1981) 195.
50. J. S. CHEN, E. KOLAWA, M. -A. NICOLET and R. P. RUIZ, *Solar Cells* **30** (1991) 451.
51. D. S. ALBIN, G. D. MOONEY, J. CARAPELLA, A. DUDA, J. TUTLE, R. MATSON and R. NOUFI, *ibid.* **30** (1991) 41.
52. K. N. TU, *Acta Metall.* **21** (1973) 347.
53. M. HANSEN and K. ANDERKO, "*Constitution of Binary Alloys*", 2nd Edn. (McGraw-Hill, New York, 1958).
54. V. SIMIĆ and Ž. MARINKOVIĆ, *Thin Solid Films* **209** (1992) 181.
55. Ž. MARINKOVIĆ and V. SIMIĆ, *ibid.* **101** (1983) L37.
56. *Idem, ibid.* **98** (1982) 95.
57. T. L. NGAI, R. C. SHARMA and Y. A. CHANG, *Bull. Alloy Phase Diag.* **9** (1988) 586.
58. M. F. SINGLETON and P. NASH, *ibid.* **9** (1988) 592.
59. P. NASH and A. NASH, *ibid.* **6** (1985) 350.
60. V. SIMIĆ and Ž. MARINKOVIĆ, *J. Less-Common Metals* **95** (1983) 259.
61. *Idem, Thin Solid Films* **249** (1994) 168.
62. *Idem.*, unpublished data.
63. *Idem, J. Less-Common Metals* **106** (1985) 287.
64. R. HALIMI, D. HAMANA and E. M. CHPILEVSKI, *Thin Solid Films* **139** (1986) 147.
65. R. HALIMI, E. M. CHPILEVSKI and D. A. GORBATCHEVSKI, *ibid.* **148** (1987) 109.
66. V. SIMIĆ and Ž. MARINKOVIĆ, *ibid.* **176** (1989) L173.
67. R. M. WALSER and R. W. BENÉ, *Appl. Phys. Lett.* **28** (1976) 624.
68. M. VENKATRAMAN and J. P. NEUMANN, *Bull. Alloy Phase Diag.* **9** (1988) 159.
69. V. SIMIĆ and Ž. MARINKOVIĆ, *Thin Solid Films* **191** (1990) 165.
70. J. L. MURRAY (ed.), "*Phase Diagrams of Binary Titanium Alloys*" (American Society of Metals, Metals Park, OH, 1988).

71. W. M. ROBERTSON, *Metall. Trans.* **3** (1972) 1443.
72. J. L. MURRAY, *Bull. Alloy Phase Diag.* **7** (1986) 165.
73. Ž. MARINKOVIĆ and V. SIMIĆ, *Thin Solid Films* **129** (1985) 315.
74. S. LEUNG, A. G. MILNES and D. D. L. CHUNG, in "*Interfaces and Contacts, MRS Symposia Proceedings*, Vol. 18, edited by R. Ludeke and K. Rose (North-Holland, Amsterdam, 1983) p. 109.
75. J. M. POATE, K. N. TU and J. W. MAYER (eds.), "*Thin Films Interdiffusion and Reactions*" (Wiley, New York, 1978).
76. P. G. SHEWMAN, "*Diffusion in Solids*" (McGraw-Hill, New York, 1963).
77. T. T. TISONE and J. DROBEK, *J. Vac. Sci. Technol.* **9** (1971) 271.
78. J. M. VANDENBERG, F. J. A. DEN BROEDER and R. A. HAMM, in "*Thin Films and Interfaces*", MRS Symposia Proceedings, Vol. 10, edited by P. S. Hó and K. N. Tú (North-Holland, New York, 1982) p. 285.
79. Ž. MARINKOVIĆ and V. SIMIĆ, *Thin Solid Films* **156** (1988) p. 105.
80. *Idem, ibid.* **195** (1991) 127.
81. C. G. HOPKINS, S. M. BAUMANN and R. J. BLATTNER, *Thin Films and Interfaces II*, MRS Symposia Proceedings Vol. 25 edited by J. E. E. Baglin, D. R. Campbell and W. K. Chu (North-Holland, New York, 1984) p. 87.
82. J. E. E. BAGLIN, F. M. D. HEURLE and W. N. HAMMER, in "*Thin Film Phenomena-Interfaces and Interactions*", Symposium Proceedings Vol. 78-2, edited by J. E. E. Baglin and J. M. Poate (Electrochemical Society Princenton, NJ, 1978) p. 171.
83. R. J. WAGNER, S. S. LAU, J. W. MAYER and J. A. ROTH, *ibid.* Vol. 78-2 p. 59.
84. R. G. KIRSCH, J. M. POATE and M. EIBSCHUTZ, *ibid.*, Vol. 78-2, p. 165.
85. D. P. KOLESNIKOV, A. F. ANDRUSHKO and E. I. SUKHININA, *Fiz. Met. Metalloved.* **34** (1972) 529 (in Russian).
86. S. K. SEN, A. GHORAI and A. K. BANDYOPADHYAY, *Thin Solid Films* **155** (1987) 243.
87. A. K. BANDYOPADHYAY, S. K. SEN and S. SEN, *ibid.* **186** (1990) 87.
88. J. HAUSER, *J. Phys. Coll. C4, suppl.* 10, **42** (1981) C4-943.
89. K. N. TU, *J. Appl. Phys.* **48** (1977) 3400.
90. Ž. MARINKOVIĆ and V. SIMIĆ, *Thin Solid Films* **217** (1992) 26.
91. S. S. LAU and R. C. SUN, *ibid.* **10** (1972) 273.
92. S. Z. BOKSHTEIN, "*Stroenie i svoistva metallicheskih splavov*" (Gosenergolzdat, Moscow, 1971) (in Russian).
93. R. W. BALLUFFI and J. M. BLAKELY, *Thin Solid Films* **25** (1975) 363.
94. S. U. CAMPISANO, in "*Proceedings of the Symposium on Thin Film Phenomena: Interface and Interactions*" edited by J. E. E. Baglin and J. M. Poate (Electrochemical Society, Princeton, NJ, 1978) Vol. 78-2, p. 129.
95. S. NAKAHARA and R. J. McCOY, *Thin Solid Films* **88** (1982) 285.
96. E. MA, C. V. THOMPSON and L. A. CLEVENGER, *J. Appl. Phys.* **69** (1991) 2211.
97. K. BARMAK, C. MICHAELSEN, J. RICKMAN and M. DAHMS, *Mater. Res. Soc. Symp. Proc.* **403** (1996) 51.
98. K. P. MINGARD and B. CANTOR, *J. Mater. Res.* **8** (1993) 274.
99. K. R. COFFEY, L. A. CLEVENGER, K. BARMAK, D. A. RUDMAN and C. V. THOMPSON, *Appl. Phys. Lett.* **55** (1989) 852.
100. C. MICHAELSEN, G. LUCADAMO and K. BARMAK, *J. Appl. Phys.* **80** (1996) 6689.
101. K. BARMAK, C. MICHAELSEN and G. LUCADAMO, *J. Mater. Res.* **12** (1997) 133.
102. L. A. CLEVENGER, C. V. THOMPSON, R. R. de AVILLEZ and E. MA, *J. Vac. Sci. Technol.* **8** (1990) 1566.
103. S. B. NEWCOMB and K. N. TU, *Appl. Phys. Lett.* **48** (1986) 1436.
104. C. V. THOMPSON, *Mater. Res. Soc. Symp. Proc.* **343** (1994) 3.
105. Ž. MARINKOVIĆ, PhD, Thesis, University of Belgrade (1986).
106. H. LEVINSTEIN, *J. Appl. Phys.* **20** (1949) 306.
107. V. V. SLUDSKAYA, "*Tonkie Plenki V Tekhnike Sverkhvysokih Tscastot*" (Moscow, 1962) (in Russian).
108. I. KARAKAYA and W. T. THOMPSON, *J. Phase Equilib.* **12** (1991) 56.
109. W. B. PEARSON, "A Handbook of Lattice Spacings and Structure of Metals and Alloys" (Pergamon, Oxford, 1964).
110. F. A. SHUNK, "*Constitution of Binary Alloys*", 2nd Suppl. (McGraw-Hill, New York, 1969).
111. C. J. SMITHELLS, "*Metals Reference Book*", Vol. 1–3 (Butterworths, London, 1976).
112. R. W. BENE, *Appl. Phys. Lett.* **41** (1982) 529.
113. H. T. G. HENTZELL, R. D. THOMPSON and K. N. TU, *J. Appl. Phys.* **54** (1983) 6923.
114. E. G. COLGAN and J. W. MAYER, *J. Mater. Res.* **2** (1987) 8.
115. J. K. HOWARD, R. F. LEVER, P. J. SMITH and P. S. HO, *J. Vac. Sci. Technol.* **13** (1976) 68.
116. E. G. COLGAN, *J. Appl. Phys.* **62** (1987) 1224.
117. *Idem, ibid.* **62** (1987) 2269.
118. JIAN LI, J. W. STRANE, S. W. RUSSELL, S. Q. HONG, J. W. MAYER, T. K. MARAIS, C. C. THERON and R. PRETORIUS, *ibid.* **72** (1992) 2810.
119. F. M. D'HEURLE and R. GHEZ, *Thin Solid Films* **215** (1992) 26.
120. R. PRETORIUS, A. M. VREDENBERG, F. W. SARIS and R. DEREUS, *J. Appl. Phys.* **70** (1991) 3636.
121. R. PRETORIUS, T. K. MARAIS and C. C. THERON, *Mater. Sci. Eng.* **10** (1993) 1.
122. K. MATHUR and A. KUMAR, *Thin Solid Films* **146** (1987) L27.
123. P. R. SUBRAMANIAN and D. E. LAUGLIN, *Bull. Alloy Phase Diag.* **10** (1989) 554.

Received 20 December 1996
and accepted 24 July 1997